TRIBHUVAN UNIVERSITY

INSTITUTE OF ENGINEERING

PULCHOWK CAMPUS

THESIS NO: 079/MSPSE/003

Performance Evaluation Of PV-ESS-Integrated Grid Using ANN Tuned UPQC For Power Quality Enhancement

by

Ashish Oliya

A THESIS

SUBMITTED TO THE DEPARTMENT OF ELECTRICAL ENGINEERING IN PARTIAL FULFILLMENT OF THE REQUIREMENTS FOR THE DEGREE OF MASTER OF SCIENCE IN POWER SYSTEM ENGINEERING

DEPARTMENT OF ELECTRICAL ENGINEERING

LALITPUR, NEPAL

APRIL, 2025

COPYRIGHT©

CERTIFICATE OF APPROVAL

The undersigned certify that they have read and recommended to the Institute of Engineering for acceptance, a dissertation entitled **"Performance Evaluation of PV-ESS-Integrated Grid Using ANN Tuned UPQC for Power Quality Enhancement"**, submitted by **Ashish Oliya** in partial fulfillment of the requirement for the award of the degree of **Master of Science in Power System Engineering**.

Assoc. Prof. Dr. Sujan Adhikari

Hillside College of Engineering
(External Examiner)

Asst. Prof. Dr. Bishal Silwal

Program Coordinator
M.Sc. in Power System Engineering
Pulchowk Campus, Lalitpur
(Supervisor)

Assoc. Prof. Dr. Basanta K. Gautam

Head of Department
Department of Electrical Engineering
Pulchowk Campus, Lalitpur
(Supervisor)

April 2025

Tel: +977-1-5443081, Email: doee@pcampus.edu.np, Website: www.doee.pcampus.edu.np

ABSTRACT

The growing integration of renewable energy sources into power grids has posed major challenges to maintaining power quality and system stability. Therefore, this study proposes an Artificial Neural Network (ANN)-based Unified Power Quality Conditioner (UPQC) for enhancing the power quality of a grid-connected photovoltaic (PV) and energy storage systems (ESS), mitigation of power quality issues of renewable energy integration to grid is the main contribution made by this research.

In this paper, UPQC utilizes the NPC converter in both series and shunt active filters. The study examines THD improvement, PF compensation, voltage regulation under nonlinear loads, grid disturbances, and faults (L-G and L-L-L-G) in ANN-tuned UPQC against PI-controlled UPQC. The Series Voltage Conditioner (SVC) mitigates voltage magnitude sagging, swelling, and imbalance, whereas the Shunt Current Conditioner (SHVC) mitigates harmonic distortion, load imbalance, and reactive power. FUZZY logic MPPT is implemented for optimal PV extraction with fast and stable convergence. In addition, ESS with FUZZY Logic Controller (FLC) supports grid stability by handling power variations and improving dynamic response. MATLAB/Simulink simulations verify THD reduction, mitigate voltage sag/swell and Power Factor (PF) improvement, of the system and establish the dominance of ANN-based control over traditional ones.

The Cesar Apartment, located in Lalitpur, Nepal, is the real-world test system under consideration here, and it is already equipped with PV modules as well as ESS. Despite this, the system suffers from power quality issues such as harmonics and fluctuating PF, in addition to being poor in extracting the maximum power from the PV modules. This proposal involves utilizing a UPQC with ANN-based control to provide solutions for these issues. Furthermore, FLC algorithm for control schemes was designed to improve ESS performance and maximize power point tracking of PV. The results from the simulations show significant improvement in power quality, as well as energy utilization, have been obtained.

ACKNOWLEDGEMENT

I would like to express my deepest gratitude to my supervisors, Associate Prof. Dr. Basanta Kumar Gautam, and Assistant Prof. Dr. Bishal Silwal, for their invaluable guidance, insightful comments, and continuous support and encouragement throughout the progress of this research work. Special thanks to Er. Pradip Humagain from Gham Power Pvt. Ltd. for providing the Cesar Apartment data. Furthermore, I am immensely thankful to the whole team of Department of Electrical Engineering, IOE, Pulchowk Campus for providing the necessary resources and environment conducive to academic growth and learning.

I would like to take this opportunity to express my sincere gratitude and thankfulness to my family members for their encouragement and continual source of inspiration during the entire period of this thesis work. Thank you all for believing in me and for being part of this journey.

TABLE OF CONTENTS

LIST OF FIGURES

LIST OF TABLES

LIST OF ABBREVIATIONS

ANN	Artificial Neural Network
PV	Photo Voltaic
ESS	Energy Storage System
UPQC	Unified Power Quality Control
NPC	Neutral Point Clamped
PF	Power Factor
SVC	Series Voltage Conditioner
SHVC	Shunt Voltage Conditioner
MPPT	Maximum Power Point Tracking
RE	Renewable Energy
MLP	Multi Layer Perceptron
MATLAB	Matrix Laboratory
THD	Total Harmonic Distortion
FFT	Fast Fourier Transform

CHAPTER ONE: INTRODUCTION

1.1 Background

Renewable energy sources, including photovoltaic (PV) systems, and battery storage are becoming more common in the power grid. This can create opportunities and challenges for power quality. For instance, this thesis considers power quality issues on the distribution grid. The PV system and battery storage are connected through the point of common coupling (PCC) to the grid and this system serves both resistive and non-linear loads. The work is based on a hypothetical model and tested with real-time data collected over a period, with the main metrics such as active power, reactive power, total harmonic distortion (THD), power factor and stability.

In a world of transition, the energy sector is now converging to replace regular forms of energy such as fossil fuels and nuclear power with Renewable Energy Sources (RESs) such as solar, wind, and tidal energy.The increasing socio-economic environmental issues of large-scale power plants have led researchers and policymakers to explore alternative energy solutions, such as hybrid renewable energy systems (HRES), which integrate multi-renewable sources to improve energy efficiency and reliability, resulting in greater diversity and resilience in the current power infrastructure[1]. Among others, the changing aspects toward this direction are a crucial requirement for sustainable energy supply, rising environmental awareness, and the market growth of renewable energy technology. Various RESs have been appreciated as bright suitors for conventional energy sources because of their nature of being abundant, accessible, and kind to Mother Nature. Different from fossil fuels, RESs do not, in other modalities, foster depletion of natural reserves while they apply a big contribution into greenhouse gas emissions reduction. The resultant use of RESs purportedly mitigated global warming effects and carbon footprint, thus theoretically serving as an answer to the struggles against aspects of climate change [2].

Variable Renewable Energy Resources (VRER), namely solar and wind, are central to achieving a cleaner, more sustainable energy future, yet they pose real challenges in terms of grid stability and reliability due to their variability. These challenges were examined and possible solutions were considered, including better forecasting, energy storage options, and supportive policy programs. Ultimately, with planning and collaboration, the integration of VRER is manageable, and we can create or hold accountable a power system that is resilient and environmentally responsible.[3]. While renewable energy sources, that is, wind and solar, provide numerous advantages, they are also quite limited due to

their reliance on specific weather conditions as well as geographical location. Variability in sunlight and wind patterns translates to fluctuation in power generation, causing instability in the grid, hence posing a direct and significant challenge to backup supply, especially at peak times. The output of RES can also be hard to predict, causing voltage and frequency fluctuations that can substantially affect the grid performance as well as operational efficiency [4].

Recently, a variety of Maximum Power Point Tracking (MPPT) methods have been studied to optimize the efficiency of photovoltaic (PV) systems under various environmental conditions, such as temperature and irradiance.To deal with these challenges, the joint use of RE Sources with Energy Storage Systems has become a solution with high potential. ESS is very important for balancing the energy supply and demand since it stores any excess energy when the production is high and releases it when it is needed. Battery storage, pumped hydroelectric storage, and supercapacitors possess much value added to quality of enhancing grid ability to assimilate renewable energies, while keeping stable and reliable. The combination of RES and ESS adds a surely more resilient power system, contributing to manage probably better variations in energy supply and demand and, thus, making a contribution to the enhancement in the efficiency of renewable energy consumption [5].

In recent years, AI techniques such as ANN, FLC controller, and machine learning algorithms have been explored for optimizing the performance of integrated RES-ESS systems to reach the desired target values. Real-time predictions, decision-making, and adaptive control can be accomplished using these smart control techniques to maintain power system's effectiveness and reliability. The grid can, therefore, be applied directly for dynamic response to changes in RES generation to keep the power supply system more stable and sustainable by the means of AI technologies.

The data collected from Jan-March of 2025, revealed significant fluctuations in active and reactive power, Total Harmonic Distortion (THD), and solar generation output, indicating serious operational issues. On 20/03/2025 Active power loading ranged considerably over the course of the day, with peaks of net around 64,871.789 W consumed load at 1 AM on Off PV timeframe, There was a similar tendency with reactive power, having a peak of 57,655.805 VAR at peak load indicating power factor around -0.745 reactive power corrective issues. Also, the THD values were above acceptable limits for the Load AC Current across all A, B, and C phases, On 12/03/2025, THD are peaking at 252.28%, 308.08%, and 193.07% around 7 AM. Similarly, THD occurred on March 25, 2025, at 15:00, when the Load AC Current THD (Phase A) reached 205.24%. The THD for phase B was 149.26%, and for phase C, it was 361.62%. During that same hour, we also observed

the system exhibiting a power factor of 0.861. In most cases, the THD value fluctuates between 30% and 60%. This demonstrates significant distortion in the waveform of the source, possibly as a result of heavy non-linear loads and from an inverter. Alternatively, the best case for THD and poor case for PF occurred on March 9, 2024 at 7:00 AM, beginning with the THD of current Phase A at 5.23, Phase B at 5.91, and Phase C at 6.06, on the contrary the power factor was lagging and this is not favorable i.e. 0.717 using load net active power of 42.681 kW, and reactive power of 41.366 kVAR with a total apparent power of 59.439 kVA, concurrently the solar generation for that time period was approximately 9 kW. With all the available data voltage THD seems quite satisfying which ranges from 2-4% which is under IEEE 519 standard.

Solar energy production exhibited a natural diurnal variation with the peak production of 46,293.238 W at 11:00 PM on 31/03/2025, and negligible production at night. The net active power supplied is 33,204.805 w with net reactive power consumed of 5,720.606 VAR at active irradiance time, suggesting that electricity is being fed back to the system. and at the same time THD value of current of phase A, B and C are 5.6%, 8.75% and 9.3% respectively with PF of 0.985. Similarly, on March 4, 2024 at 12:00 PM, PV generates 40,136.078 W with net active power supply to grid of 14,193.986 W. At this time system has PF of 0.884 and load current THD of Phase A, B and C are 40.63%, 26.39% and 50.001% respectively which is very above the IEEE 519 Standard.

First of all, in this project we are developing the efficient model for research, The proposal is for a three-wire, three-phase grid that incorporates PV and ESS via a phase inverter. The equivalent nonlinear loads cause harmonic disturbances, swells, and dips in the voltage under working conditions. A consistent frequency of 50 Hz is maintained together with an AC voltage Ph to ground of 230 V. The regulation of fault voltage circumstances is done with a UPQC. Alongside a roughly 60 kW rated PV system, and a DC-coupled Energy Storage System, a nine 48V 30Ah battery with rated capacity 13 kWH with a battery bank linked via a bidirectional converter is used in conjunction. In the current study, ANN is utilized as a controller in the NPC converter inside UPQC, and the FLC approach has produced the suggested MPPT for a PV system.

In this aspect, it has been proposed that ANN-based UPQC is an best approach for improving power quality in grid-connected PV-ESS systems. In addition, capable of always learning and adapting to the dynamics of a system, AI provides a precise control and an effective mechanism for real-time improvement in power quality. Although ANN would be time-consuming with the training, high accuracy and reliability, in turn, make it a prospective control tool of power quality devices within the renewable energy systems.

1.2 Problem Statement

The rise of renewable energy, especially photovoltaic (PV) systems, has brought to light many issues, such as fluctuations in voltage, intermittent generation. At the same time, Energy Storage Systems (ESS) are faced with issues such as control, operation, and coordination of renewable generation. New modern, sensitive loads are more susceptible to power quality issues such as voltage sags and swells, harmonic disturbances, or unbalanced conditions caused by caused by non-linear loads and inverter-based generation, resulting overheating in electrical equipment, and inefficient power transfer. Further to this, imbalances in voltage and reactive power result in an inherent instability on the grid, leading to higher losses, inefficient operation in electrical loads, as well as penalties for non-compliance with grid standards. Voltage sags and dips are the extreme case as industries mostly are reliant on fragile electronics, while harmonics and flicker decrease the life of electrical components. The existing mitigation devices that can be used to address these emerging and challenging situations have demonstrated limitations on their effectiveness in more complicated scenarios, mostly due to dynamic grids with high levels of renewable and ESS penetration.

1.3 Objectives

The objective of the study are mentioned below:

- To enhance solar energy extraction of PV system using FUZZY MPPT and to integrate an ESS with the grid using FLC-based control for grid support.

- To develop an ANN-based control strategy of UPQC with NPC controllers which gives efficient voltage regulation, harmonic elimination, and perform active/reactive power compensation to improve power factor compared to traditional controllers.

1.4 Scope

The main scope includes:

- Enhance the quality of power in the distribution system utilizing a UPQC with NPC type inverters to alleviate the impact of voltage disturbance, harmonics, and reactive power in the distribution network

- Create intelligent control with ANN based schemes for adaptive and robust operation under varying loading and source conditions of supply.

- Implement PV and ESS for efficient energy management, renewable energy usage, and peak shaving during higher load demand.

1.5 Limitation

- Some key assumptions made within this analysis might not make room for real-world complications.

- Does not take into consideration the cost-effectiveness or economic aspects of ESS sizing.

- The power quality and stability are prioritized while large grid dynamics are neglected.

- A limited study on extreme situations-such as long durations of low PV or ESS degradation.

1.6 Thesis Organization

The dissertation is organized into five chapters. This section enlists a brief outline of each chapter and its contents.

- This chapter gives brief introduction of the dissertation. The problem statement is described and followed by the objectives of the thesis.

- Chapter 2 explores the necessary literature review done for this dissertation.

- Chapter 3 describes the research methodology of the dissertation including the MATLAB simulation and workflow.

- Chapter 4 discusses the obtained results and performs the analysis of the ANN-based control system of UPQC compared with conventional controller and also compare the real system o/p data with updating the real i/p data to proposed model.

- Chapter 5 concludes the thesis work.

Finally, this thesis will end with a list of references and the relevant appendices.

CHAPTER TWO: LITERATURE REVIEW

This chapter explores the necessary literature review done for this dissertation. It covers the overview and fundamentals of PV, energy storage system, unified power quality conrol and machine learning theory.

2.1 Overview

Renewable energy integration relies on power electronic devices like converters and inverters, which can degrade power quality on both the source and load sides. Additionally, non-linear loads at the point of common coupling (PCC) introduce harmonics, worsening existing issues. Common power quality problems include voltage sags, swells, flicker, and harmonic distortions [6].

The primary concerns of power quality are: Voltage and current variations caused by uncontrollable variability of renewable energy processes. Renewable energy resources cause intermittent supply due to the variability of weather conditions that change with time, causing variations in frequency and voltage at the interconnected power system. Harmonics, which are caused by power electronics that are used in the generation of renewable energy. When the penetration level of renewable energy resource is higher, then the effect of harmonics could be significant [7].The growing penetration of renewable energy (RE) sources has raised power quality (PQ) issues due to their intermittent nature and relevant interfacing converters connecting them to the grid. Numerous approaches have been used to detect and classify PQ disturbances in RE-penetrated utility networks, using feature extraction methods, even in noisy environments. Additionally, advanced signal processing methods and machine learning approaches have been widely reviewed, which serve to maximize state estimation, monitoring and mitigation of PQ issues [8].

Different methods are used to mitigate the power quality concern in grid. These include FACTS devices such as UPFC, UPFC-FLC, GUPFC, UPQC, and SVC, which are used to mitigate THD and enhance power quality for bettering grid performance [9]. addition, in the literature [10] deals with the use of UPQC to alleviate power network and harmonic disturbances via PV-BESS. A PV-BESS integrated UPQC ensures voltage support and stable power even in times of voltage interruptions . This too is far superior to SVC, Statcom, and DVR with respect to voltage enhancement, harmonic alleviation, current enhancement, and improvement of system power quality [11]. In the presence of linear and nonlinear loads simultaneously, the UPQC outperformed the DVR. The UPQC was able to effectively mitigate voltage sag, and voltage swell, and account for harmonics plus

the UPQC was faster, and restored better voltage waveforms when compared to the DVR. Furthermore, the UPQC kept THD within acceptable levels making it better at keeping voltage stable thus helping with power quality makes for better microgrids [12].

The SRF and dq0 concept based control strategies are used for series and shunt connected active power filter of UPQC. UPQC reduces voltage fluctuations and harmonic distortions with series and shunt active power filters implemented with SRF and dq0 strategies [13].

In comparison with the classical PI controller, the UPQC-ANN-RE system is able to achieve slightly better THD in load-side voltage and currents, while being capable of eliminating harmonics due to the operation of nonlinear loads. Both systems meet IEEE 519 harmonic distortion standards [14]. The FLC-based MPPT is superior to ANN-based MPPT in PV, Wind, and ESS for an efficient and economical use of power. They give electric vehicles the flexibility to consume power and assist the grid during peak load and off-peak periods if proper controllability and grid integration are provided. Real-time predictions, decision-making, and adaptive control can be accomplished using these smart control techniques to maintain power system's effectiveness and reliability [15].

Uncertainty in RE sources can be avoided when using FLC-based MPPT algorithms. The FLC-based MPPT is known to have been carried out for avoiding the uncertainties from climate conditions related to solar [16], Several parameters, such as irradiation and temperature, must be analyzed when modeling PV systems, as RESs are sensitive to both weather and location. A variety of Maximum Power Point Tracking (MPPT) methods have been studied to optimize the efficiency of photovoltaic (PV) systems under various environmental conditions, such as temperature and irradiance. Because fuzzy logic control (FLC) responds quickly to changes in the environment and is insensitive to changes in circuit characteristics, it is a remarkable method when used for MPPT. The accuracy benefits shown by the FLC MPPT technique have boosted the system's ability to operate at the Maximum Power Point (MPP) [17].

Energy storage devices, including batteries and ultracapacitors, contribute significantly to the improvement of transient stability by reducing power variations. The study [18], which evaluates system response with various DG types, fault scenario types and fault levels of penetration, verifies that storage is effective at enhancing stability/reliability within a power system and improves the integration of DG in contemporary power systems. ESS is very important for balancing the energy supply and demand since it stores any excess energy when the production is high and releases it when it is needed.

2.2 Solar PV System

Solar cells are semiconductor devices used to convert sunlight directly into electrical energy in a PV solar system. Considered a clean, renewable energy source, solar power has become one of the biggest renewable sources of energy for the benefit of the earth, reducing greenhouse emissions, and contributing to the goals of sustainable energy development. A PV system consists of four standard components: solar panels, inverters, optional battery storage, and a connection to the grid. Since they can supply power in a continuous manner, PV systems are now also of interest with regard to their integration in conjunction with energy storage systems (ESS) or hybrid systems.

The working principle of a photovoltaic system is explained by the photovoltaic effect. In this effect, sunlight represented by its photons excited the electrons of the semiconductor material and hence developed the electric current. The performance of a PV cell is guided by its respective parameters, namely:

Open-circuit voltage (Voc): The voltage across the PV cell terminals when there is no load;

Short-circuit current (Isc): The current that passes when the terminals are shorted;

Maximum power point (MPP): The point at which the PV cell works at its maximum efficiency in terms of both voltage and current. The electrical power output from solar panels will depend on the intensity of light, the area of the panel, and the characteristics of the cell.

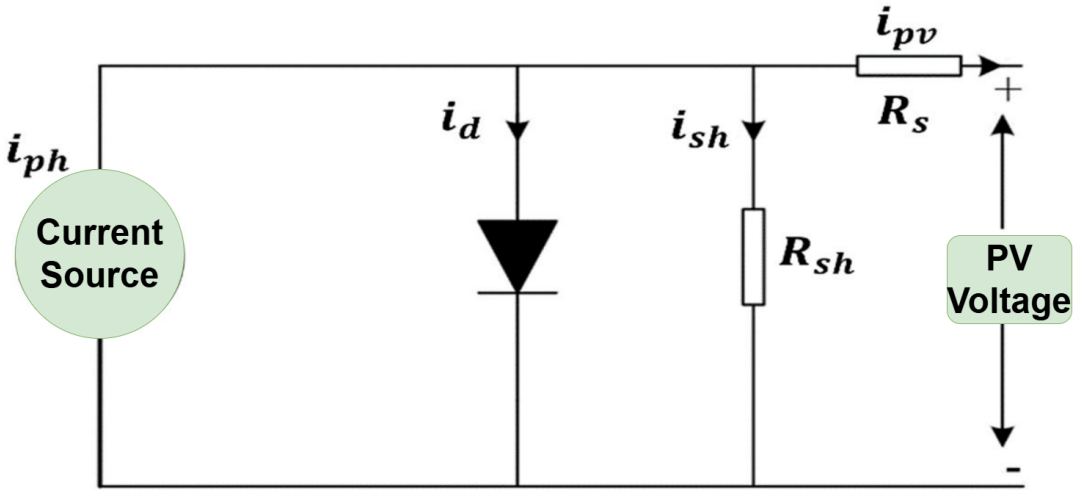

Figure 2.1: PV Single Module

A PV module uses the single-diode equivalent model to generate power dependent on temperature and solar irradiation. The following factors control the I-V characteristics:

$$I_L = I_S - I_{\text{sat}} \left[\exp\left(\frac{V + I_L R_{\text{series}}}{c V_T} \right) - 1 \right] - \frac{V + I_L R_{\text{series}}}{R_{\text{parallel}}} \tag{2.1}$$

$$V_T = \frac{kT}{q} Q_d N_{\text{cell}} N_{\text{ser}} \tag{2.2}$$

Where: - I_L = Output current from the PV panel - I_S = Photogenerated current (depends on irradiance) - I_{sat} = Reverse saturation current - V_T = Thermal voltage - c = Diode quality factor - R_{series} = Series resistance - R_{parallel} = Parallel resistance **Temperature and Irradiance Effects**

$$I_S = I_{SC} \times \frac{G}{G_{\text{ref}}} \tag{2.3}$$

$$V_{OC} = V_{OC,\text{ref}} + k_T (T - T_{\text{ref}}) \tag{2.4}$$

Where: - I_{SC} = Short circuit current - V_{OC} = Open circuit voltage - G = Solar irradiance - T = Module temperature - k_T = Temperature coefficient

Power Calculation

$$P_{PV} = V_{PV} \times I_{PV} \tag{2.5}$$

2.3 Energy Storage System

Even though electricity has, by and large, been regarded as a non-storage able product even though pumped hydro and electrochemical battery technologies have been around for a considerable period. Explain things that have been omitted or viewed as not sufficiently practical – everything from excess building costs, to not enough operational capacity for use of energy in electric power systems – is extensive. Current and advanced storage technologies, and the ongoing effort to enhance electric energy storage (EES), are getting significant attention today. Given existing market structure and the new potential of EES technologies, numerous EES applications have been developed and are under investigation. Every ESS system converts electrical forms of energy into other forms of energy like mechanical, chemical, thermal, etc. Based on the storage energy nature ESS have different technologies, configurations, and characteristics. ESS can be classified according to their storage technologies as electrical, thermal, mechanical, chemical, electrochemical, and hybrid systems. Among these, let us talk about the electrochemical energy storage system.

2.3.1 Electrochemical Energy Storage System

Electrochemical storage refers to battery technology, which is the storage of chemical energy that has a reversible conversion into electrical energy. Battery technology is an old and mature technology and is available in various ranges of energy capacity, cost, life cycle, and material, and is overtaking energy storage technology, day after day. Battery cells can be connected in series and parallel combinations to obtain the required voltage and current rating of the battery bank.

Lead-Acid battery This battery is one of the most traditional and widely utilized types of battery and a well-established, mature, and secondary storage battery. The anode of the cell consists of lead peroxide (PbO2) and the cathode consists of sponge pure lead (Pb), and as an electrolyte it uses dilute sulphuric acid (H2SO4). The reactions occurring during the discharge of the battery can be summarized in terms of oxidation reactions at the anode and cathode as:

$$\text{Oxidation:} \quad \text{Pb} \rightarrow \text{Pb}^{2+} + 2e^{-}$$

$$\text{Reduction:} \quad \text{Pb}^{4+} + 2e^{-} \rightarrow \text{Pb}^{2+}$$

Both oxidation and reduction reaction gives rise to lead sulphuric acid (PbSO4) as their by-product. The overall red-ox reaction can be given as:

$$\text{Pb} + \text{PbO}_2 + 2\text{H}_2\text{SO}_4 \rightleftharpoons 2\text{PbSO}_4 + 2\text{H}_2\text{O}$$

Lithium-ion Battery This is a rechargeable battery. The anode is made up of graphite and the cathode is made up of lithium metal oxide (LiMO2). An electrolyte made up of lithium salt contains a separator made up of Polyethylene (PE), Polypropylene (PP). During charging the reaction at two electrodes can be given as:

$$\text{At cathode:} \quad \text{LiMO}_2 \rightarrow \text{Li}^{+} + \text{MO}_2 + e^{-}$$

$$\text{At anode:} \quad \text{C}_6 + \text{Li}^{+} + e^{-} \rightarrow \text{LiC}_6$$

$$\text{Overall Redox Reaction:} \quad \text{LiMO}_2 + \text{C}_6 \rightarrow \text{MO}_2 + \text{LiC}_6$$

At the cathode, lithium metal oxide produces lithium ions and a free electron. The liberated ion passes through a porous membrane inside an electrolyte, reaches the anode, and combines with graphite to form lithiated carbon (LiC6).

During discharging lithium ion and a free electron is released from lithiated carbon. Free electron flows through an external path and lithium-ion follows an electrolytic membrane path to reach the cathode. At the cathode, metal oxide combines with lithium ion and free electron to form a lithium metal oxide.

$$\text{At cathode:} \quad \text{Li}^+ + \text{MO}_2 + e^- \rightarrow \text{LiMO}_2$$

$$\text{At anode:} \quad \text{LiC}_6 \rightarrow \text{C}_6 + \text{Li}^+ + e^-$$

$$\text{Overall Redox Reaction:} \quad \text{MO}_2 + \text{LiC}_6 \rightarrow \text{LiMO}_2 + \text{C}_6$$

Lithium-ion battery cell voltage varies from 3.8 – 4.2 volts. There are several lithium-ion batteries based on lithium metal oxide used. Some examples are Lithium manganese oxide (LiMn2O2), Lithium nickel manganese cobaltoxide (LiNiMnCoO2), Lithium iron phosphate (LiFePO4), and Lithium Titanite (Li4Ti5O12).

Nickel Batteries These batteries are old battery technologies. In nickel-based batteries, anodes are made of nickel oxyhydroxide, cathode by any one metal (Cd/MH/Fe/Zn or H2), and potassium hydroxide as an electrolyte. Among several nickel batteries, Ni-Cd and Ni-MH are commercially available. Ni-Cd is the most successful. The red-ox reaction can be given as:

$$\text{At cathode:} \quad \text{Cd} + 2\text{OH}^- \rightarrow \text{Cd(OH)}_2 + 2e^-$$

$$\text{At anode:} \quad \text{NiOOH} + \text{H}_2\text{O} + e^- \rightarrow \text{OH}^- + \text{Ni(OH)}_2$$

$$\text{Overall Reaction:} \quad \text{Cd} + 2\text{NiOOH} + 2\text{H}_2\text{O} \rightarrow \text{Cd(OH)}_2 + 2\text{Ni(OH)}_2$$

2.4 Unified Power Quality Control (UPQC)

The Unified Power Quality Conditioner (UPQC) is considered to be the most advanced power quality improvement device, incorporating advantages of both a Series Active Power Filter (APF) and Shunt Active Power Filter (APF) into a single combined unit.

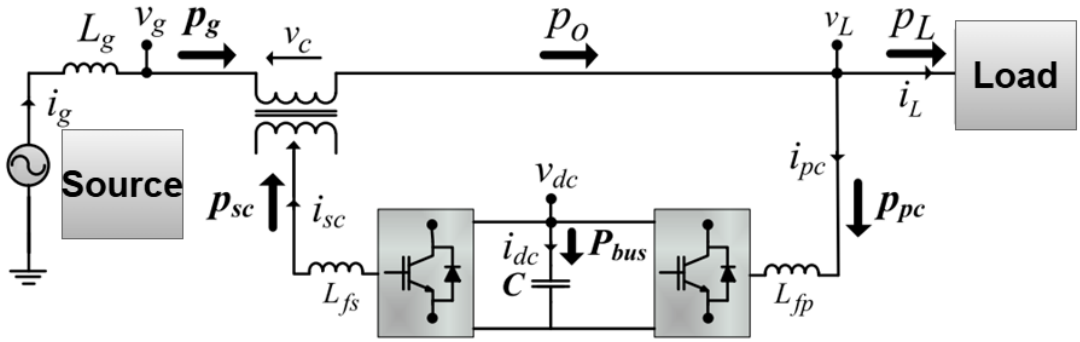

Figure 2.2: UPQC Circuit Structure

Power quality problems such as voltage sags, swells, harmonics and transients may seriously affect the performance of sensitive equipment, especially in commercial and industrial settings. Various specialized power gadgets have been developed to mitigate these disturbances. The UPQC stands out as a unique power quality conditioner combining both series and shunt compensation, thus becoming useful in integrated power quality maintenance. The UPQC integrates into itself the traditional devices, the DSTATCOM and the DVR. It therefore provides a holistic solution for these power quality issues by integrating both a series and a shunt inverter into a single device for enhancing the voltage profile and the current profile and thereby improving the overall reliability of power. From single-function devices, power quality conditioners have entered a multi-functional domain. The initial solutions, such as static var compensators (SVCs) and dynamic voltage restorers (DVRs), addressed a number of important power quality issues such as voltage sags and reactive power compensation. However, these devices were limited in their operating range of multiple disturbances at the same time. Therefore, a more holistic solution was sought in the UPQC platform, UPQC was introduced for the very first time in literature with a concept of bridging two power electronics devices to tackle both voltage and current quality issues together. As in [19], the UPQC can be defined as a series inverter for voltage waveform restoration at the PCC and a shunt inverter for current harmonic and reactive power compensation from the load side.

In recent literature, the control strategies for UPQC have been a major focus of research. Traditional methods of control, which involve PI controllers, have come under scrutiny in modern control scenarios. An example of this is given in [20], which proposes an MPC control strategy for UPQC to improve performance concerning series and shunt inverters. The MPC control strategy provides better dynamic performance in mitigating voltage sags and harmonics. Likewise, intelligent control techniques, like fuzzy logic controllers and ANNs, have been investigated for the UPQC systems. For developing an ANN-based UPQC control strategy for improving voltage regulation and harmonic mitigation, reference [14] and [15] utilized testing in this system under various load conditions, establishing improved performance compared to conventional methods.

UPQC is applicable in numerous domains. It is popularly used in industrial and commercial applications to increase the quality of power supplied for their efficient operation; sensitive equipment, such as microprocessors, data centers, and industrial machinery, are involved. It is also utilized in all renewable energy systems to compensate for intermittency and variability of the renewable power generated. Integration of Electric Vehicles in the Power Grid has been another application area wherein UPQC systems are emerging as frontline solutions to address issues arising due to charging stations and power quality disturbances.

2.5 Machine Learning

Machine Learning is a part of Artificial Intelligence that enhances system performance through learning derived from data. It is founded on statistical principles and algorithms analogous to the processes humans use to learn. The result is a system or machine that is able to increase performance and accuracy over time. Some of the main areas in which Machine Learning is used are Natural Language Processing (NLP), speech recognition, and classification. In regard to Machine Learning, training an algorithm is the act of teaching the algorithm to recognize patterns, provide decisions or predictions without being explicitly programmed to do so. Algorithms for machine learning will learn from massive amounts of data, uncovering the underlying patterns and relationships among the data in each data set. Once the algorithms learn these patterns, systems can adapt and enhance their accuracy over time, depending on the effectiveness of the training. This adaptive learning process is especially relevant in e.g. interact natural language conversations with humans, recognize speech patterns, differentiate speakers, or categorize data.Machine Learning is versatile and has broad applications in many industries such as healthcare and finance. Machine Learning, because of research and innovation, is constantly evolving and futuristically proficient, advancing artificial intelligence with practical applications in

many scalar situations and settings. Machine learning approaches can be categorized into three main types:

(i) **Supervised Learning**
Supervised learning consists of a training dataset where each instance is defined as a vector of input variables and respective desired outputs, presented as a matrix. One of the goals is to maximize a given function; typically, a loss or cost function, which generates model parameters that maximize or minimize the function. In so doing, the model learns to predict outputs accurately for new inputs by deriving patterns and relationships within the training dataset. Consequently, supervised learning is considered foundational to fields like image identification and predictive analytics. Commonly utilized algorithms include support vector machines, linear regression, K-nearest neighbour, neural networks, naive Bayes, and random forest.

(ii) **Unsupervised Learning**
Unsupervised learning is based on a collection of unlabeled data and identifies shared or common features to classify into meaningful (or meaningful) groups or partitions. The model then acts on the collection of data sets based upon whether or not those features are present. Commonly used algorithms include Hopfield learning, maximum likelihood, Hierarchical clustering and partial least square..

(iii) **Reinforcement Learning**
Reinforcement learning is an interactive method involving a Markov process that is used to optimize actions and fulfill objectives. Feedback or rewards would often be utilized to optimize actions based on the current state or the current state and action. Some commonly used approaches include Monte Carlo, temporal differences, and SARSA.

2.5.1 Artificial Neural Network, Multi Layer Perceptron

Artificial Neural Networks (ANNs) are increasingly relevant in addressing a wide variety of complex problems within numerous disciplines including, but not limited to, pattern recognition, classification, regression, and forecasting. In MATLAB, NFTool or Neural Network Fitting Tool is one of several tools introduced that provides a GUI (Graphical User Interface) to construct and train ANNs for data fitting problems modeled with a multilayer perceptron (MLP). This review paper contains information in MLP using the NFTool regarding structure, training approach, and practical examples.

The Multi Layer Perceptron (MLP) is a type of artificial neural network, which is recognized for its feedforward architecture that involves multiple layers that include, an input layer, one or often more hidden layer(s), and an output layer, all layers are fully interconnected,Here input vector x and evaluates the weighted sum $\sum_{i=1}^{n} x_i w_i + b$ where b is is bias term in addition to the perceptron similar to weighted inputs, allows for added flexibility in modeling complex patterns in the input data but is usually omitted in the network architecture. The activation function calculates the output based on the weighted sum of the inputs.

Some of the commonly used activation function are:

1. Sigmoid function
   The sigmoid activation function transforms real-numbered inputs into a range between 0 and 1. The sigmoid is defined as:

$$f(x) = \frac{1}{1+e^{-x}} \tag{2.6}$$

   The Figure 2.3 shows the sigmoid function.

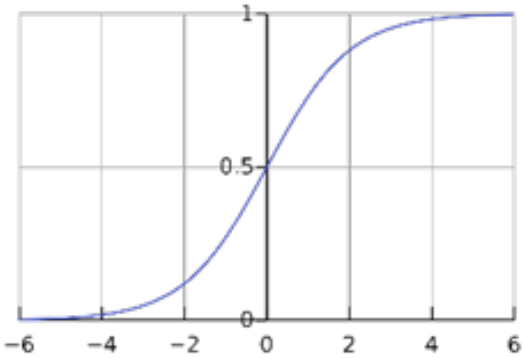

Figure 2.3: Sigmoid activation function

2. Hyperbolic tangent function
   The hyperbolic tangent function is very similar to the sigmoid activation function, has the same S-shape, and in this case, the output ranges from -1 to 1. For tanh, as the input increases (becomes more positive), the output goes towards 1.0, and as it decreases (becomes more negative), the output goes towards -1.0. The tanh is defined as:

$$f(x) = \frac{e^{x}+e^{-x}}{e^{x}-e^{-x}} \tag{2.7}$$

   The Figure 2.4 shows the tanh function.

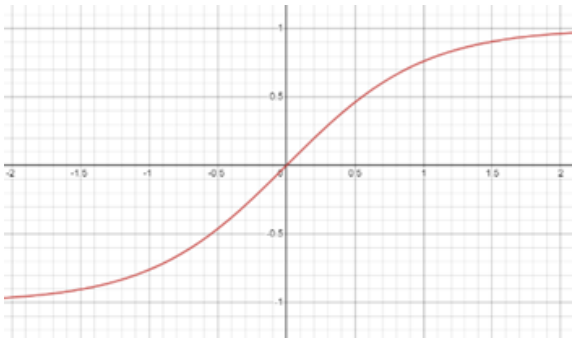

Figure 2.4: tanh activation function

3. ReLU function

   ReLU, which stands for rectified linear unit, simply converts the input to either zero or itself. ReLU operates by producing an output of zero for any zero or negative input or by producing the same input when the input is a positive value. ReLU is mathematically expressed as:

$$f(x) = max(0, x) \tag{2.8}$$

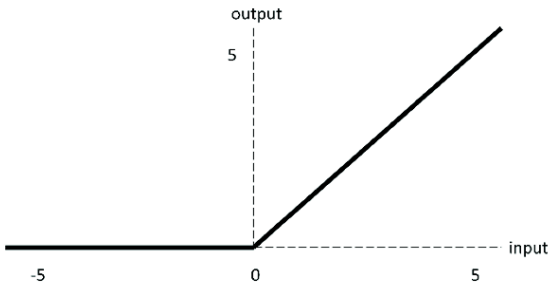

Figure 2.5: ReLU activation function

4. Leaky ReLU

   Leaky ReLU is a type of activation function for artificial neural networks. While it is a variation of the traditional ReLU activation function, it was specifically made to address "dying ReLU" the issue of neurons that can be inactive during training due to repeated negative outputs. In simple terms, Leaky ReLU allows for a non-zero small gradient for the activation function when the input is less than zero, as opposed to ReLU which would just return zero. The mathematical definition of

Leaky ReLU is:

$$f(x) = \begin{cases} x, & \text{if } x \geq 1 \\ ax, & \text{if } x < 1 \end{cases} \tag{2.9}$$

5. SoftMax

   SoftMax is simply a function that converts input of k real values into an output of k real values that sum to 1 which can be perceived as probabilities. If one of the inputs is a small or negative number, the softmax will turn that variable into a small probability, and if that input is a big number, the softmax will turn that variable into a big probability. The softmax can be defined as:

$$\sigma(x_i) = \frac{e^{x_i}}{\sum_{j=1}^{k} e^{z_k}} \tag{2.10}$$

   The softmax is used as an activation for output layer of multi class classification networks.

Each layer in an MLP is composed of several perceptrons. Connecting these layers in sequence forms the MLP architecture. The width of a layer is determined by the number of perceptrons in a layer, while the network's depth is defined by the total number of these interconnected layers. The output layer, located at the final stage of the network, is responsible for producing the desired output.

For MLP, if each layer transform the input via function f_1, f_2, f_3, f_4, respectively from input to output layer. Then for an input vector x, the output vector will be $f_4(f_3(f_2(f_1(x))))$.

MLP Learning involves the iterative adjustment of connection weights between neurons, a process critical for the network to learn patterns and relationships from data. The ANN model is generated using the Neural Fitting Tool (nftool) of the MATLAB using Levenberg-Marquardt backpropagation(LMBP) for training and hence gives great convergence and accuracy because it uses the approximation of the Hessian matrix instead of simple gradient descent.

By minimizing MSE, such an ANN-based controller brings in power quality, adaptability, and robustness in UPQC applications. Unlike traditional controllers, ANNs learn nonlinear system behavior and offer self-learning capabilities and substantially improved stability under disturbances with greater speed of the dynamic response and very efficient real-time implementation for superior power compensation.

CHAPTER THREE: METHODOLOGY

This chapter describes the workflow of the research starting from the PV -ESS system modeling, integrating them with grid for power efficiency and stability and apply ANN tuned UPQC to improve power quality issues, voltage sag/swell and to compensate reactive power.

3.1 Approach

The UPQC-ANN Tuned, PV-ESS system methodology integrates the Unified Power Quality Conditioner with the Artificial Neural Networks for the action of enhancing and

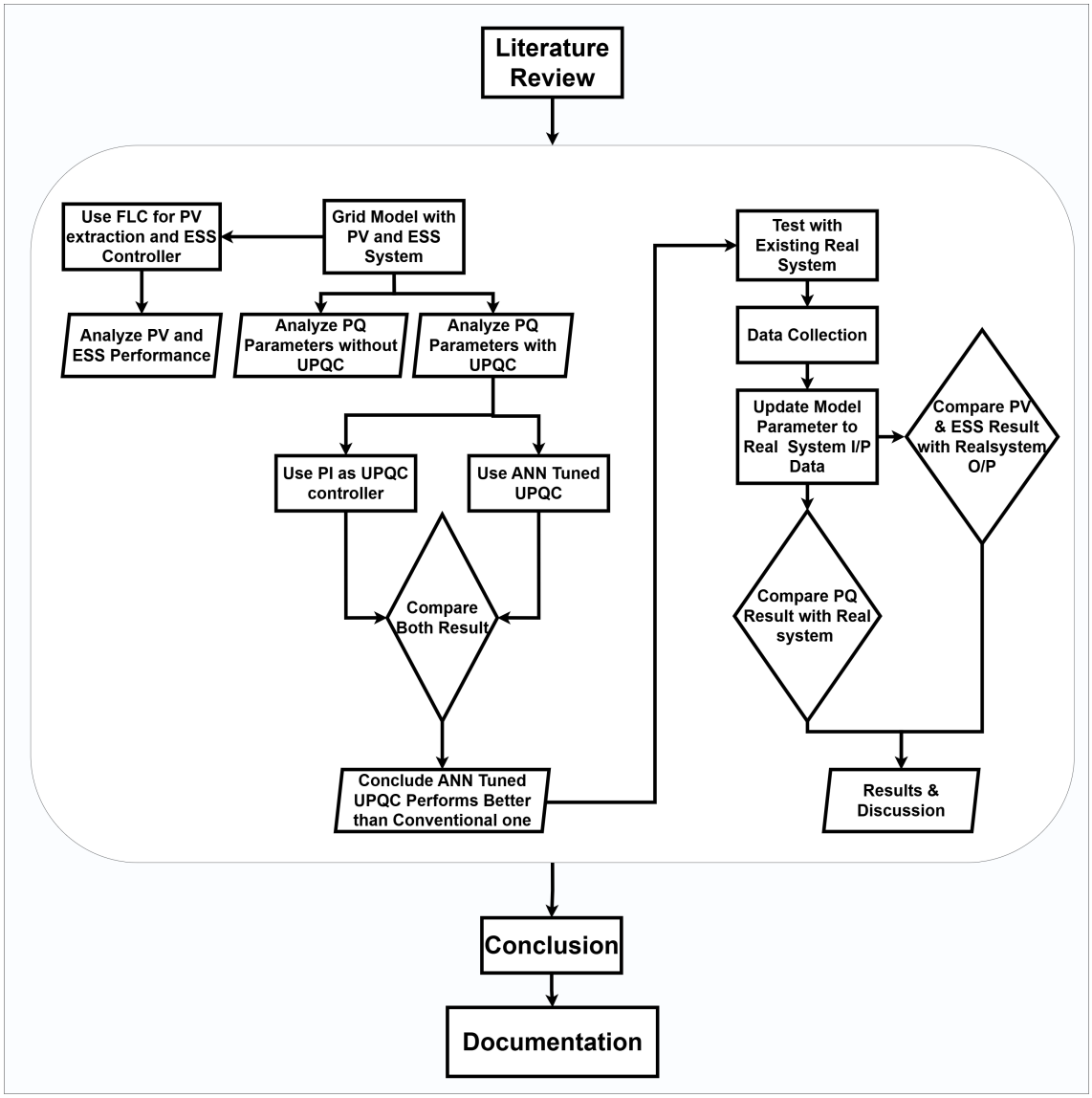

Figure 3.1: Methodology Approach

managing power quality using a PV-ESS-enabled setup. The overall methodology that has been utilized in this dissertation is shown in figure 3.1. The UPQC is for mitigating voltage disturbances arising from sags and swells by compensating voltage disturbances occurring on both the source and load sides.The ANN optimizes the control strategy of the UPQC to the current load, irradiation from solar, and grid status. The PV-ESS system assures that renewable energies are produced while also ensuring the storage of the excess power for stable and sufficient supply for all the units. Performance and stability of the system are also improved through efficient active/reactive power management, integrated renewable energy resource with protection of high power quality under dynamic grid and supply conditions..

Figure 3.2 illustrates a DG System RE-Based With UPQC in which solar PV with energy storage system and utility power is supplied. Three-phase source/substation supplies power through feeder line that have three-phase breaker and stepped down to 11/0.4 kV. PV system with MPPT and DC/AC converter supplies power to the system, supported by an EES (Battery) and EES Controller for the management of energy storage. There exists a linear, nonlinear and DC load present in the system and a fault block indicates possible disruptions in the system.

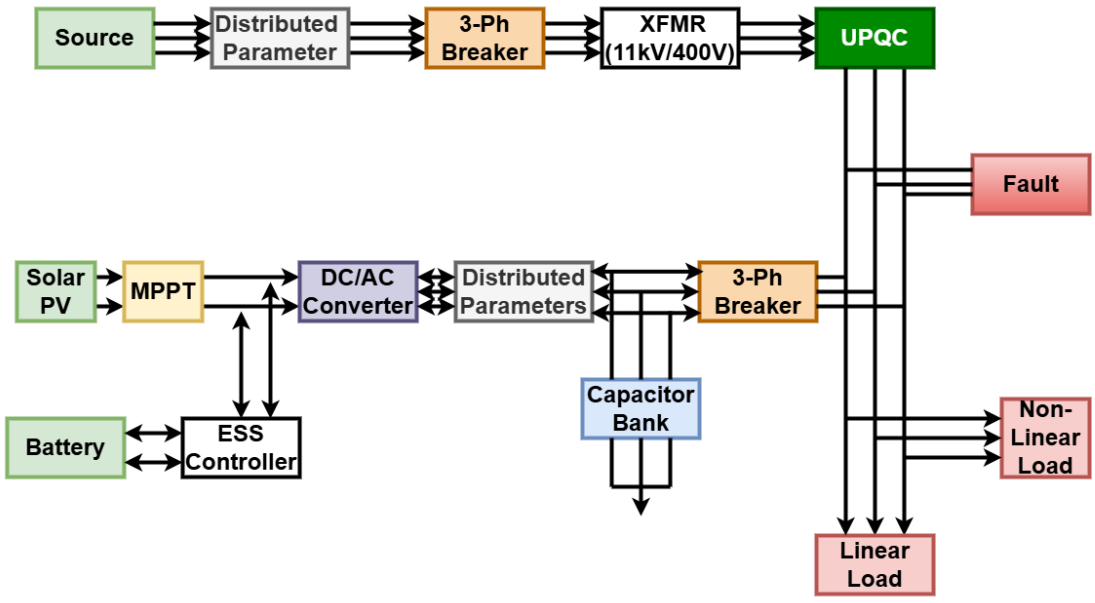

Figure 3.2: Overall Proposed System

Overall system modeling in MATLAB is shown in Figure 3.3 below.

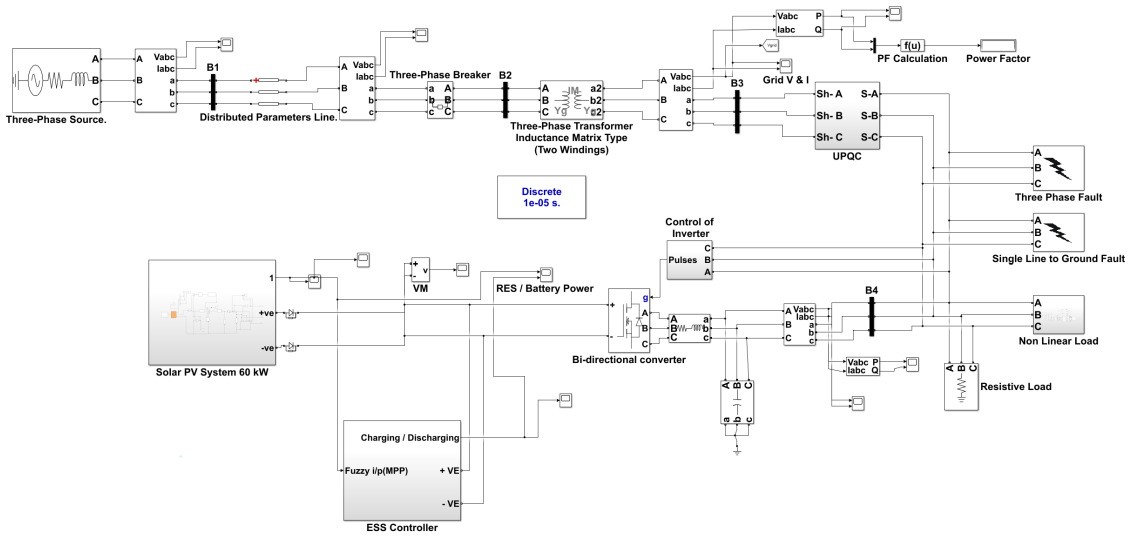

Figure 3.3: Overall System MATLAB Model

3.2 PV Modelling

The overall PV system, including MPPT and a boost converter, feeds into an AC/DC bidirectional converter, as shown in figure 3.13. This same converter is also shared by the battery system via the DC bus. The PV system uses a Fuzzy Logic Controller (FLC) as

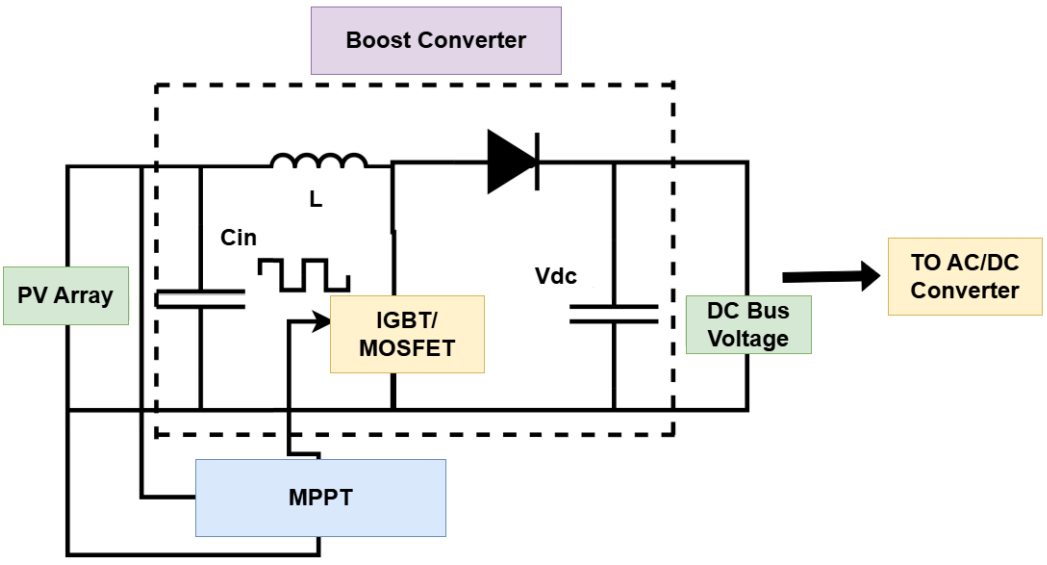

Figure 3.4: MPPT and Boost Converter for Maximum PV Power

shown in MATLAB model in figure 3.5 to accomplish Maximum Power Point Tracking (MPPT), which optimizes power extraction by dynamically regulating the duty cycle of

the boost converter.The FLC-based MPPT provides better flexibility and decision-making, allowing for more effective tracking in dynamic situations than conventional MPPT methods like Perturb and Observe (P & O) and Incremental Conductance, which have trouble with abrupt changes in irradiance and partial shading[15].

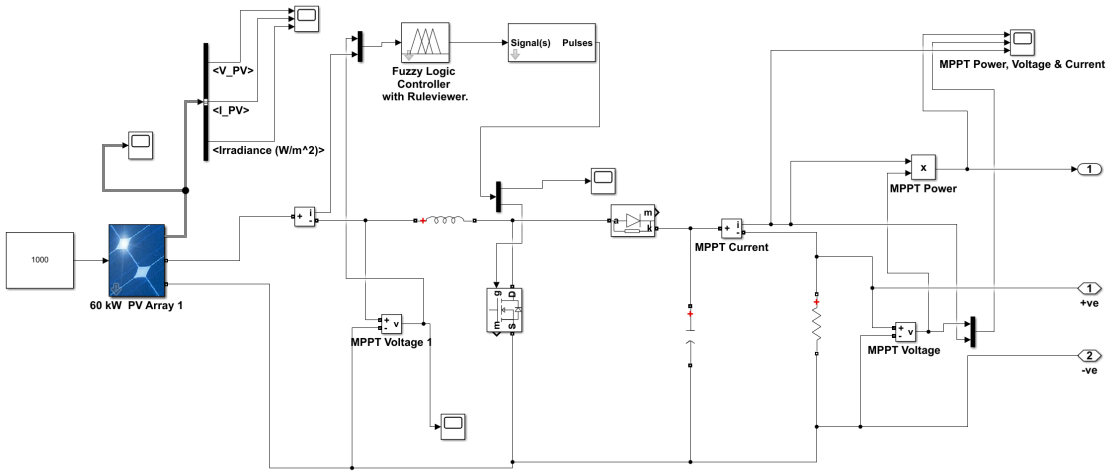

Figure 3.5: FUZZY MPPT MATLAB model of PV

Fuzzy Logic Controller for MPPT

Fuzzification Fuzzification converts crisp inputs (PV voltage and current) into fuzzy values using membership functions.

Inputs:

- V_{pv} (PV Voltage)
- I_{pv} (PV Current)

Membership Functions:

- Voltage (V) → LV- Low Voltage, MV- Medium Voltage, HV- High Voltage
- Current (I) → LI- Low Current, MI- Medium Current, HI- High Current

Inference (Rule-Based Decision Making) Fuzzy rules are applied based on the power slope condition:

$$EV(q) = \frac{P_V(q) - P_V(q-1)}{I_V(q) - I_V(q-1)} \tag{3.1}$$

Decision Rules:

- If $EV(q) > 0$, then increase duty cycle.
- If $EV(q) < 0$, then decrease duty cycle.
- If $EV(q) \approx 0$, then Maximum Power Point (MPP) is reached.

The change in error is given by:

$$dEV(q) = EV(q) - EV(q-1) \tag{3.2}$$

This determines whether the power is increasing or decreasing. **Fuzzy Rules**

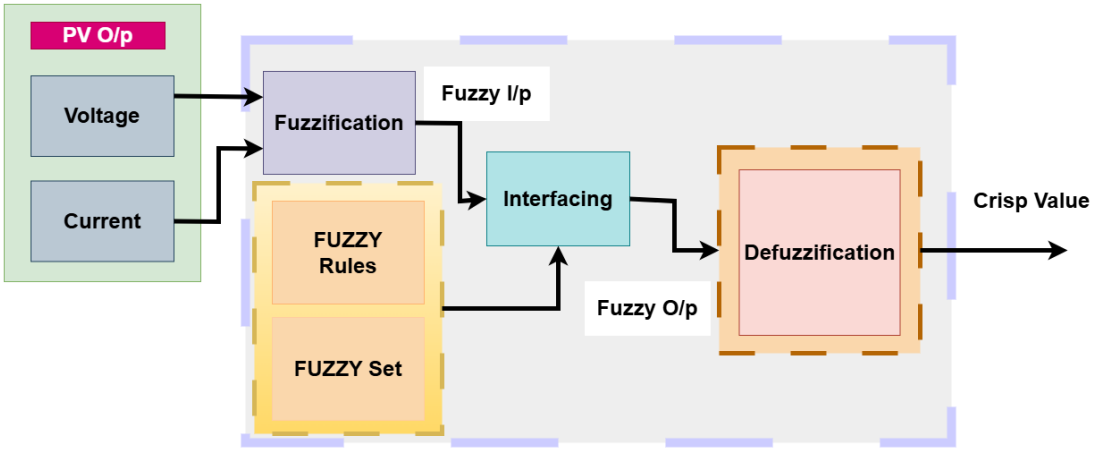

Figure 3.6: Block diagram of FLC-based MPPT employed to control duty cycle of boost converter in PV system

- If V_{pv} is LV and I_{pv} is LI, then Duty Cycle is HD (High Duty Cycle).
- If V_{pv} is MV and I_{pv} is MI, then Duty Cycle is MD (Medium Duty Cycle).
- If V_{pv} is HV and I_{pv} is HI, then Duty Cycle is LD (Low Duty Cycle).

Defuzzification Defuzzification converts the fuzzy duty cycle into a crisp value using the centroid method:

$$D = \frac{\sum(\mu_i \cdot d_i)}{\sum \mu_i} \tag{3.3}$$

Where:

- μ_i = Membership degree
- d_i = Corresponding duty cycle

Boost Converter Control The duty cycle D is used to control the boost converter:

$$V_{\text{out}} = \frac{V_{\text{in}}}{1 - D} \tag{3.4}$$

The fuzzy MPPT dynamically adjusts D to maintain maximum power output.

Table 3.1: Fuzzy Control Rules for MPPT V & I as Input

V \ I	Low Current	Medium Current	High Current
Low Voltage	High Duty	Medium Duty	Medium Duty
Medium Voltage	High Duty	Medium Duty	Medium Duty
High Voltage	Medium Duty	Low Duty	Low Duty

3.3 ESS Modeling

The power management approach identifies how much power may be transferred to the battery, or the PV system, or the grid in hopes of achieving an optimal power flow. In the proposed model, battery(ESS) is DC coupled with the PV system and overall system with buck/boost converter feeding with the same AC/DC converter is shown in figure 3.7. ESS is charged whenever there is power surplus, and discharging occurs whenever

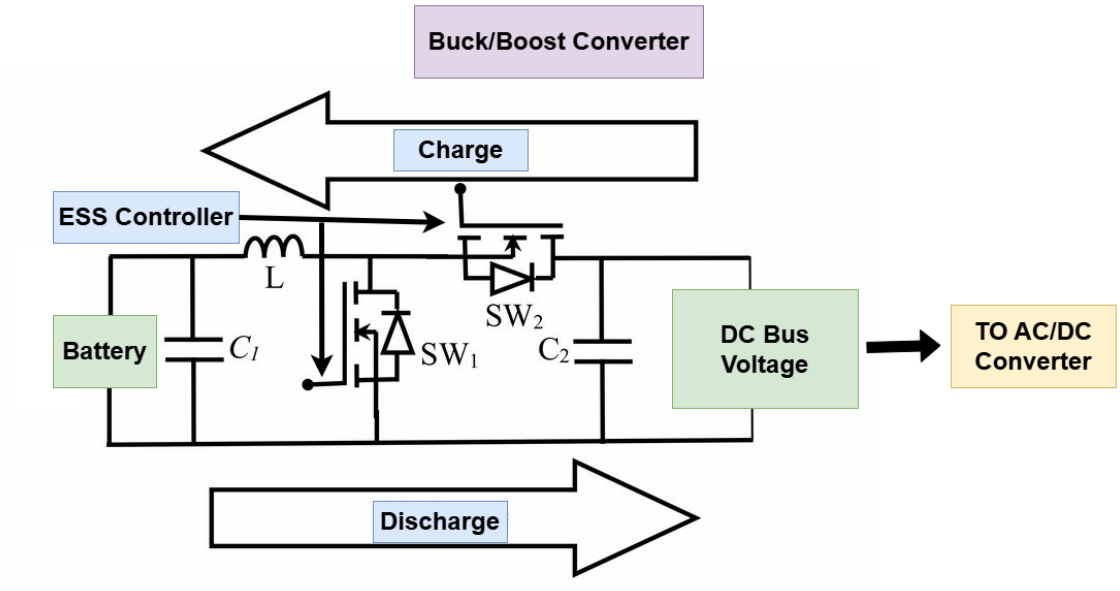

Figure 3.7: Battery controller and Buck/Boost Converter for ESS

there is a power deficit at the point of common coupling (PCC). The difference between active power at the PCC and reference load power is computed and improved through the element controlled by the fuzzy logic controller (FLC) to improve the active power values. Appropriate power should be provided to meet load demands to maintain a reliable and efficient grid system. The ESS plays a significant role in providing the extra power demand or storing the surplus energy. Solar energy is dependent on weather, and the ESS can act as a backup supply for providing power at any time. MATLAB model of FUZZY Logic Controller is shown in figure 3.8. It gets its regulation of charging and

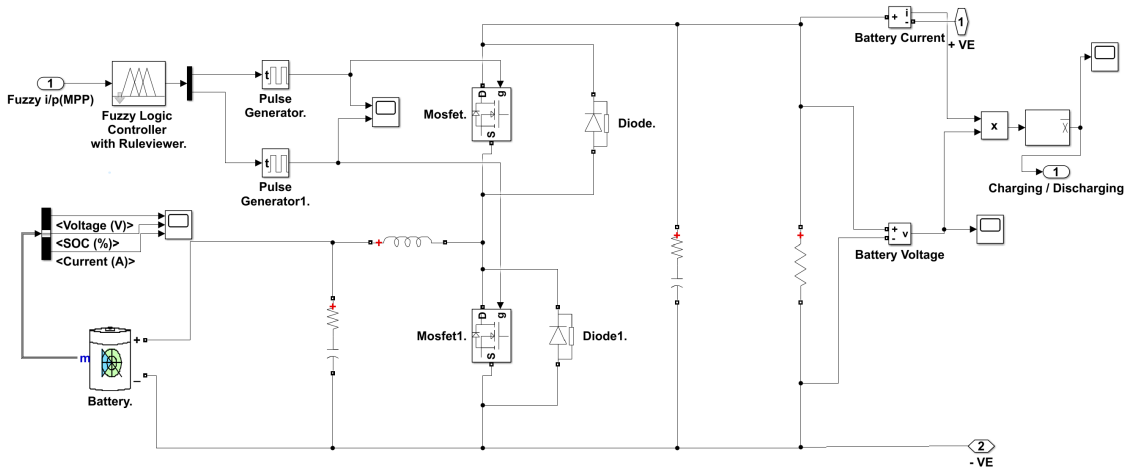

Figure 3.8: MATLAB model of FLC controller of ESS

discharging via a Fuzzy Logic Controller (FLC) that is set to optimize the power flow while maintaining the system stable. The SOC represents the available battery capacity and is given by:

$$SOC(t) = SOC(0) + \frac{1}{C_{\text{rated}}} \int_0^t I_{\text{batt}}(t)\, dt \tag{3.5}$$

For discrete-time simulation, SOC is updated as:

$$SOC(k+1) = SOC(k) + \frac{I_{\text{batt}}(k) \times \Delta t}{C_{\text{rated}}} \tag{3.6}$$

Where:

- $SOC(t)$ = State of Charge at time t (%).
- $SOC(0)$ = Initial SOC.
- C_{rated} = Rated battery capacity (30Ah).

- $I_{\text{batt}}(t)$ = Battery charging/discharging current (A).
- Δt = Time step for simulation.

SOC Behavior:

- Charging: If $I_{\text{batt}} > 0$, SOC increases.
- Discharging: If $I_{\text{batt}} < 0$, SOC decreases.

SOC is constrained between 0% and 100%:

$$0 \leq SOC(t) \leq 100\% \tag{3.7}$$

The battery terminal voltage is given by:

$$V_{\text{batt}} = V_{\text{oc}} - I_{\text{batt}} R_{\text{int}} \tag{3.8}$$

Where:

- V_{batt} = Battery terminal voltage (V).
- V_{oc} = Open-circuit voltage (V).
- I_{batt} = Battery current (A).
- R_{int} = Internal resistance (0.14667Ω).

The open-circuit voltage V_{oc} is a function of SOC:

$$V_{\text{oc}} = a \cdot SOC^3 + b \cdot SOC^2 + c \cdot SOC + d \tag{3.9}$$

Where:

- a, b, c, d are coefficients determined from the battery characteristics.

The power supplied or absorbed by the battery is given by:

$$P_{\text{batt}} = V_{\text{batt}} \cdot I_{\text{batt}} \tag{3.10}$$

Including charging/discharging efficiency:

- **Charging:**

$$P_{\text{batt}} = \eta_{\text{ch}} \cdot V_{\text{batt}} \cdot I_{\text{batt}} \tag{3.11}$$

- **Discharging:**

$$P_{\text{batt}} = \frac{V_{\text{batt}} \cdot I_{\text{batt}}}{\eta_{\text{dis}}} \tag{3.12}$$

Where:

- η_{ch} = Charging efficiency.
- η_{dis} = Discharging efficiency.

The FLC approach is developed to manage battery charging and discharging depending on the power imbalance (Error) in the grid, defined as the difference between generation and load demand.

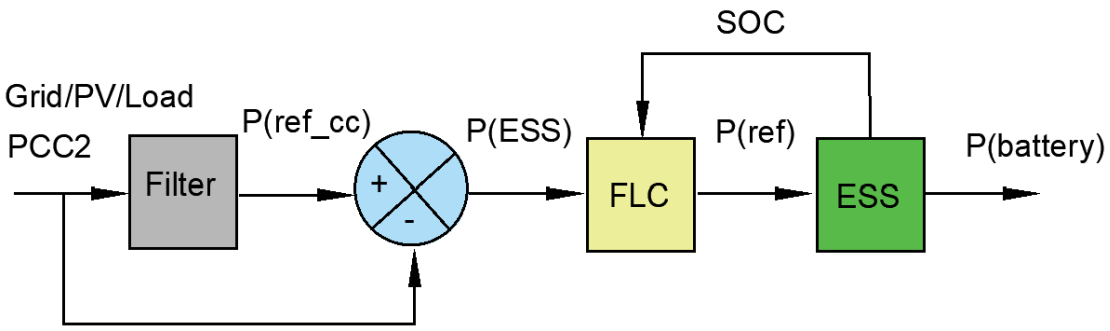

Figure 3.9: Fuzzy Logic Controlled ESS connected with grid for support

- Deficit Power (Error ≤ 0): Signifies that the grid is short on power (generation is less than demand). In this condition, the system defaults to battery discharging (BD = High, BC = Low)
- Excess Power (Error > 0): Signifies the grid has excessive power as generation exceeds demand. In this case the system switches to enable battery charging (BC = High, BD = Low).

The crisp duty cycle D is computed using the centroid method:

Table 3.2: Fuzzy Control Rules for Error, BC, and BD

Rule No.	Error (Input1)	BC (Output1)	BD (Output2)
1	Low Error (≤ 0)	High (1)	Low (0)
2	High Error (> 0)	Low (0)	High (1)

$$D = \frac{\sum \mu_D(x) \cdot x}{\sum \mu_D(x)} \tag{3.13}$$

Where:

- x represents the discrete values of D.
- $\mu_D(x)$ is the aggregated membership function of D.

This determines the final duty cycle for the bidirectional converter.

3.4 UPQC-ANN Tuned, PV-ESS TOPOLOGY

Below Structure figure 3.10 symbolizes the architecture of a UPQC-ANN, PV-ESS system planned to boost the power quality in an integrated green energy setup. This System

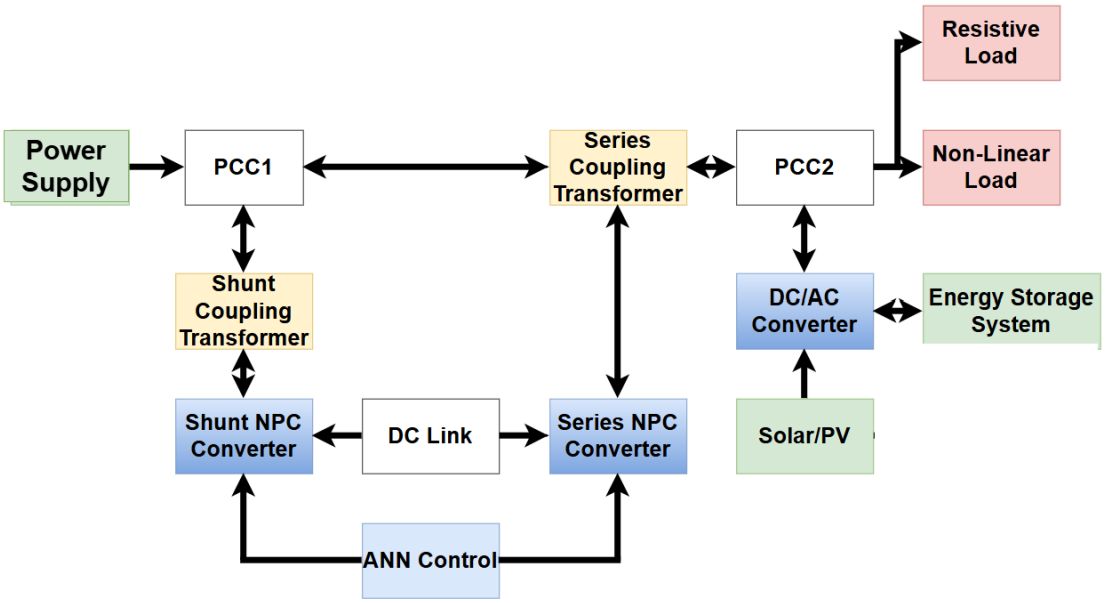

Figure 3.10: UPQC-ANN, PV-ESS Topology

utilizes the dual compentation approach as it consists of a Shunt NPC converter utilizing its power architecture to compensate for current, connected through a Shunt Coupling Transformer to regulate reactive power and neutralize harmonics and the series-connected NPC converter through a series coupling transformer provides for voltage compensation through appropriate voltage injection. The two converters are linked by a DC Link which maintains power balance. The ANN-based control keeps optimizing UPQC performance by instantaneously modifying its operation in instances of disturbances. The system contains two Points of Common Coupling (PCC1 and PCC2) where PCC1 connecting the main supply of the electrical grid and PCC2 feeds linear and nonlinear loads, an ESS-PV providing integrated renewable energy by means of a converter, besides assisting voltage stability and power factor enhancement. Shunt and series connection to form the UPQC utilizing NPC converter is shown in figure 3.11.

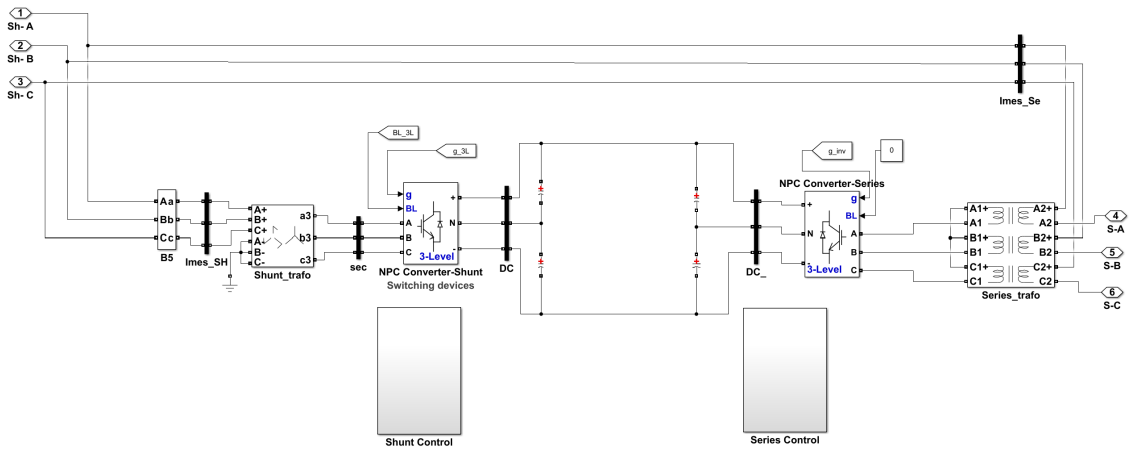

Figure 3.11: MATLAB Model of UPQC with NPC converter

A NPC converter serves in the UPQC system for series and shunt compensation. The NPC topology has a common DC link and, since the voltage across each switching device is half of the DC-link voltage, this reduces voltage stress and increases reliability. The three-level converter can withstand larger voltage levels and has lower switching losses than traditional two-level converters. The three level NPC converter topology is shown in figure 3.12 through MATLAB blocks.

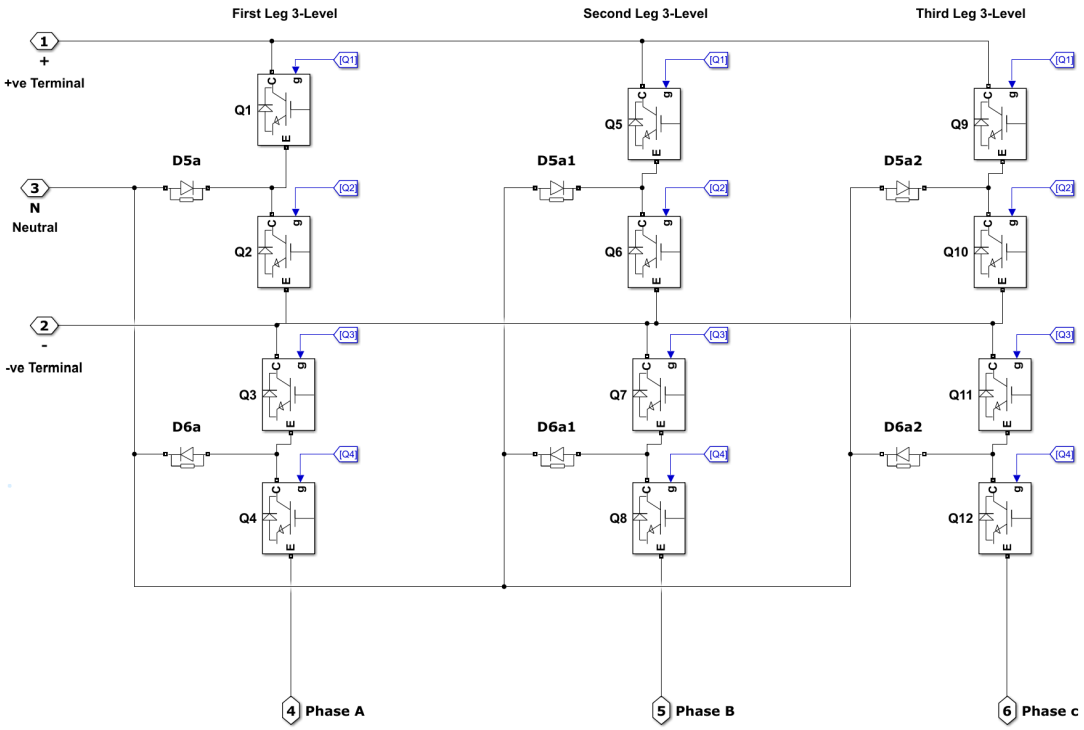

Figure 3.12: Three Level NPC converter circuit

The ANN model is generated using the Neural Fitting Tool (nftool) of the MATLAB using Levenberg-Marquardt backpropagation(LMBP) for training and hence gives great convergence and accuracy because it uses the approximation of the Hessian matrix instead of simple gradient descent.

By minimizing MSE, such an ANN-based controller brings in power quality, adaptability, and robustness in UPQC applications. Unlike traditional controllers, ANNs learn nonlinear system behavior and offer self-learning capabilities and substantially improved stability under disturbances with greater speed of the dynamic response and very efficient real-time implementation for superior power compensation.

Error Minimization:) The Mean Squared Error (MSE) is given by:

$$MSE = \frac{1}{N}\sum_{k=1}^{N}(T_k - O_k)^2 \tag{3.14}$$

where:

- T_k is the target output

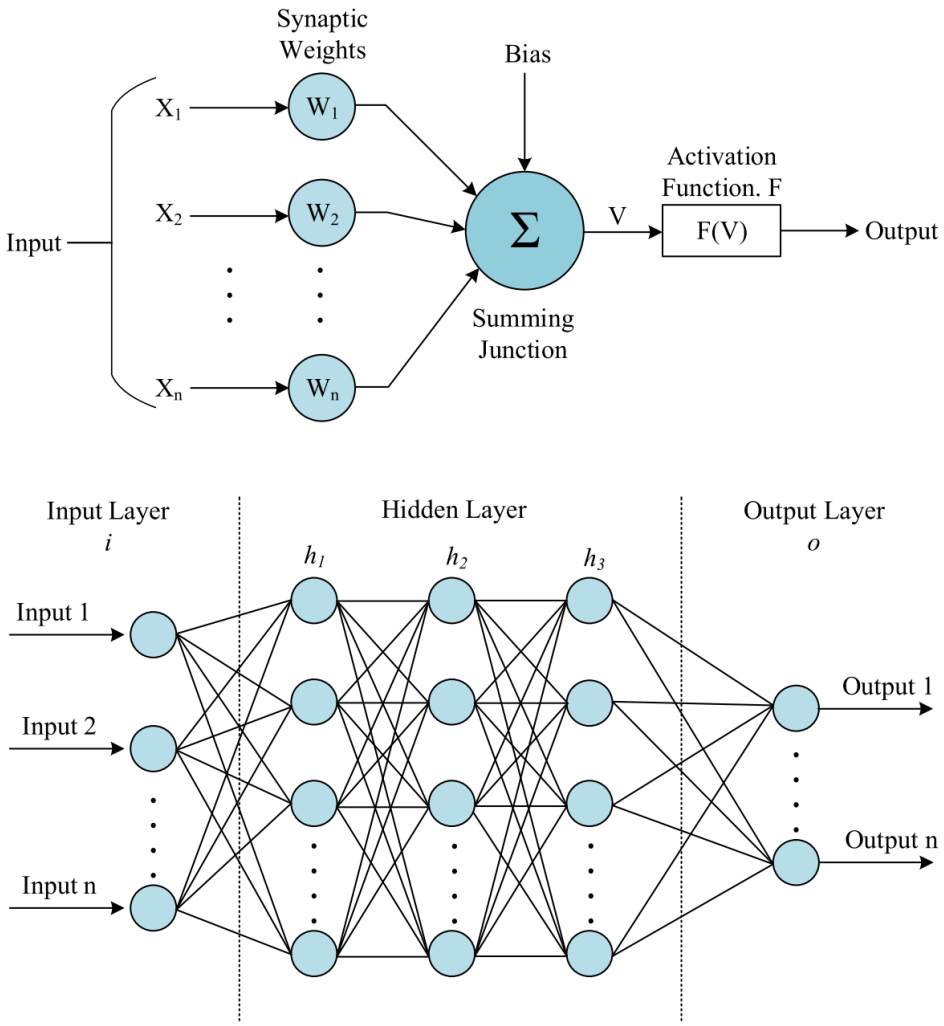

Figure 3.13: Basic ANN Structure.

- O_k is the ANN output
- N is the number of training samples

Weight Update Rule The weight update using gradient descent is:

$$W_{ij}(t+1) = W_{ij}(t) - \eta \frac{\partial MSE}{\partial W_{ij}} \tag{3.15}$$

where:

- $W_{ij}(t+1)$ is the updated weight

- $\frac{\partial MSE}{\partial W_{ij}}$ is the gradient of the error function
- η is the learning rate

3.4.1 NPC Shunt Inverter Control

The load currents i_{La}, i_{Lb}, i_{Lc} are transformed into the $dq0$ frame using Park's transformation:

$$\begin{bmatrix} i_d \\ i_q \\ i_0 \end{bmatrix} = \frac{2}{3} \begin{bmatrix} \cos\theta & \cos(\theta - 120°) & \cos(\theta + 120°) \\ \sin\theta & \sin(\theta - 120°) & \sin(\theta + 120°) \\ \frac{1}{2} & \frac{1}{2} & \frac{1}{2} \end{bmatrix} \begin{bmatrix} i_{La} \\ i_{Lb} \\ i_{Lc} \end{bmatrix} \tag{3.16}$$

The low-pass filter (LPF) removes oscillating components in i_d and i_q. The compensating current reference is generated:

$$i_{dsh} = i_d - i_{dref}, \quad i_{qsh} = i_q - i_{qref} \tag{3.17}$$

The reference current is then computed and converted back to the abc frame using inverse Park transformation:

$$\begin{bmatrix} i_a^{sh} \\ i_b^{sh} \\ i_c^{sh} \end{bmatrix} = \begin{bmatrix} \cos\theta & \sin\theta & 1 \\ \cos(\theta - 120°) & \sin(\theta - 120°) & 1 \\ \cos(\theta + 120°) & \sin(\theta + 120°) & 1 \end{bmatrix} \begin{bmatrix} i_d^{sh} \\ i_q^{sh} \\ i_0^{sh} \end{bmatrix} \tag{3.18}$$

The Voltage Source Inverter (VSI) injects the compensatory current using switching pulses produced by the hysteresis current controller. The shunt inverter regulates DC-link voltage

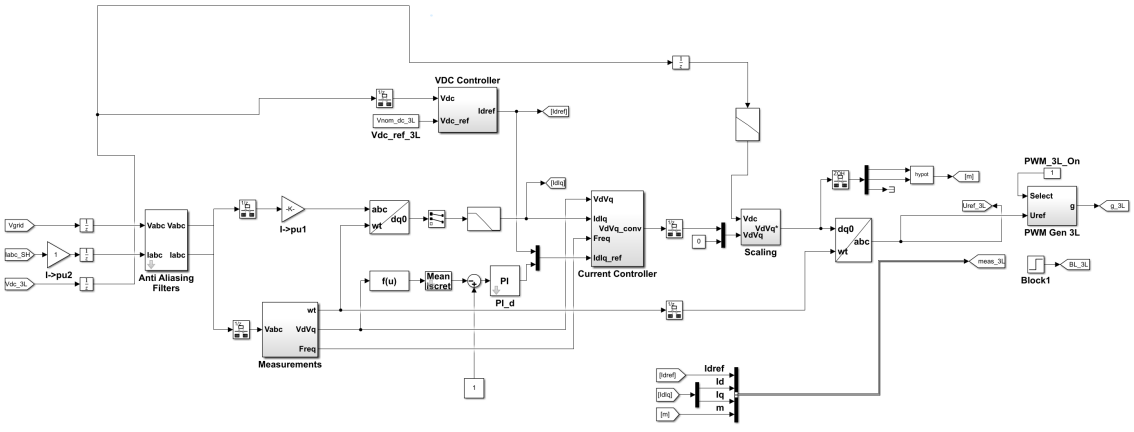

Figure 3.14: MATLAB model of NPC shunt controller

and compensates for reactive power and current harmonics using an ANN-based control strategy. Similarly, the voltage v_a, v_b, v_c are transformed into the $dq0$ frame using Park's

transformation for the phase synchronization. MATLAB model of Shunt NPC converter is shown in figure 3.11.

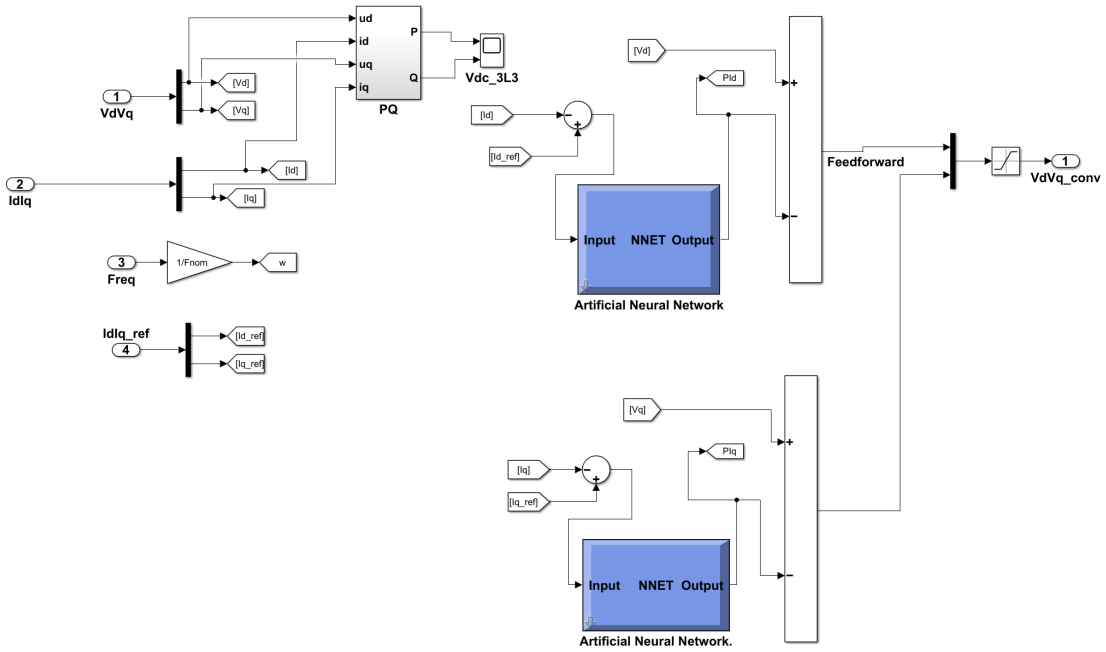

Figure 3.15: MATLAB model of current controller of shunt controller

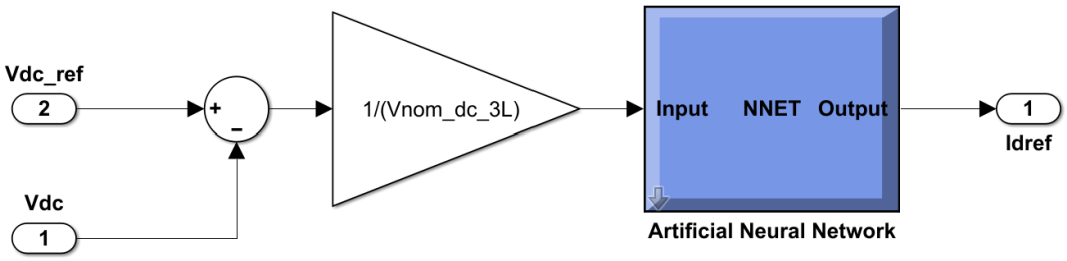

Figure 3.16: MATLAB model of voltage controller of shunt controller

Inputs to ANN:

- DC-link voltage error:

$$e_{vdc}(t) = V_{dc,ref} - V_{dc} \tag{3.19}$$

- Change in DC-link voltage error:

$$\Delta e_{vdc}(t) = e_{vdc}(t) - e_{vdc}(t-1) \tag{3.20}$$

- Load current components in dq-frame:

$$i_{Ld}, i_{Lq} \tag{3.21}$$

ANN Output:

- Reference currents for the shunt inverter:

$$i^*_{shd}, i^*_{shq} = f_{ANN}(e_{vdc}, \Delta e_{vdc}, i_{Ld}, i_{Lq}) \tag{3.22}$$

These reference currents are converted to the abc-frame and controlled using hysteresis current control to generate switching pulses for the inverter. The shunt controller injects current to compensate for power disturbances:

$$I_{inj} = I_{ref} - I_{sensed} \tag{3.23}$$

where:

- I_{inj} is the injected current
- I_{ref} is the reference current from ANN
- I_{sensed} is the measured system current

3.4.2 NPC Series Inverter Control

The reference voltage is extracted using the SRF theory: Convert supply voltage V_s to $dq0$ frame:

$$\begin{bmatrix} V_d \\ V_q \\ V_0 \end{bmatrix} = \frac{2}{3} \begin{bmatrix} \cos\theta & \cos(\theta - 120^\circ) & \cos(\theta + 120^\circ) \\ \sin\theta & \sin(\theta - 120^\circ) & \sin(\theta + 120^\circ) \\ \frac{1}{2} & \frac{1}{2} & \frac{1}{2} \end{bmatrix} \begin{bmatrix} V_{sa} \\ V_{sb} \\ V_{sc} \end{bmatrix} \tag{3.24}$$

The oscillating components in V_d and V_q are removed using an LPF. The reference voltage is calculated:

$$V_{ds} = V_d - V_{dref}, \quad V_{qs} = V_q - V_{qref} \tag{3.25}$$

The compensatory voltage is computed and returned to the ABC frame after filtering. Similarly,it converts the source current i_{sa}, i_{sb}, i_{sc} are transformed into the $dq0$ which is used for the power computation and system synchronization. The gate pulses for the series inverter are produced using a Sinusoidal Pulse Width Modulation (SPWM) approach. The series inverter compensates for voltage sags/swells by injecting appropriate voltage using an ANN-based controller.

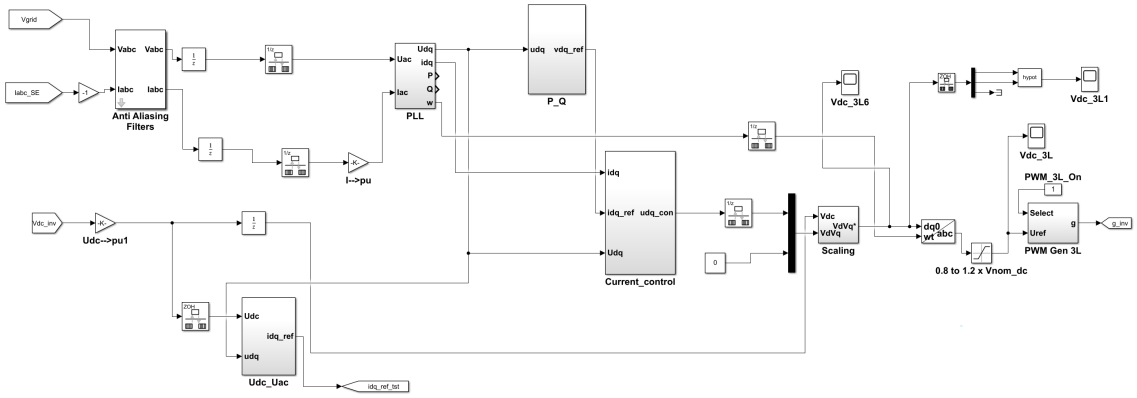

Figure 3.17: MATLAB model of NPC series controller

Inputs to ANN:

- Voltage error:

$$e_{vs}(t) = V_{s,ref} - V_s \tag{3.26}$$

- Change in voltage error:

$$\Delta e_{vs}(t) = e_{vs}(t) - e_{vs}(t-1) \tag{3.27}$$

- Supply voltage dq-components:

$$v_{sd}, v_{sq} \tag{3.28}$$

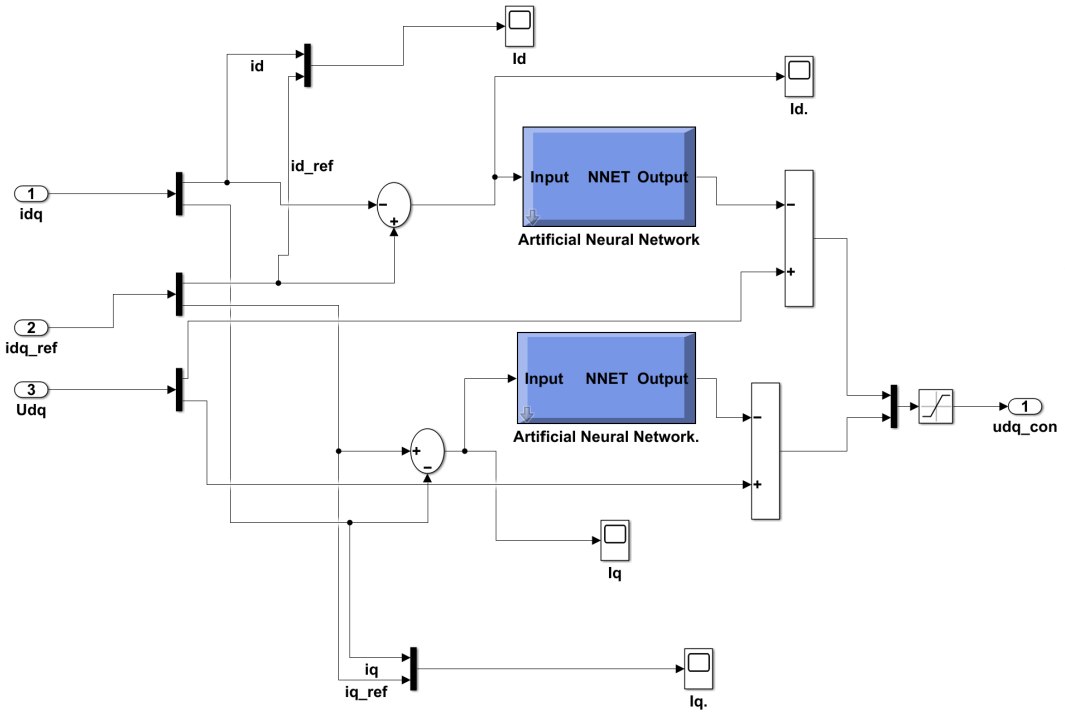

Figure 3.18: MATLAB model of voltage controller of series controller

ANN Output:

- Reference voltage signals for the series inverter:

$$v_{sd}^{*}, v_{sq}^{*} = f_{ANN}(e_{vs}, \Delta e_{vs}, v_{sd}, v_{sq}) \tag{3.29}$$

These reference voltages are converted to the abc-frame and used for PWM-based voltage injection . The series controller injects voltage to maintain system stability:

$$V_{inj} = V_{ref} - V_{sensed} \tag{3.30}$$

where:

- V_{inj} is the injected voltage
- V_{ref} is the reference voltage from ANN
- V_{sensed} is the measured system voltage

3.5 Real Test system

The real system setup is taken from Cesar Apartment, located in Lalitpur, Nepal, which receive its power supply from the Teku Feeder of 11 kV distribution network. The real workiing conditions have harmonic disturbances from the equivalent non linear loads and inverter based generation. Cesa Apartment, lalitpur is connected to three-phase grid with a 250kVA transformer of 11/0.4 kV L-L with PV-ESS, through a phase inverter. The AC L-L voltage is 400 V at load side, and the frequency is kept constant at 50 Hz. In the study,In Cesar Apartment PV system consists of N-type i-TOPCon Bifacial dual glass monocrystalline modules connected with 16 series-connected modules per string and 8 mppt parallel strings for efficient power. The solar photovoltaic system of approximately

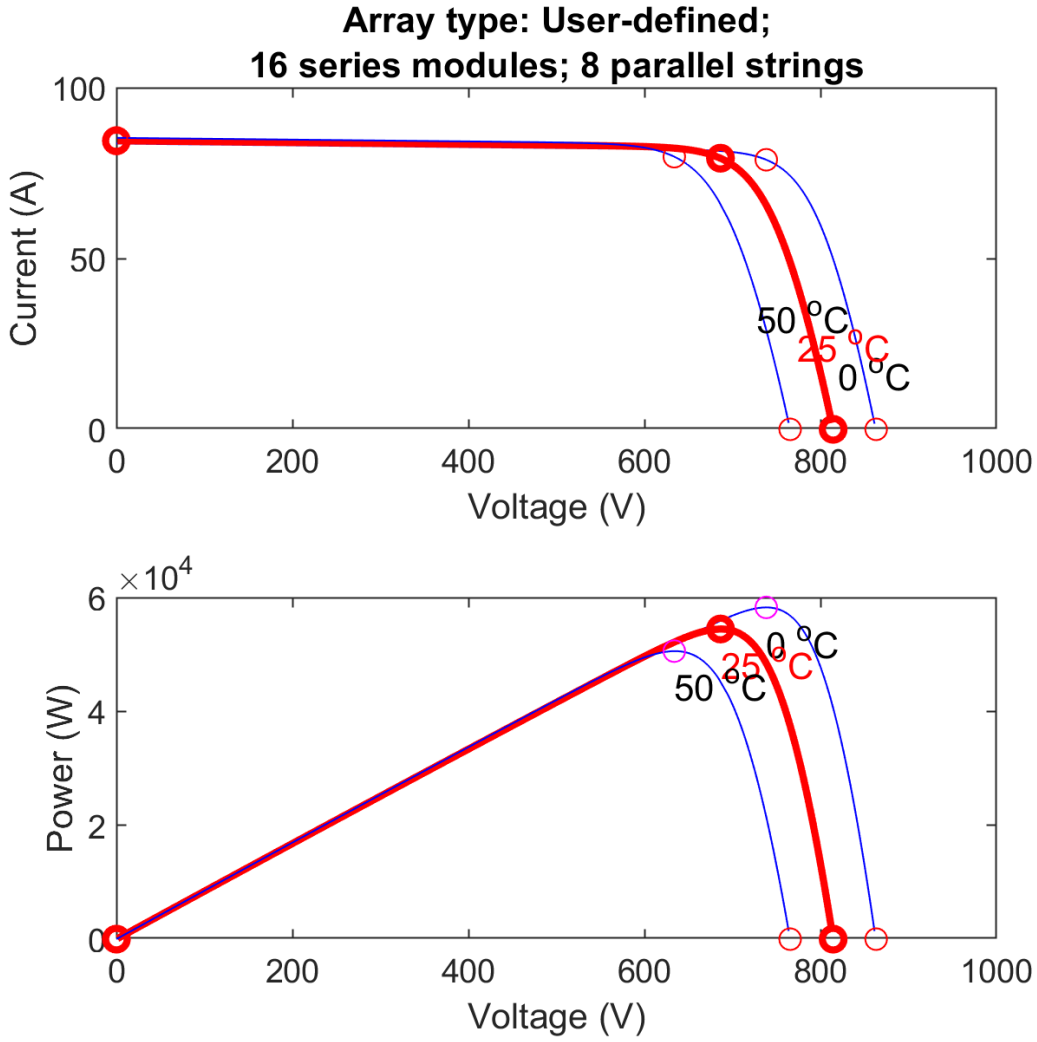

Figure 3.19: Real test system PV I-V and P-V characteristics

54.4 kW uses an open circuit voltage (Voc) equal to 50.9 V, a short circuit current (Isc) 10.56 A, a MPP voltage (Vmp) is 42.9 V and MPP current (Imp) is 9.93 A under STC

conditions. The graph for all of this input data is shown in figure 3.19. The energy storage system which is AC-Coupled with the grid and PV, comprises of LiFePO batteries having a total nominal capacity of 210.6 kWh, made up of 36 modules, rated at 48 V, in 9-series and 4-parallel (9S4P) configuration to satisfy the system's voltage and capacity specifications. The system's nominal voltage is 432 V; the rated capacity is 462.96 Ah. Every battery is rated 200 kWh (0.5C rate of discharge) and energy calculations typically include round-trip efficiency, its battery discharge characteristic is shown in figure 3.20. The system is paired with an AI-driven Energy Management System (EMS) by Swanbarton, that adaptively adjusts charge-discharge cycles, dispatches energy, and reduces losses using predictive and real-time controls. Our system also utilizes a Fuzzy Logic Controller (FLC) to provide a more adaptive and more efficient energy management system. This

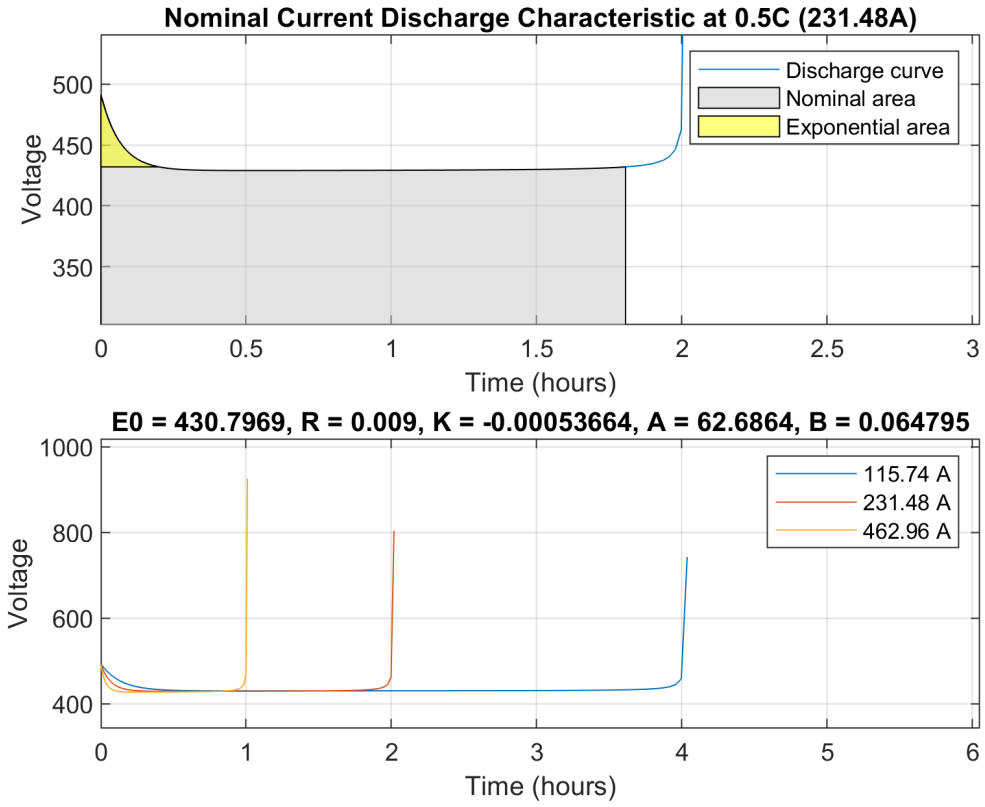

Figure 3.20: Real test system battery discharge characteristics

real system now utilizes the FUZZY as MPPT to exract PV and FLC controller in ESS and whole system utilizes the proposed UPQC model to mitigate power quality issues. MATLAB model of real system is shown is figure 3.21.

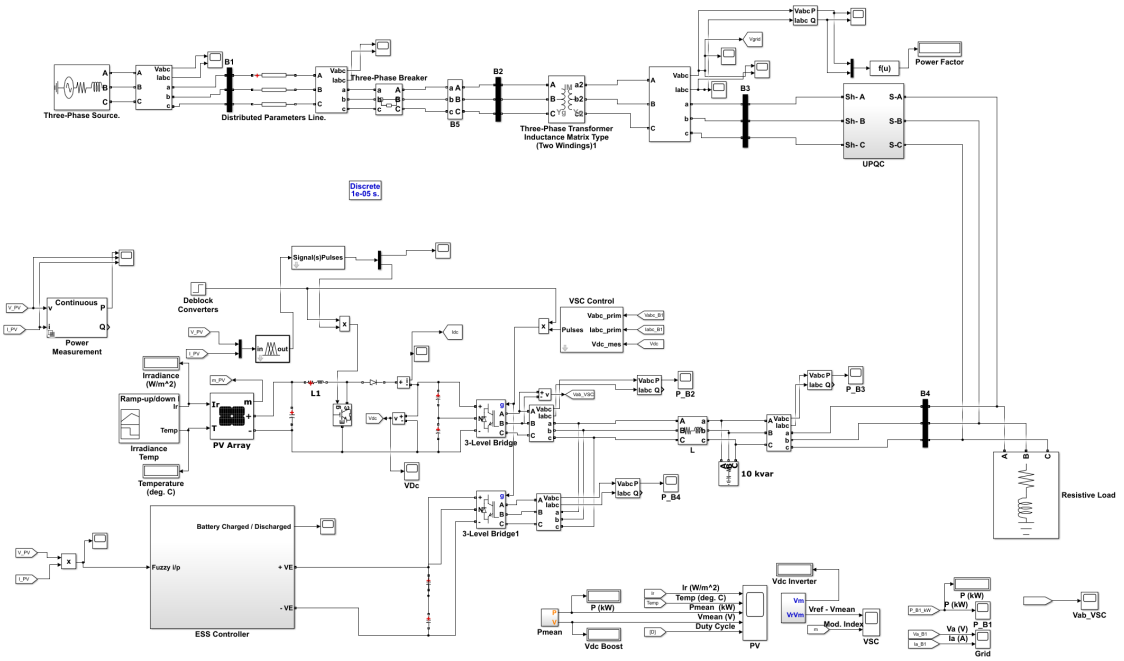

Figure 3.21: MATLAB Model of Real System

3.6 Tools and Software

This section lists the tools and software used in this dissertation.

3.6.1 Microsoft Office

Microsoft Office comprises a suite of software applications created by Microsoft, including a word processing program (Word), a spreadsheet application (Excel), and a presentation software (PowerPoint), among other tools. In this dissertation, Word is utilized for initial report drafting, while Excel is employed for storing the extracted features.

3.6.2 Matlab

Matlab is a software platform for programming, and numerical computing, created by MathWorks. In this research, Matlab simulink is used to create model and all data are extract from simulation results. Nftool is used for train and test the data for ANN.

3.6.3 Overleaf

Overleaf is an innovative online platform and LaTeX editor designed specifically for academics, researchers, and professionals involved in scientific writing and publishing. Overleaf provides a collaborative environment where users can create, edit, and manage LaTeX

documents seamlessly, without the need for local LaTeX installations or complex setup. It offers LaTeX templates from various reputable journals. In this dissertation, overleaf is used for preparing the reports.

CHAPTER FOUR: RESULTS AND DISCUSSION

This chapter presents the results obtained using the methodology described in Chapter 3.

4.1 Proposed Model

In this section, we describe the simulation results and analysis of a PV-ESS system proposed with FUZZY MPPT to extract solar energy & FLC in ESS for power management, ANN Tuned UPQC and NPC as series and shunt converter. The performance of the system was tested under different fault conditions, including steady-state operation, dynamic disturbances, and power quality analysis. Some overview of data and concept of project are shown table below.

Table 4.1: System Components and Specifications

Category	Component	Specifications/Details
Power Source & Grid	Three-phase YG Source	11kV (L-L), 50 Hz
	Transmission Line	Distributed parameter, 100 km
	Step-down Transformer	11kV $\rightarrow$ 0.4kV (L-L)
	Swing Bus	100 kW power
Renewable Energy & Storage	PV System	60 kW, 1kW/m^2, 25°C, Fuzzy MPPT
	Battery Storage	30Ah, Charge/Discharge Control
	ESS	Fuzzy-based controller, Manages power flow
Power Electronics	Buck-Boost Converter	MOSFETs, IGBTs, Fuzzy Logic Control
	NPC Converter	PI/ANN Controller
Loads	Linear Grid Load	30 kW Resistive
	Nonlinear Load	100 kW (Diode Bridge + RLC)
Power Quality & Control	UPQC	Voltage Regulation & Harmonic Mitigation
	Shunt Inverter (NPC)	Current Compensation
	Series Inverter (NPC)	Voltage Sag/Swells Compensation
Control Strategies	MPPT	Fuzzy Logic
	PI/ANN Controller	NPC Converter

4.1.1 Solar PV MPPT

PV system consists of First Solar FS-272 modules connected with 26 series-connected modules per string and 33 parallel strings for efficient power. Each module comprises 116 cells and has Open-Circuit Voltage(Voc) equal to 94.57 V, Short-Circuit Current(Isc) 1.18 A, MPP Voltage(Vmp) 70.56 V, and MPPt Current(Imp) 1.01 A under STC conditions. The performance of the photovoltaic (PV) system was analyzed in two scenarios: the

first in an optimal condition without MPPT and the second using MPPT control based on FUZZY logic. Figures 4.1 show the I-V and P-V characteristics of the PV array at 25°C for different levels of irradiance: 1 kW/m², 0.75 kW/m², 0.5 kW/m², and 0.25 kW/m². With decreasing irradiance, one expects a drop in the amount of energy that the PV array could generate; conversely, higher irradiance allows for more power and current to be output. Each irradiance level shows a maximum power point (MPP) within the power-voltage characteristics, which explains the need for good tracking algorithms for MPPT that provide for good extraction of power. From the graph, Figure 4.1. , the Maximum

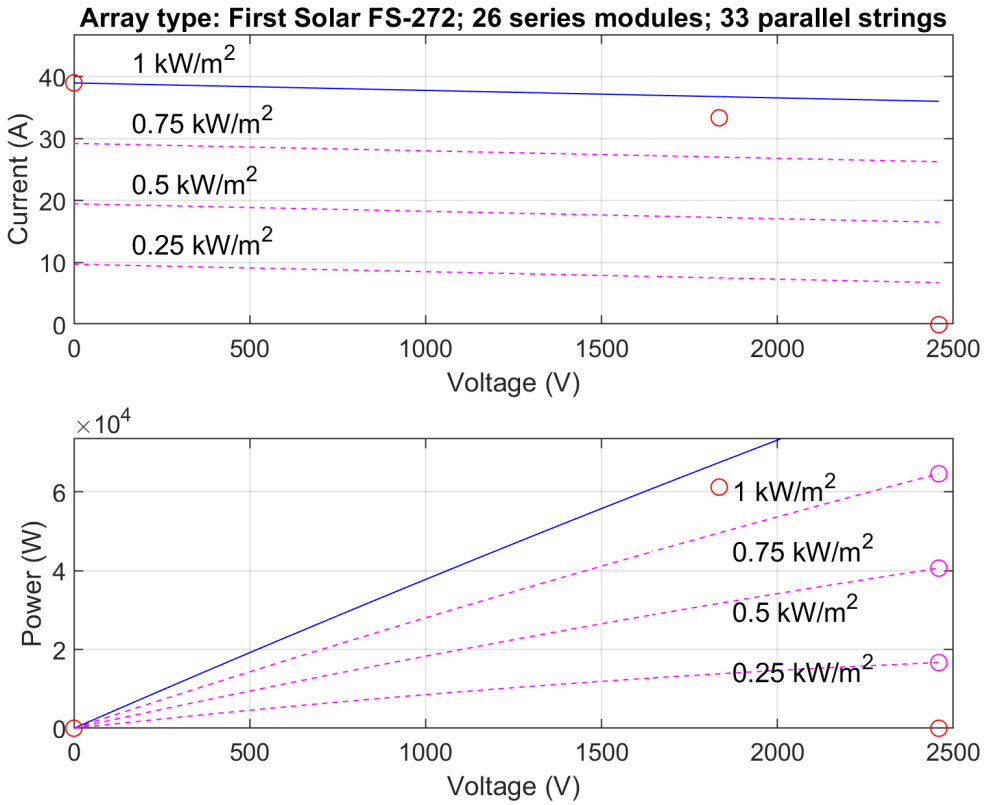

Figure 4.1: I-V and P-V Characteristics of array at 25 deg.c

Power Point (MPP) occurs at 1 kW/m² of irradiation, with a voltage of approx. 1750-1850 V and current somewhere 30-35 A. Thus,maximum power output of 60KW can achieved at ideal case. As irradiance declines, parameters such as current and power drop proportionately, affecting energy generation overall.

AFter using FUZZY as MPPT, the simulation results indicate that, the PV system has reached a stable maximum output of approx 57.5 kW with a corresponding voltage of approx. 1800 v and a current of approx. 32 A with efficiency of nearly 96%.The fuzzy MPPT realizes definitely smooth-and-fast tracking, having its stability under variable-irradiance

conditions assisted by the extra prowess in handling nonlinear and uncertainty conditions that real-world applications with constantly changing irradiance levels impose upon it. Fast and smooth tracking response with negligible oscillations is a considerable advantage of fuzzy MPPT for actual PV applications. Therefore, this approach is extremely reliable, adaptive, and efficient for enhanced performance. Such an MPPT implementation functionally becomes the preferred choice to improve PV systems over older techniques. The system is fast and smooth in tracking with minimum oscillations as shown in figure 4.2.

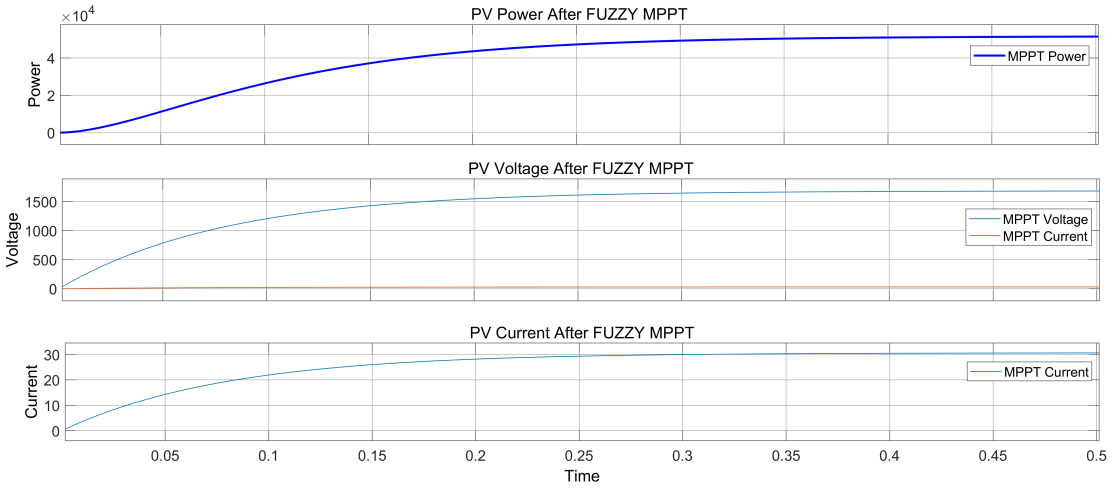

Figure 4.2: Power,Voltage, Current Plot After FUZZY MPPT

4.1.2 Energy Storage System

A key aspect of the system would involve the use of Fuzzy Logic Control for the ESS with real-time dynamic adjustment of power flows, as shown in Figure 4.5. Further, based on the fuzzy-based control approach, the fluctuations in current flow are maintained within limits to achieve uninterrupted power feeding into the system. This prevents abrupt extraction of the stored energy and helps with energy sharing among the photovoltaic system and the battery, and load. This resulted in the system's more stable performance, power quality, and efficiency, rendering it very effective in real-time applications for both grid-connected and islanded mode.

The SOC was in slow decline 4.4, which indicates that controlled discharge would take place, which also stabilizes the current over a time allowing smooth power transfer. With proper Fuzzy Logic control in EES, better performance will be achieved on the grounds that power flow adjustment would be dynamic against real-time operating conditions.

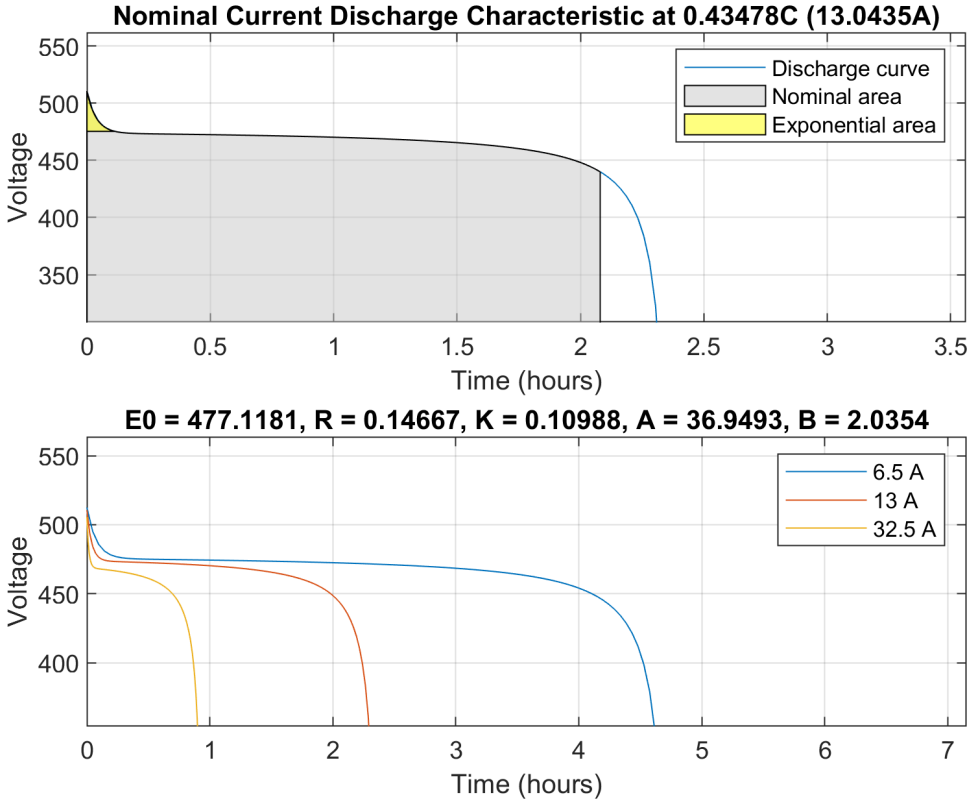

Figure 4.3: Ideal Characteristics of Battery

Figure 4.5 depicts the ESS's power dynamics, showing its ability to charge (positive values) and discharge (negative values) over a time period from 0 to 1 unit. The ESS balances energy from both the grid and PV system, storing excess energy during high supply and supplying energy during high demand. Specific intervals highlight fault conditions: from 0.2 to 0.4, the ESS responds to an L-G fault by discharging to stabilize the grid, and from 0.6 to 0.8, it addresses an L-L-L-G fault by discharging at a higher rate to maintain stability. These results demonstrate the ESS's critical role in managing power fluctuations and enhancing grid resilience during disturbances.

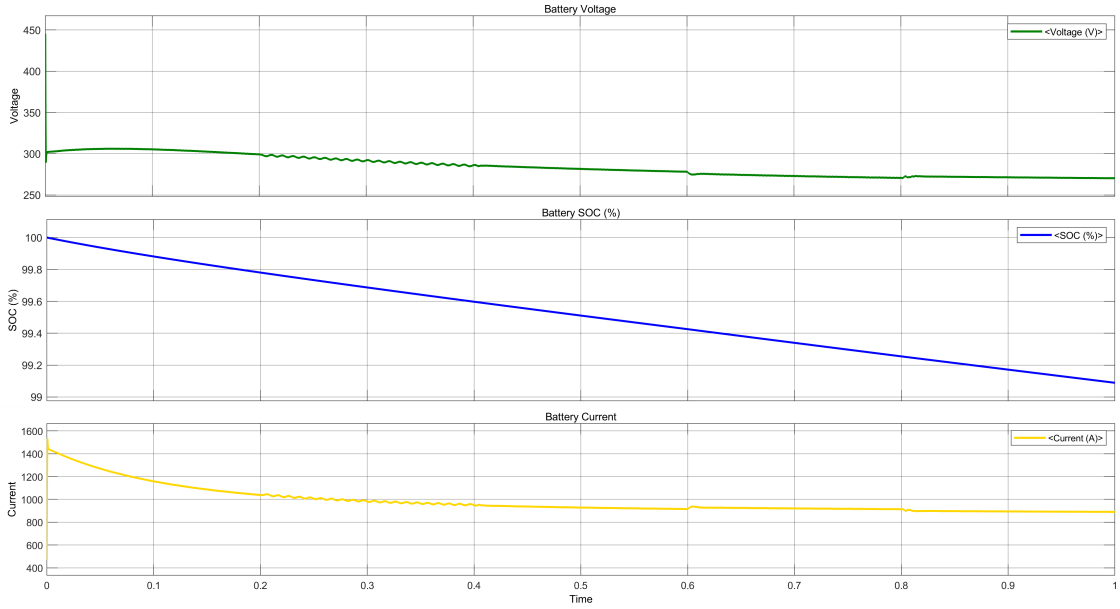

Figure 4.4: Energy Storage System Voltage, SOC %, Current

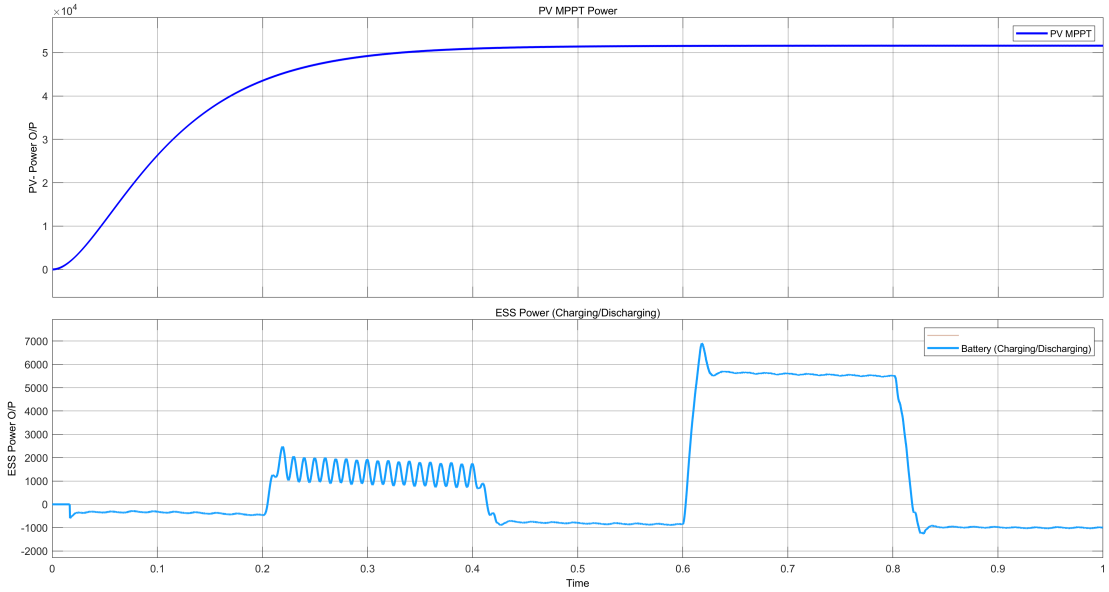

Figure 4.5: PV-MPPT Power and Charging/Discharging Power of ESS

Figure 4.6, focuses specifically on the charging power of the ESS. The graph shows the power being transferred to the battery over time, with the ESS power values ranging from 0 to -1500 units. The negative values indicate that power is being absorbed by the ESS for charging. The plot demonstrates how the ESS charges at varying rates depending on the available power from the grid and the demand.

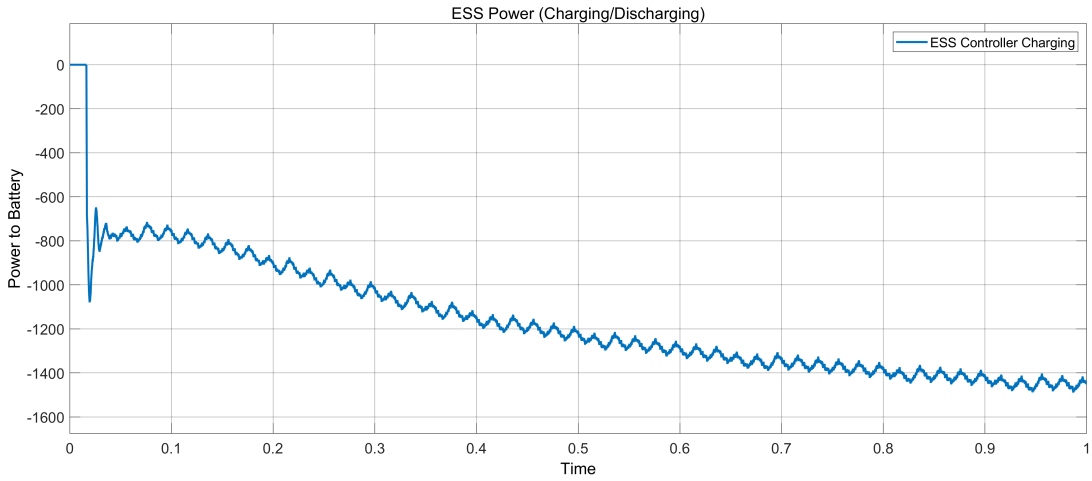

Figure 4.6: Charging Power Plot of ESS

Figure 4.7 depicts the discharging power of the ESS. Here, the ESS power values are positive, indicating that the ESS is supplying power to the grid or load. The graph shows the power output from the ESS over the same time period, with values ranging initially at 11 kW to stable 8 kW units. This plot highlights the ESS's role in providing energy when the grid's supply is insufficient to meet demand

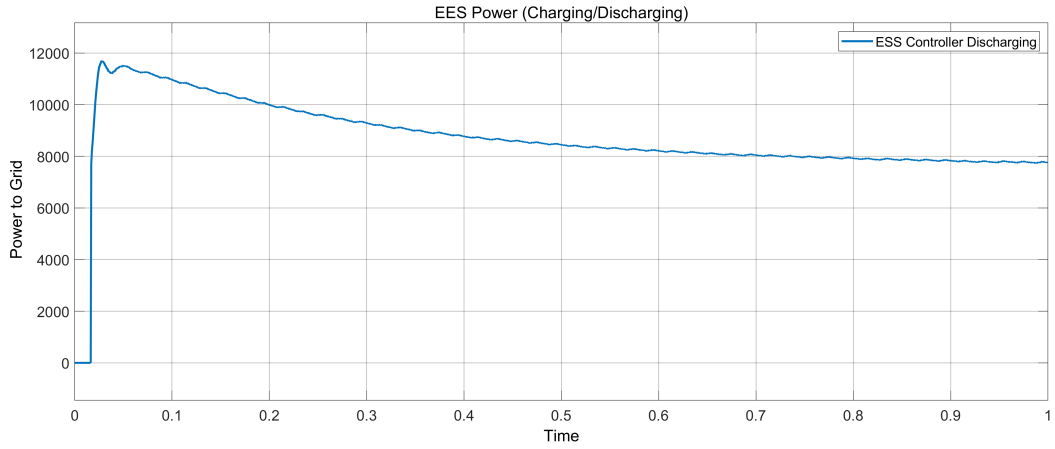

Figure 4.7: Discharging Power Plot of ESS

4.1.3 Analysis Of Grid Before Using UPQC

In this part, we are going to just Overview of System in different type of Load and Source Scenario.

Grid With Source and Resistive Load Only

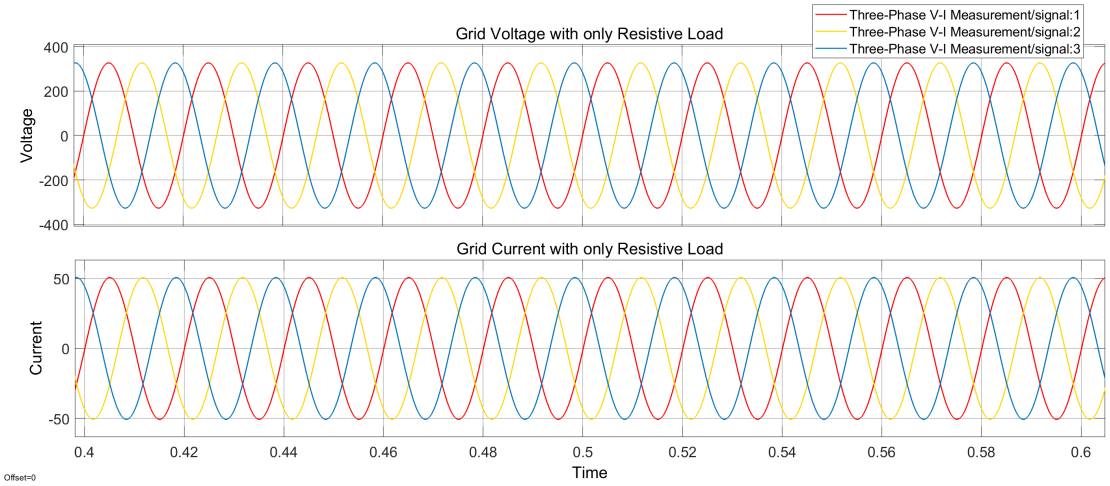

Figure 4.8: Grid V-I Waveform with Only Resistive load

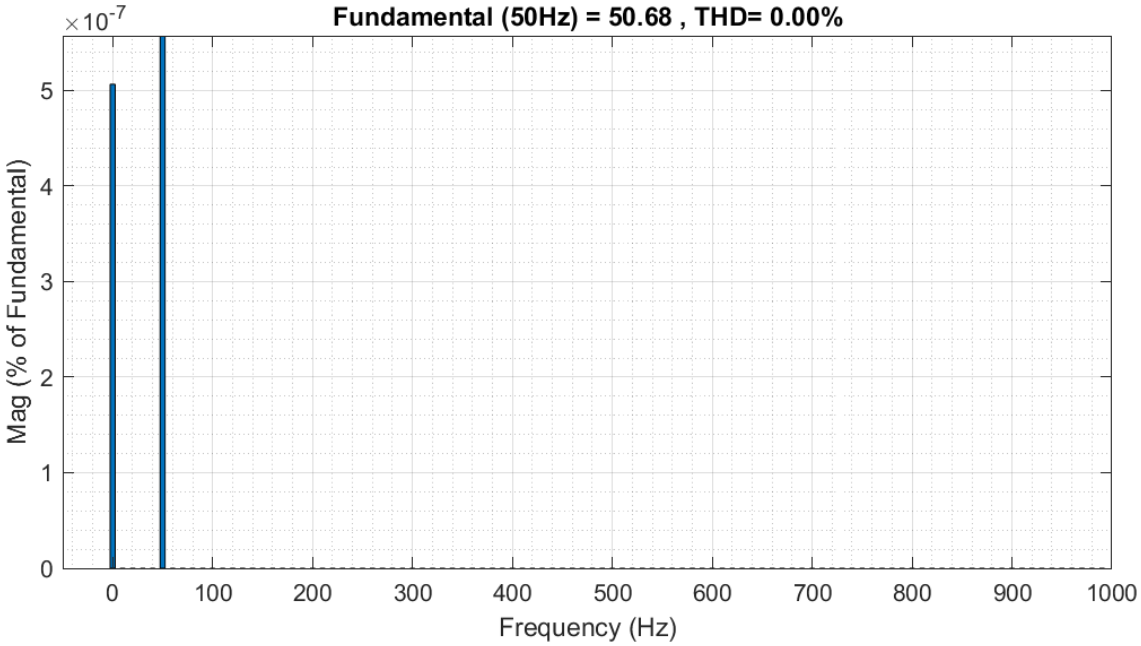

Figure 4.9: FFT of measured current signal at only Resistive Load

Grid with Resistive and Non-Linear Load

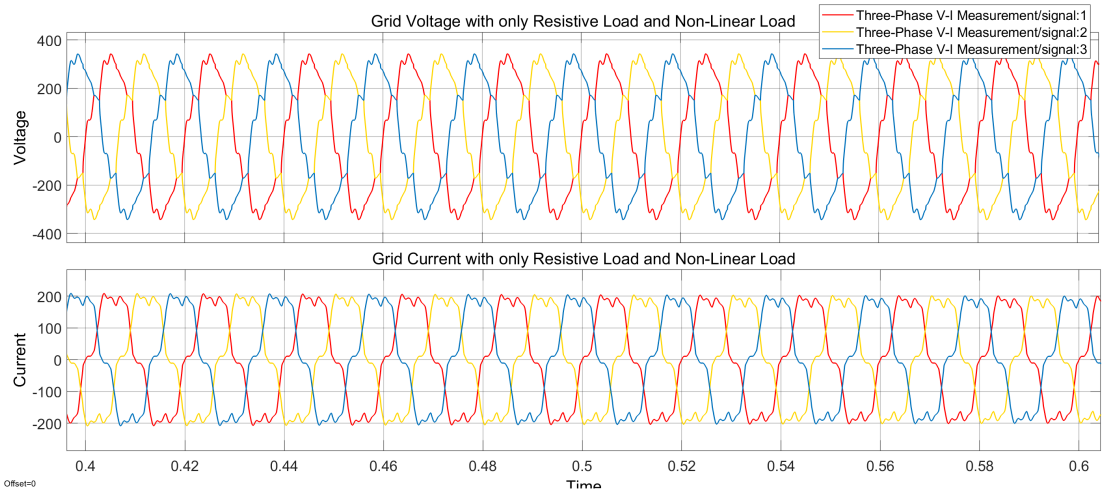

Figure 4.10: Grid V-I Waveform with Resistive and Non-Linear load

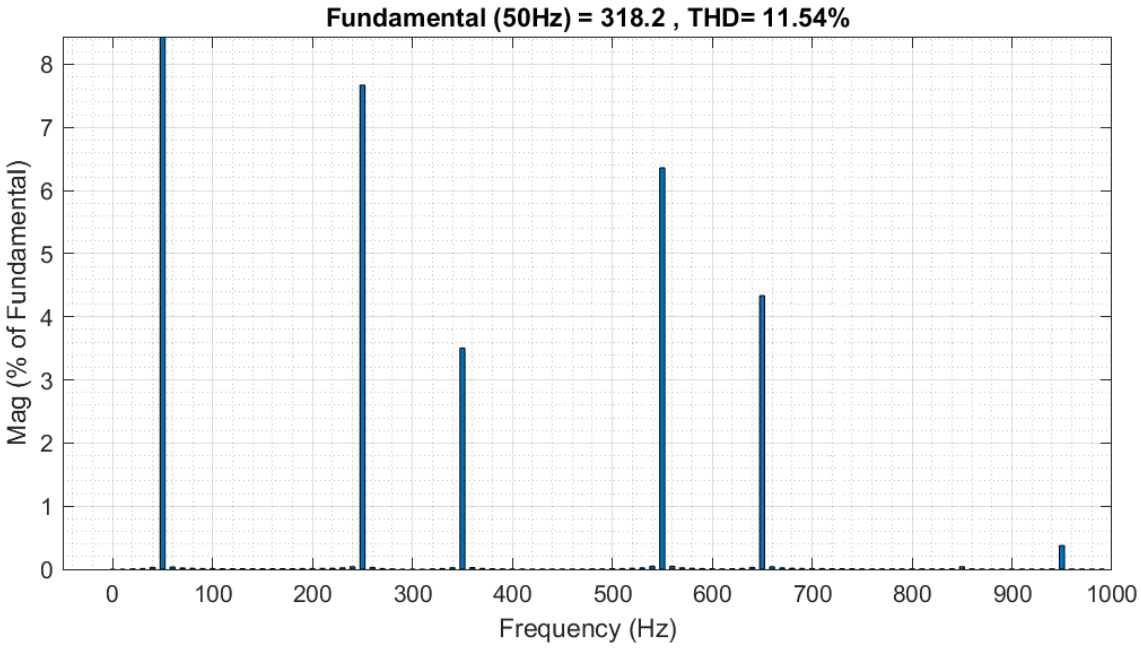

Figure 4.11: FFT of measured Voltage signal at Resistive and Non-Linear Load

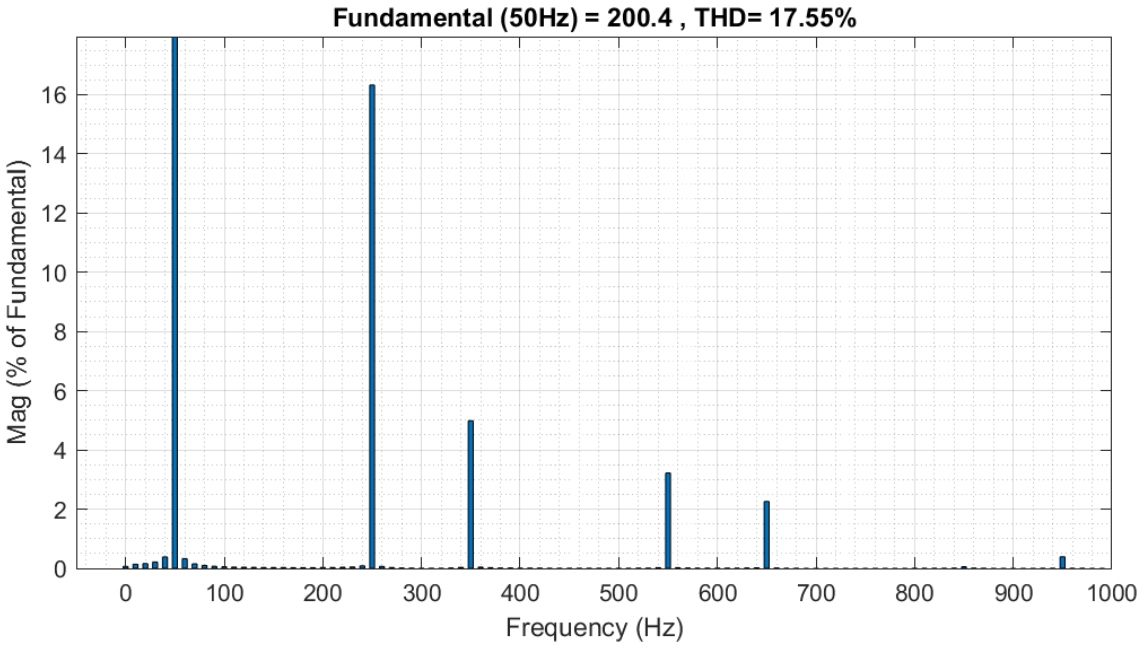

Figure 4.12: FFT of measured Current signal at Resistive and Non-Linear Load

Grid with PV-ESS,Fault, Resistive and Non-Linear Load

Before inserting the UPQC, such waveforms of grid voltage and current are immensely distorted, coming from nonlinear loads, PV-ESS integration, and fault conditions. The overall system waveform 4.13 shows irrefutable irregular voltage and current variations, indicating poor power quality. When introducing the PV-ESS, faults, and nonlinear loads 4.14, the distortion encountered has incremented, with greater harmonic content, voltage sags, and swells intensity. Evidence of voltage unbalance, radial current, and consequent possible overload in some phases is observed under an L-G fault 4.15. The most severe loss occurs in the three-phase fault case (L-L-L-G) 4.16, where huge voltage drops and highly disproportionate current waveforms attack the system to the point of almost total collapse. This makes a number of calls to implement a compensation mechanism like UPQC, with its features of harmonics cancellation, good voltage regulation, and overall stability improvement of the system.

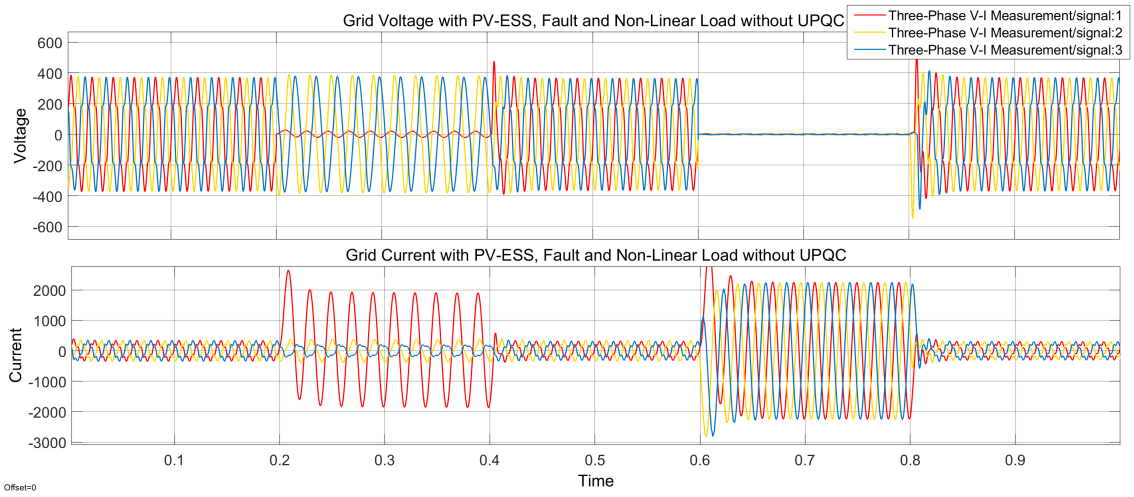

Figure 4.13: Grid V-I Waveform of Overall system without UPQC

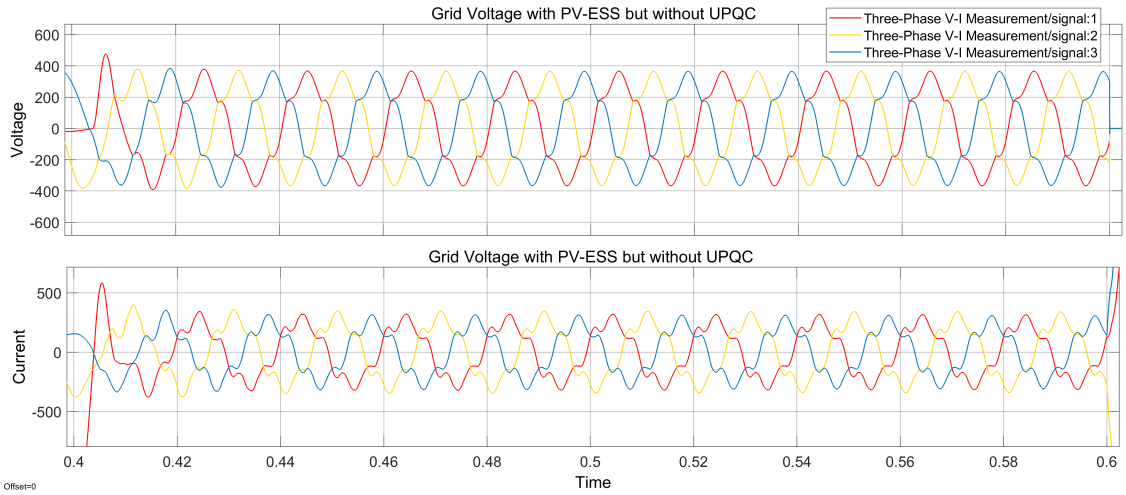

Figure 4.14: Grid V-I Waveform with PV-ESS, Fault and Non-Linear load but without UPQC

All these Figures (without UPQC), severe voltage and current distortion are observed, especially in current waveform. During an L-G fault at (0.2s-0.4s), the voltage experiences uneven peaks and a faulted phase (signal 1) drops to nearly zero and voltage swell occurs in remaing phase, while the current surges from approx. 250A to 2000A, marking 8 times/800% increase. Similarly, during L-L-L-G fault at (0.6s-0.8s) , the voltage collapses to nearly zero and the current spikes to approx.. 2200A i.e. 9 times/900% increases, indicating extreme instability.

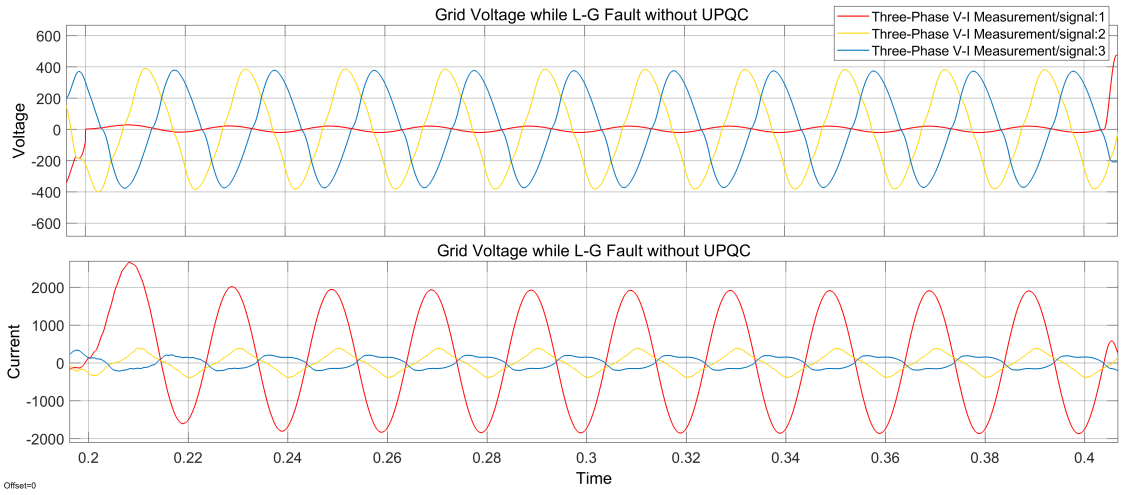

Figure 4.15: Grid V-I Waveform with L-G fault but without UPQC

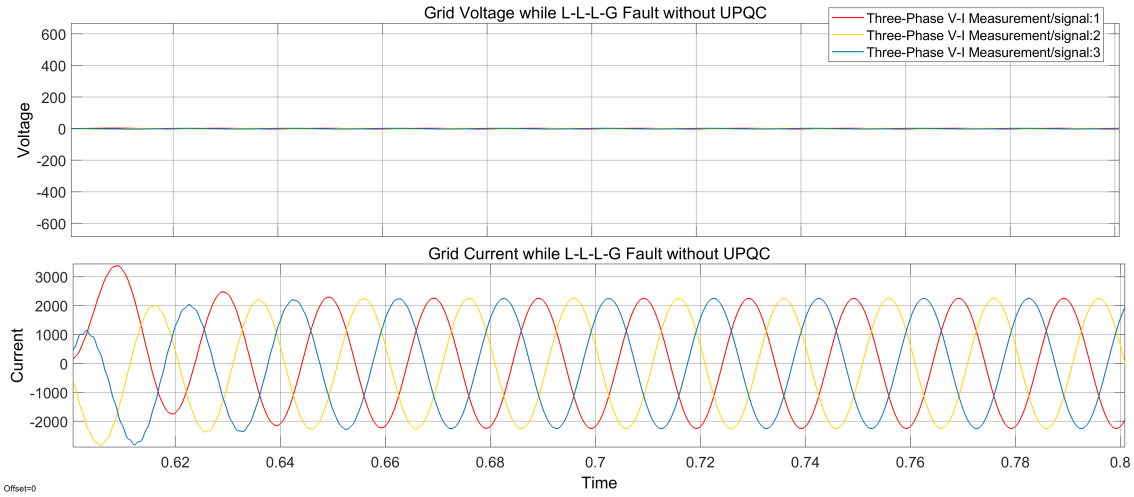

Figure 4.16: Grid V-I Waveform with L-L-L-G fault but without UPQC

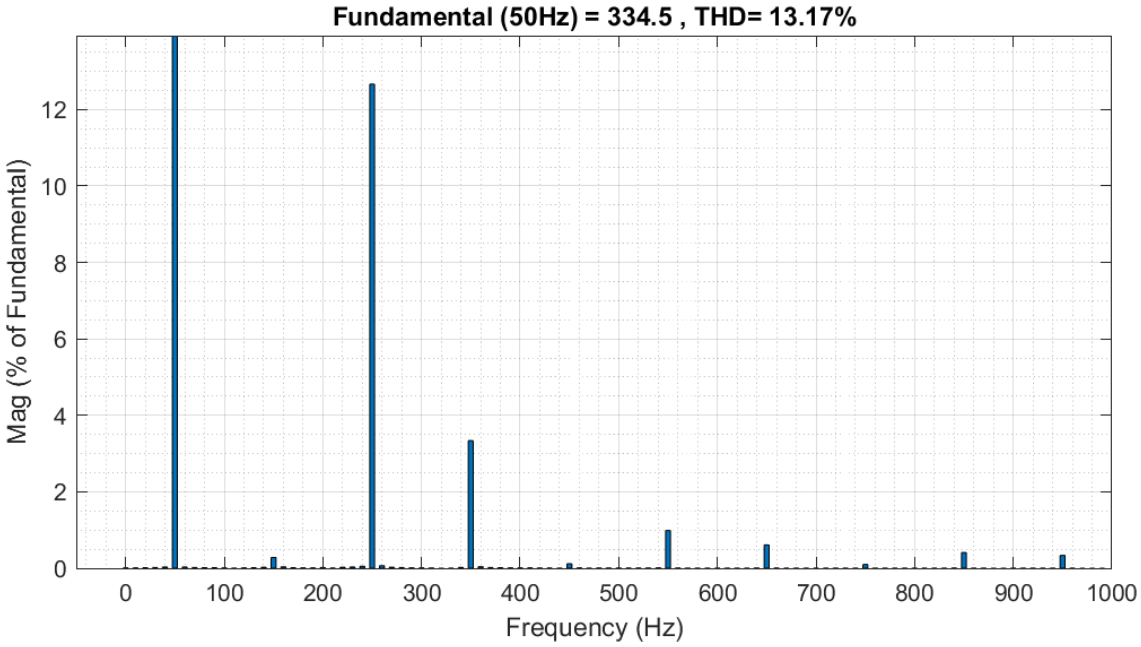

Figure 4.17: FFT of measured Voltage signal with PV-ESS and Non-Linear Load but without UPQC

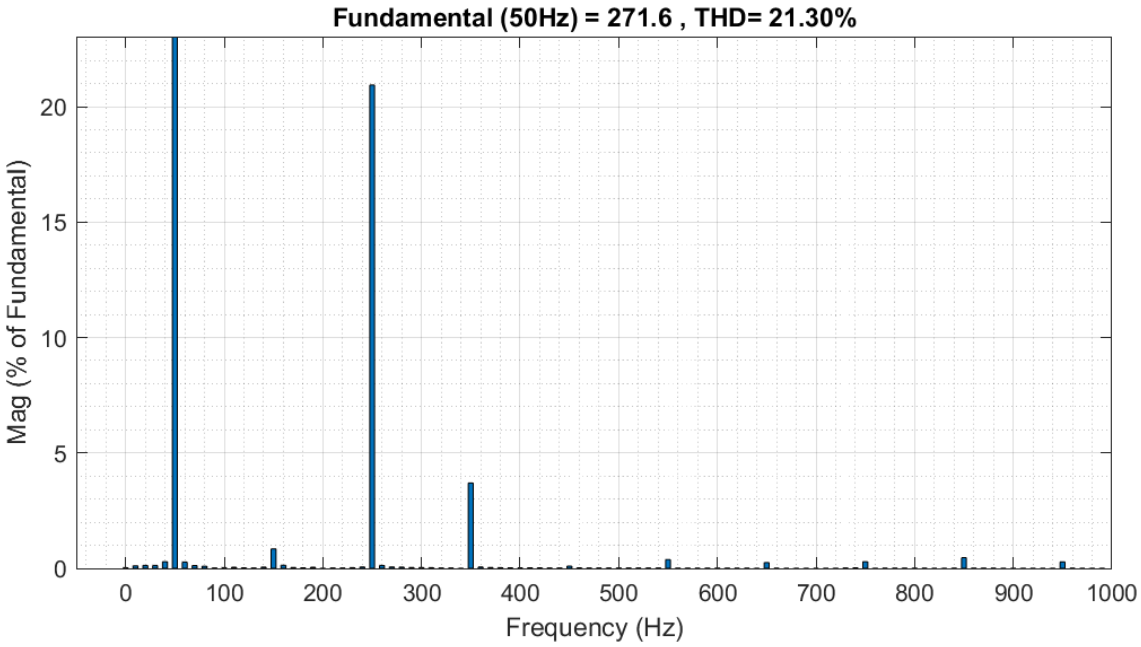

Figure 4.18: FFT of measured Current signal with PV-ESS and Non-Linear Load but without UPQC

The figures above represent THD of a grid that was obtained from MATLAB simulation over five cycles from 0.5 s. The THD is measured up to 20th harmonics(i.e 1000Hz). Under normal operating conditions without faults or PV integration in 4.11 and 4.12, the system shows little current distortion, with a THD value of voltage as 11.54% and current as 17.55%. After integration of the PV system, the voltage and the current in figure 4.23 and 4.24 THD rise to 13.17% and 21.30%, respectively, due to the fluctuating generating capacity of renewable resources, and power factor (PF) of 0.86 was observed.

4.1.4 Analysis of Grid After Using UPQC

The ANN-tuned UPQC dramatically restores the voltage and current waveforms under different operating conditions, so the general system waveform quit in Figure4.19 shows well-regulated voltage profiles and balanced sinusoidal current waveforms; hence reduced harmonic distortions and improved power stability. In connectivity with PV-ESS, faults, and some nonlinear loads in Figure4.20, the voltage stays stable while drastically reducing current distortion; hence, this validates that the UPQC has the capacity to filter power quality issues. The internal visualized demonstration during the case of L-G fault in Figure 4.21 reveals that the voltage was typically dipped during the short time and well after that quickly stabilized while the current waveform was very close to symmetrical, which again demonstrates the advantage of the UPQC against fault. The first of its unexamined cases gives concerning severe conditions of three-line ground case L-L-L-G fault in Figure4.22,

where the UPQC can entirely keep the voltage dips within reasonable limits and let no high fault currents through, which gives back to the nature of such a fault quite fast while keeping stability in this system. Therefore, PI-controlled UPQC demonstrates similar improvement in each test case so that both controllers are capable of improving power quality. However, the adaptive control-oriented dynamic features are assumed to be more appropriately fulfilled by the ANN-tuned UPQC.

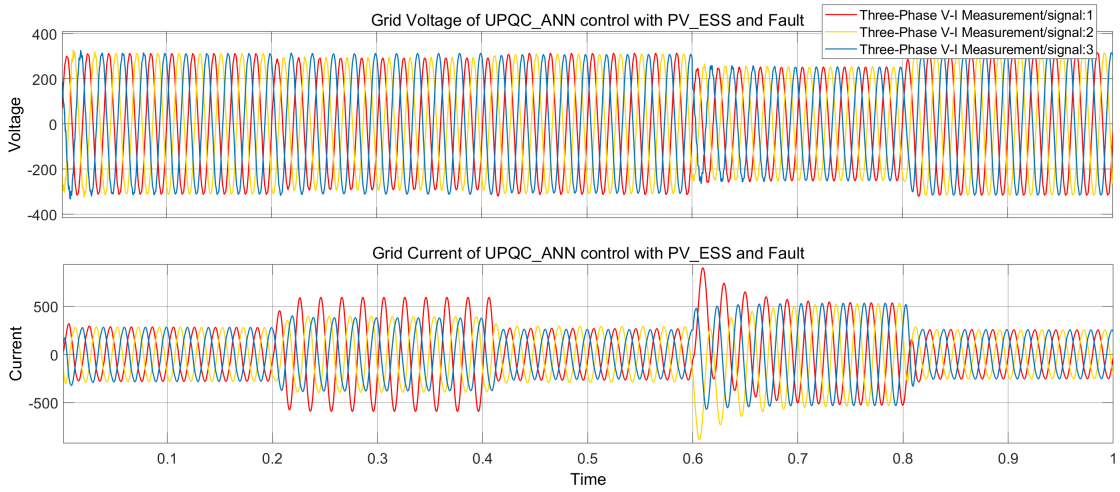

Figure 4.19: Grid V-I Waveform of Overall system with ANN Tuned UPQC

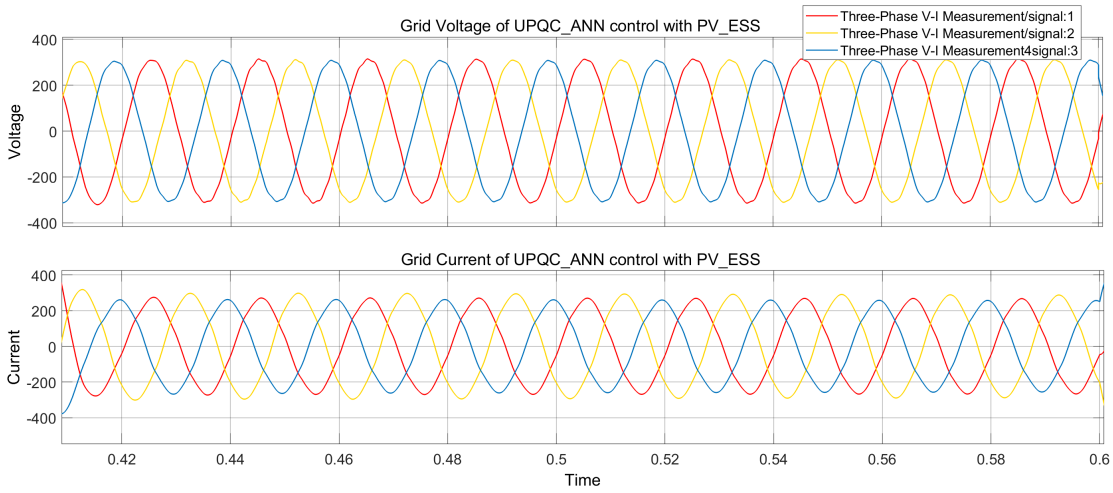

Figure 4.20: Grid V-I Waveform with PV-ESS, Fault and Non-Linear load and ANN Tuned UPQC

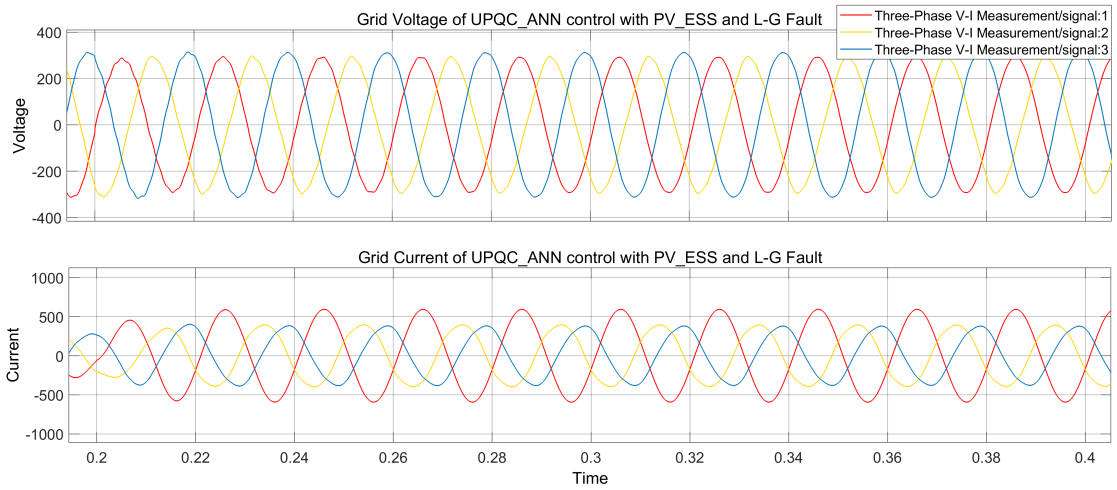

Figure 4.21: Grid V-I Waveform with L-G fault but without UPQC

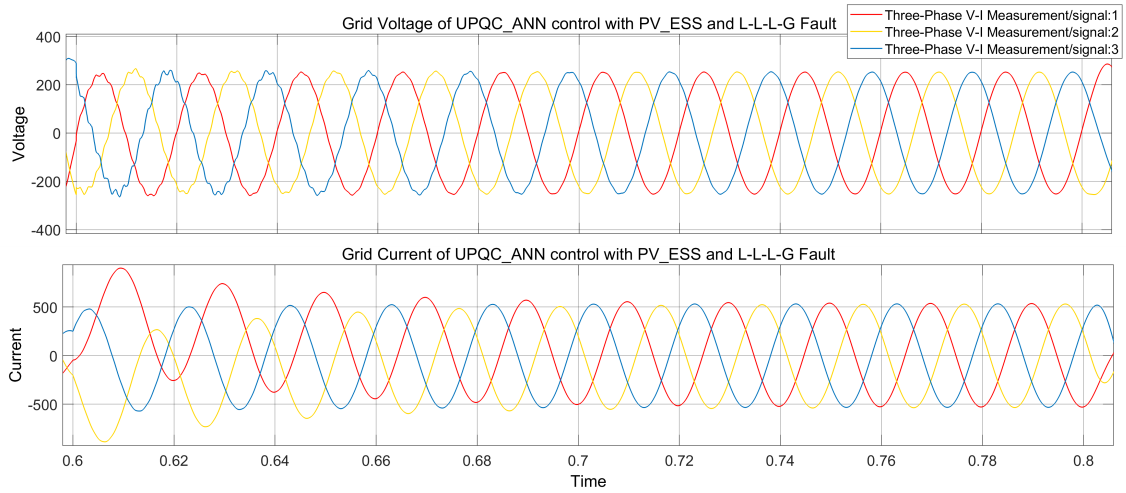

Figure 4.22: Grid V-I Waveform with L-L-L-G fault and ANN Tuned UPQC

Grid with PI control UPQC, PV-ESS, Fault and Non-Linear Load

Implementing UPQC along with a PI controller will act effectively to reduce harmonics, as the voltage and current THD was brought down to 3.13% and 3.11% respectively, which is under the IEEE 519 standard and PF improves to 0.95.

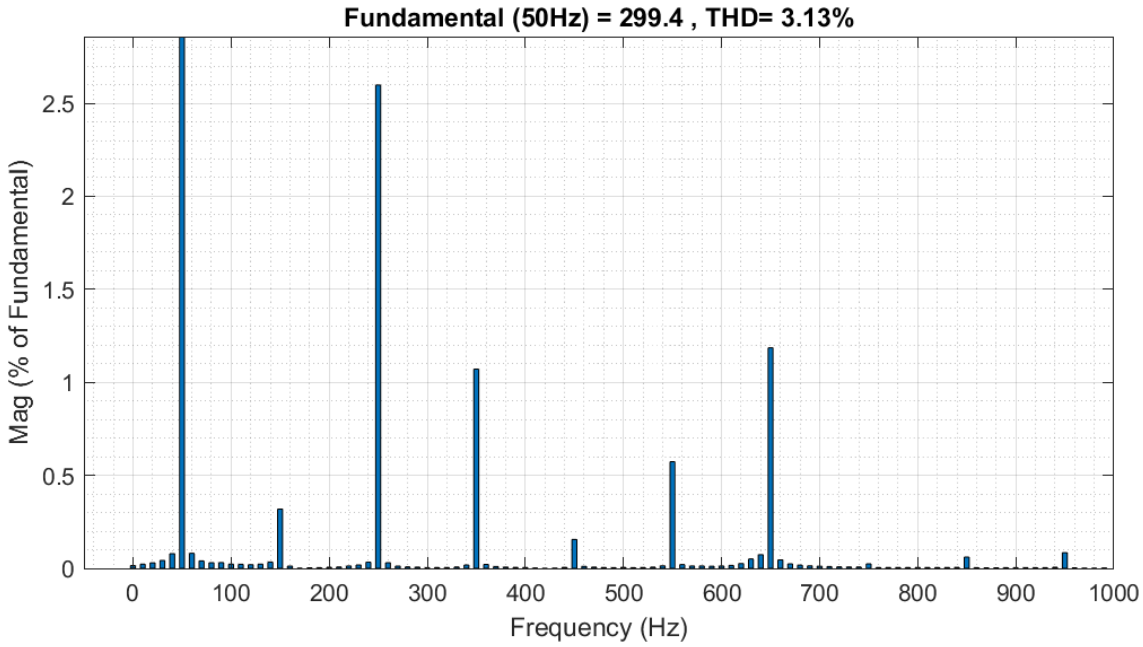

Figure 4.23: FFT of measured Voltage signal with PI control UPQC

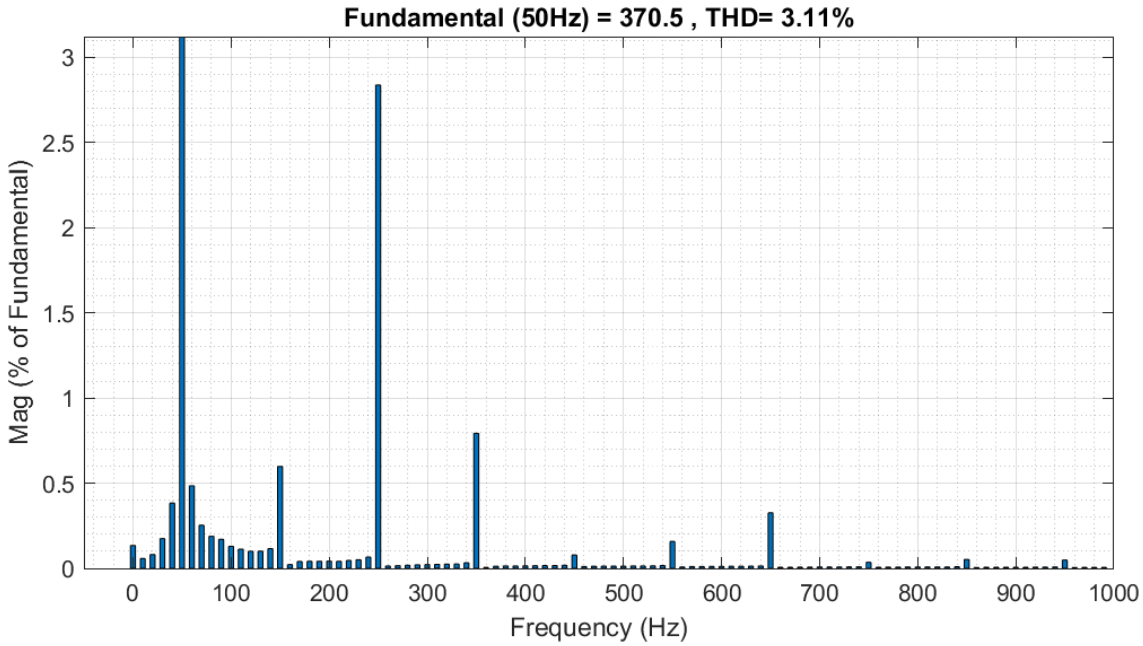

Figure 4.24: FFT of measured Current signal with PI Control UPQC

Grid with ANN Tuned UPQC, PV-ESS, Fault and Non-Linear Load

Finally, using an ANN-based controller instead of a PI controller further enhances the performance of UPQC and THD of voltage and THD of current were reduced to 1.66% and 2.48%, with stabilization over time and PF is optimized at 0.99.

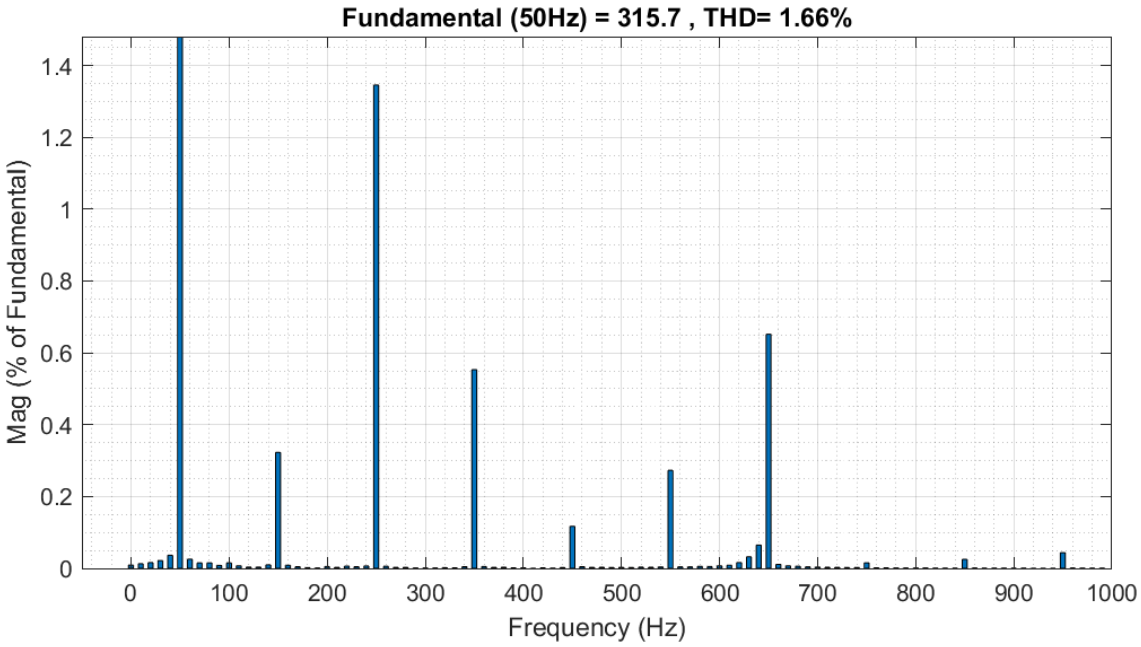

Figure 4.25: FFT of measured Voltage signal with ANN Tune UPQC

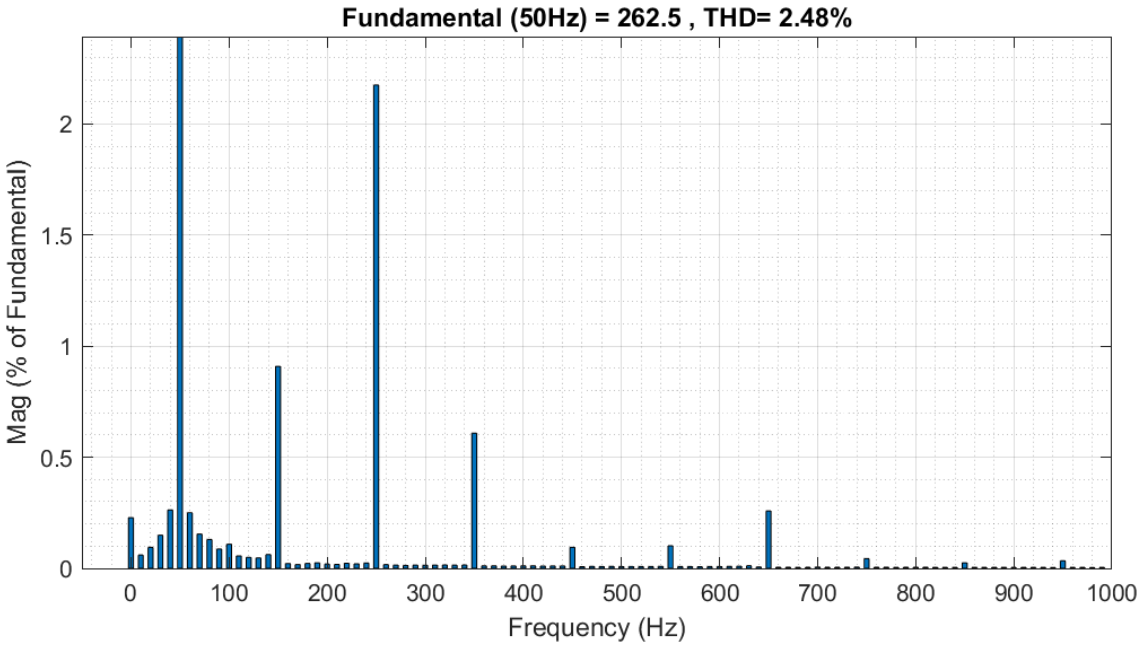

Figure 4.26: FFT of measured Current signal with ANN Tuned UPQC

A THD table in different cases seen at 0.5s through five cycles and upto 20th harmonics (1000Hz) are as follows.

Table 4.2: Grid THD Analysis Under Different Conditions

THD (%)	Without PV-ESS, Non-inear load & UPQC			Integrating PV-ESS, Non-linear load but without UPQC		
	Phase I	**Phase II**	**Phase III**	**Phase I**	**Phase II**	**Phase III**
Voltage	11.54	11.53	11.54	13.17	13.68	13.57
Current	17.55	17.54	17.58	21.30	20.46	22.93
THD (%)	**Integrating PV-ESS, Non-linear load & with PI controlled UPQC**			**Integrating PV-ESS, Non-linear load & with ANN Tuned UPQC**		
	Phase I	**Phase II**	**Phase III**	**Phase I**	**Phase II**	**Phase III**
Voltage	3.13	3.25	3.26	1.66	1.81	1.79
Current	3.11	3.21	3.39	2.48	2.66	2.87

From the above results we can conclude that FUZZY MPPT extract maximum power from PV and Energy storage system consist of FLC controller can optimized the charging and Discharging power from battery. Also, for power quality issues, we can conclude that ANN-Tuned UPQC Performs better than that of conventional (PI) one.

4.2 Test with Real Model

In this section, we will check all above result by updating the real system data to our model as mentioned on methodology portion.

The performance of this system was tested under different condition as per data availability. All the test data are mentioned on appendix portion at last.

4.2.1 Solar PV MPPT of Real System

For the real system analysis, the irradiance levels were varied between 1000 W/m² to 250 W/m² in the ramping down or up time of 0.6 to 1.7 seconds to mimic the dynamic solar conditions. A ramp-down and ramp-up profile was given to both irradiance and temperature for studying the system behavior in a varying environment. Temperature was increased from 25°C to 50°C with ramp-up pattern after 2 seconds shown in figure 4.27. This ongoing variation of irradiance and temperature was done to verify the robustness and flexibility of the system under non-homogeneous solar and thermal conditions. With the use of the fuzzy logic-based MPPT algorithm in real field simulation, the PV system achieved a maximum power of 50 kW under peak irradiance conditions (1000 W/m²) and a lowest output of about 15 kW even under low irradiance conditions (250 W/m²) as shown in figure 4.28. This performance is greatly enhanced compared to the real case without fuzzy MPPT, where the observed maximum PV power was up to about 46 kW, but the system mostly stayed between the range of 30–40 kW within the active solar window (around 11:00 AM to 2:00 PM), and dropped down as low as 5–10 kW during low irradiance.

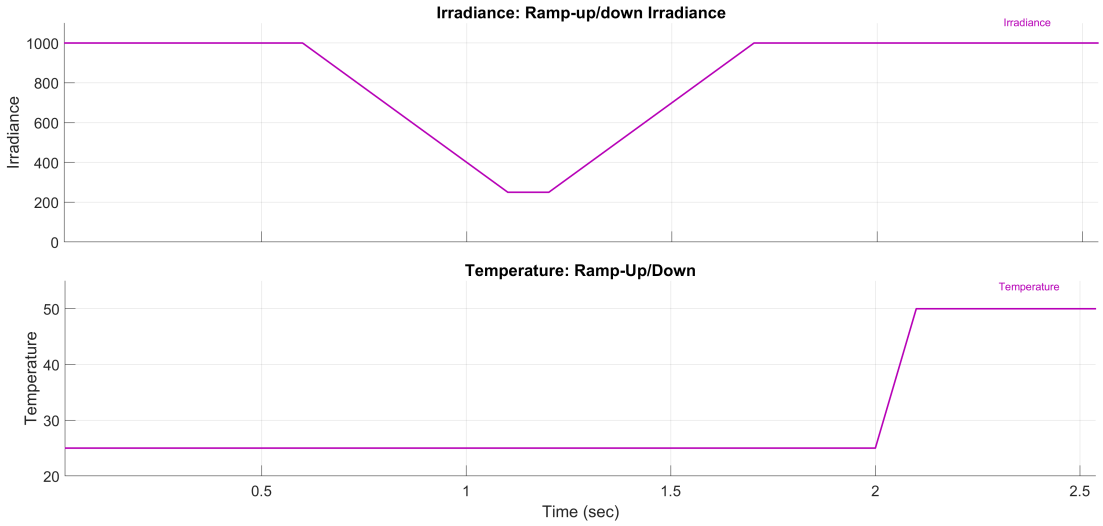

Figure 4.27: Variation in Irradiance and Temperature

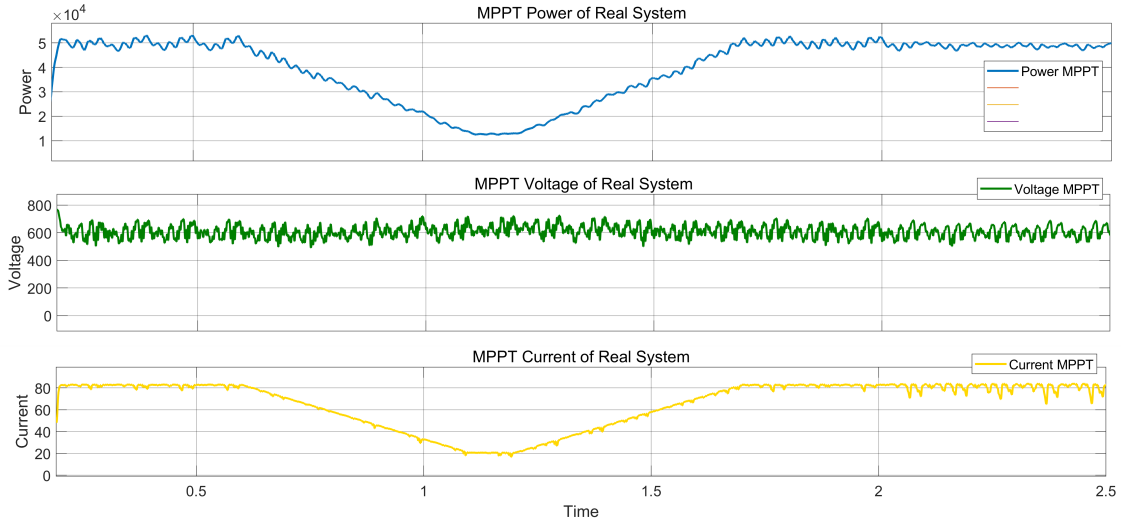

Figure 4.28: Real System PV o/p while using FUZZY Logic as MPPT

4.2.2 Energy Storage System of Real Test System

The charging in figure 4.29 and discharging power in figure 4.30 plots for the FLC-based ESS controller demonstrate how well the battery, which is AC-coupled to the system (as it is in reality) was working alongside PV generation. When the PV system was generating, and supporting the grid, the battery charged through the excess power. When the PV goes off, or output drops, the battery automatically discharged to support the load. The two configurations can provide uninterrupted service and reliability by providing the grid assistance when needed; addressing power swings; and aiding system resilience under certain conditions.

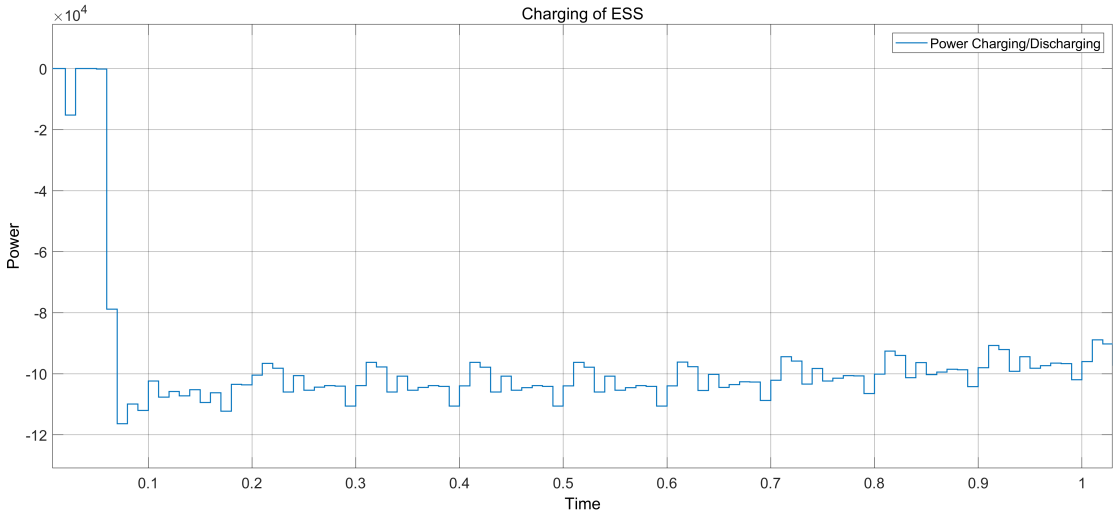

Figure 4.29: Charging of Real system Battery

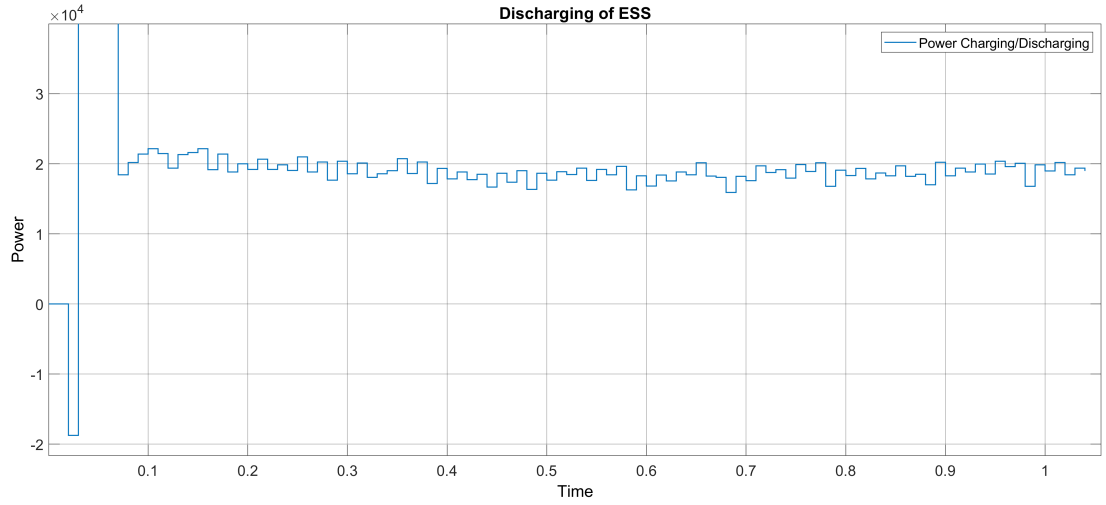

Figure 4.30: Discharging of Real system Battery

4.2.3 Analysis Of Grid After Using UPQC

The capability of the ANN-tuned UPQC for the preservation of stability of the grid during transient condition is illustrated by examining the V/I waveforms displayed in the figure 4.31. For the PV power variation (which occurs from 0.6 s to 1.7 s), there is a sharp reduction of the output of the PV array, and the system draws more power from the grid, which is shown by the increase in the amplitude of the grid current. However, the grid voltage remains sinusoidal and is stable across all phases, demonstrating the UPQC is effectively regulating the voltage. In like manner, during the load variation, the UPQC demonstrates its effectiveness in voltage stability based on the voltage sags and swells

and the grid current varies proportionally to the load. The adaptability of the UPQC is indicative of the dual functionality for conditioning both voltage and current, as evident, provides both power quality and reliability of the system, despite changes in generation and load.

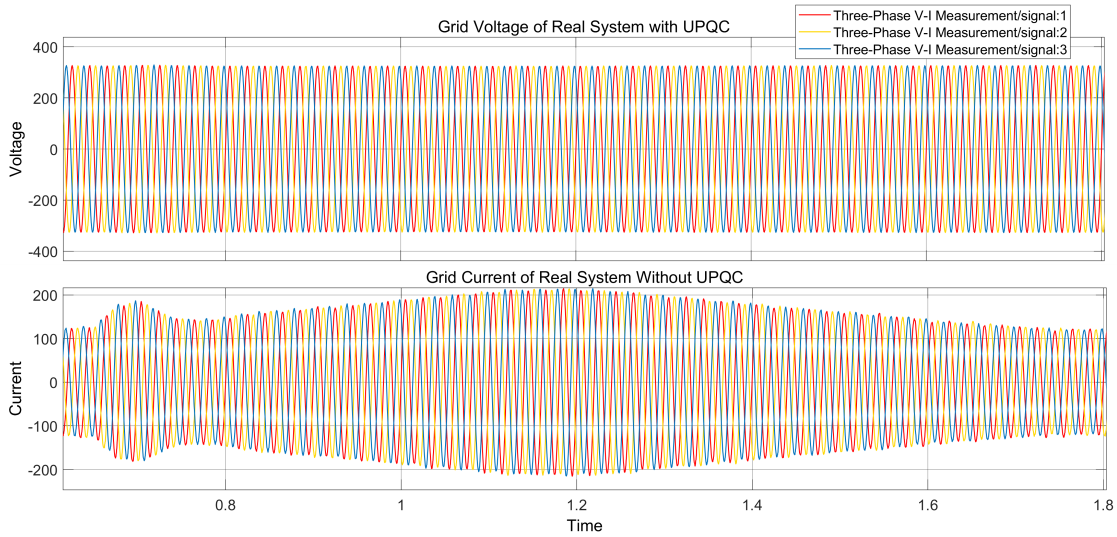

Figure 4.31: Overall Grid Support after using UPQC

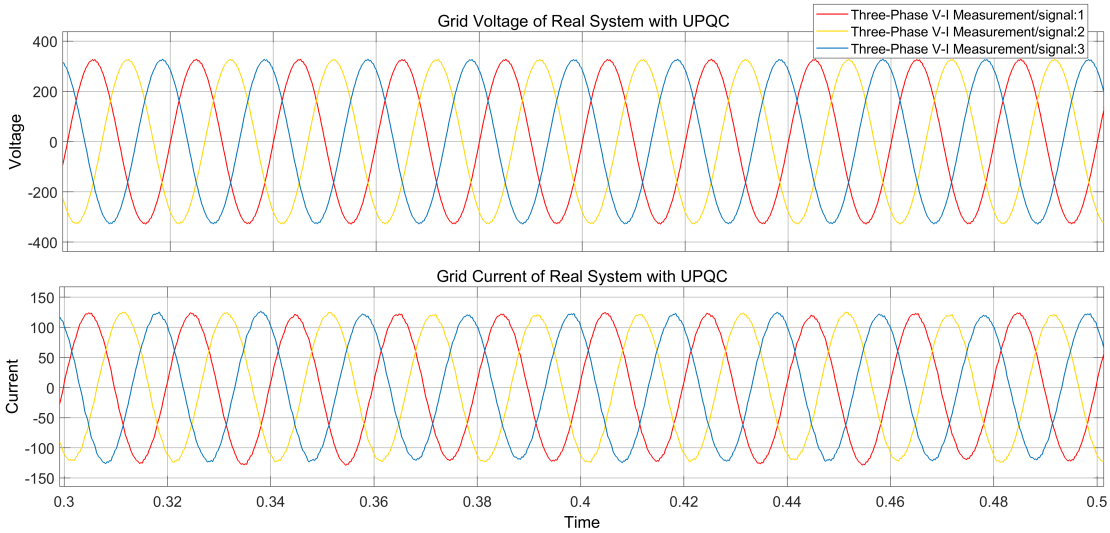

Figure 4.32: Grid Waveform of Real system after using UPQC

As shown in the appendix data below, in the real-world distribution of nepal systems, at the Cesar Apartment, the Total Harmonic Distortion (THD) levels, particularly for current, demonstrate considerable variability due to the impacts of the nonlinear loads, inverter-based DG and sudden changes in loads. Voltage THD is typically within 2% to 4%, and

current THD varies from 10% to 300% mentioned at the introduction part at these locations; typical average current THD levels are within 40% to 60%, highlighting how variable and distortion-prone practical systems can be. THD levels are driven by the increased penetration of inverter based generation systems combined with dynamic load behavior. Conversely, our proposed ANN-tuned UPQC system effectively mitigates these distortions and achieves significant improvements in overall power quality. We have tested our real system model with variable PV generation conditions and also by changing the active resistive load of the system from 20 kW to 100kW, Voltage THD was continuously maintained between 0.48% and 0.52% in figure 4.33 and current THD remained at a much lower and stable range of 1.80% to 4.5% in figure 4.34 and 4.35, even with varying loads and PV generation conditions. The THD at a 20 kW resistive load was measured at 4.40% (due to high influnce of inverter based generation in grid) and at a 100 kW load was measured at 1.88%, demonstrating the systems adaptive compensation performance as the load demand and harmonic profile vary. The measurements taken throughout the study highlight the effectiveness of the ANN-tuned UPQC provided distortion mitigation and grid stabilization while in operation under dynamic conditions that generally prove difficult for a technical system in a real-world situation while simultaneously providing IEEE -519 compliant THD figures

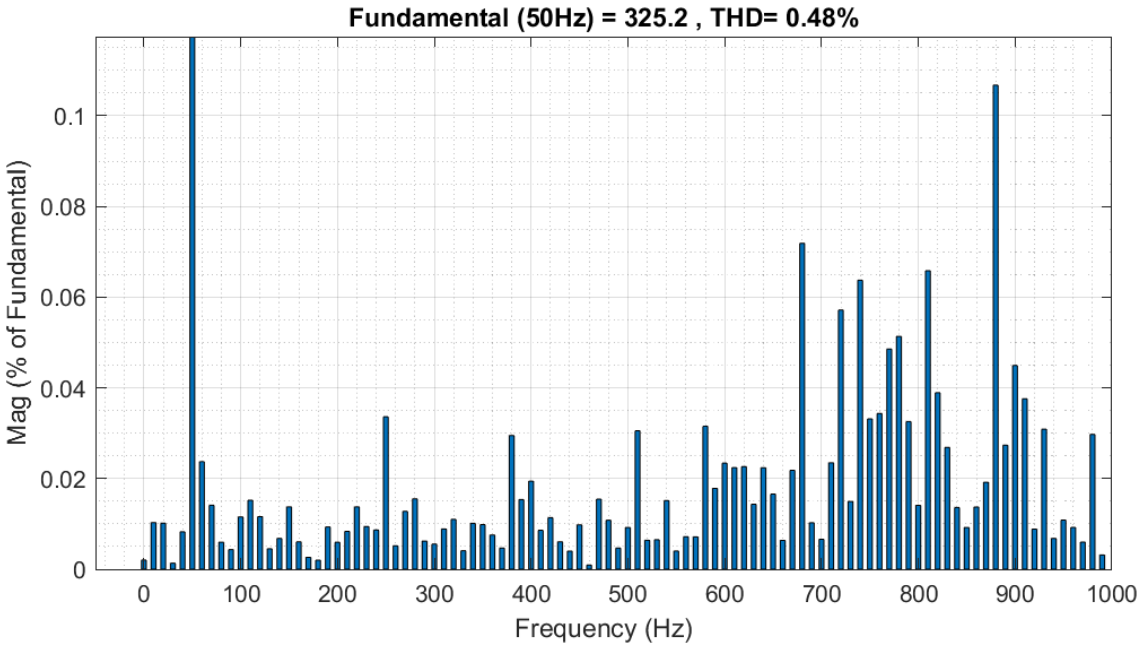

Figure 4.33: FFT of Voltage signal of Real System with ANN Tuned UPQC

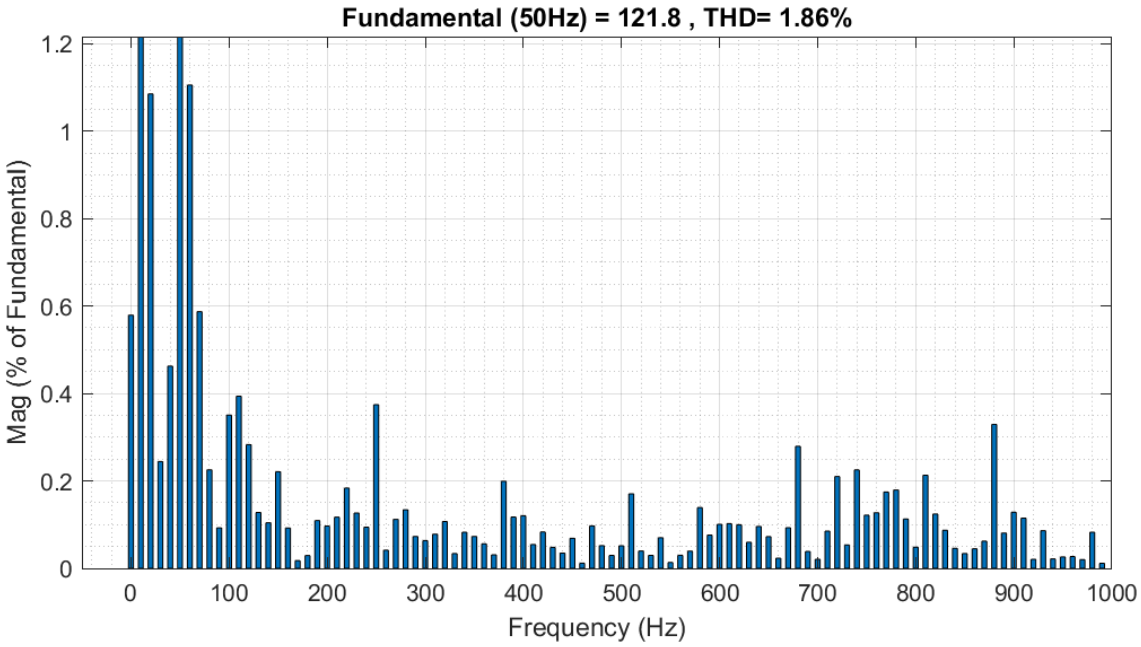

Figure 4.34: FFT of Current signal of Real System with ANN Tuned UPQC with 100kW Load

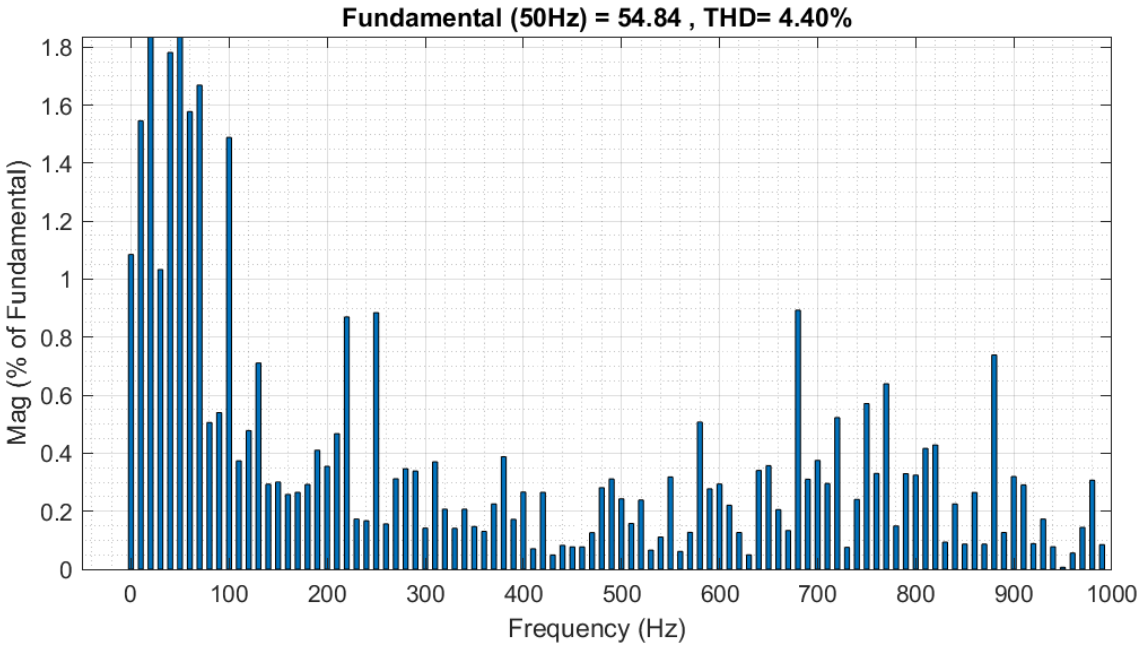

Figure 4.35: FFT of Current signal of Real System with ANN Tuned UPQC with 20kW Load

The representation seen in Figure 4.36 offers a clear indication of the proposed ANN-tuned UPQC system's capability to control the flow of active and reactive power. During periods of decreased PV power due to reduced irradiance value, the grid active power (top graph)

activates to help with the reduction in generation while maintaining the capacity of continuous power delivery to the load. The grid is also exhibiting reactive power consumption (bottom graph), especially during transient manifestations and load changes. This demonstrates the continuous efforts of the UPQC in managing reactive power exchange with the grid dynamically. Overall, the system maintains excellent power quality while registering a power factor of 0.996 which is practically unity. This is in stark contrast to practical systems that do not have compensation which, in turn, results in significant degradation of the power factor, as low as 0.7, from the inverter based generation or changes in resistive or nonlinear loads. These results demonstrate that the integration of the ANN optimized UPQC not only allows for harmonic reduction but assisting with compensation improving the overall power factor while making the system stable and efficient while approaching ideal conditions through dynamic operation.

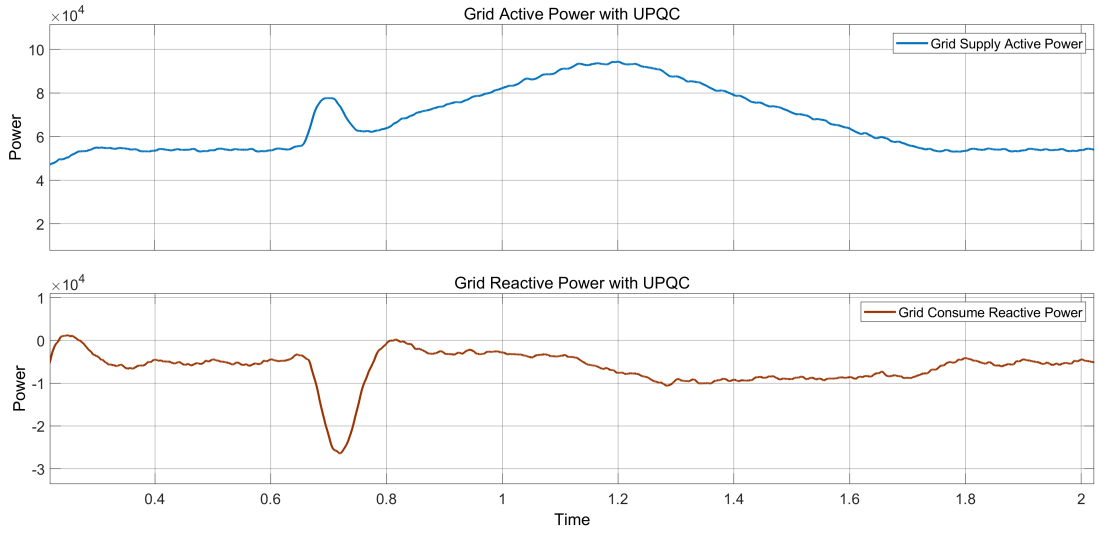

Figure 4.36: Grid Active and Reactive Power Support

CHAPTER FIVE: CONCLUSION

The proposed PV-ESS integrated UPQC system based on fuzzy MPPT, FLC based ESS controller and ANN-tuned, brings about great improvements in power quality and system stability under various working situations and fault conditions. The fuzzy MPPT controller extracts power efficiently from the PV system, converging to the maximum power point quickly with great stability and efficiency. Simulation results show that an ANN-tuned UPQC effectively mitigates voltage sag/swells, current surges, and harmonics distortions. The system experiences high harmonic distortion when operated without UPQC. The PI-controlled UPQC notably reduces the total harmonic distortion (THD) levels, while the ANN-based UPQC would achieve even better harmonic attenuation, giving both excellent performance to keep harmonics well below the IEEE-519 standard.

The ANN-based approach effects power factor correction much more effectively than the PI controller against the original, achieving very nearly unity power factor operation. Furthermore, the ESS satisfactorily maintains a balanced power transfer with the grid support, with controlled charge and discharge. In conclusion, the proposed system improves power quality, reduces harmonic distortion, and strengthens the grid's resilience towards disturbances, providing reliable and efficient solutions for modern power systems. The real implementation of the suggested system in the Cesar Apartment which was connected to the Teku 11 kV feeder, displayed better performance than under real operating conditions. The ANN based UPQC successfully reduced power quality issues including harmonics and improved the power factor. The Fuzzy Logic based MPPT extracted more power from the PV system than the typical real-case scenario, and the ESS controlling managed the charged/discharged cycles very effectively. Thus, the results showed that the test and validation of the research thesis model was successful in a real-world application and verified that the model is effective in enhancing energy extraction and energy quality in residential applications.

REFERENCES

[1] D. Gielen, F. Boshell, D. Saygin, M. D. Bazilian, N. Wagner, and R. Gorini, "The role of renewable energy in the global energy transformation," *Energy Strategy Reviews*, vol. 24, pp. 38–50, 2019. [Online]. Available: https://doi.org/10.1016/j.esr.2019.01.006

[2] R. M. Elavarasan, "The motivation for renewable energy and its comparison with other energy sources: A review," *European Journal of Sustainable Development Research*, vol. 3, no. 1, p. em0076, 2019. [Online]. Available: https://doi.org/10.20897/ejosdr/4005

[3] S. Garg and S. Tyagi, "A comprehensive review on opportunities and challenges of grid integration of renewable energy resources," in *2024 Second International Conference on Smart Technologies for Power and Renewable Energy (SPECon)*, 2024, pp. 1–6.

[4] R. M. Elavarasan, S. Afridhis, R. R. Vijayaraghavan, U. Subramaniam, and M. Nurunnabi, "Swot analysis: A framework for comprehensive evaluation of drivers and barriers for renewable energy development," *Energy Reports*, vol. 6, pp. 1838–1864, 2020.

[5] S. Devassy and B. Singh, "Performance analysis of solar pv array and battery integrated unified power quality conditioner for microgrid systems," *IEEE Transactions on Industrial Electronics*, vol. 68, no. 5, pp. 4027–4035, 2021.

[6] E. J. Coster, J. M. A. Myrzik, B. Kruimer, and W. L. Kling, "Integration issues of distributed generation in distribution grids," *Proceedings of the IEEE*, vol. 99, no. 1, pp. 28–39, 2011. [Online]. Available: https://doi.org/10.1109/JPROC.2010.2052776

[7] X. Liang, "Emerging power quality challenges due to integration of renewable energy sources," *IEEE Transactions on Industry Applications*, vol. 53, no. 2, pp. 855–866, 2017.

[8] G. S. Chawda, A. G. Shaik, M. Shaik, S. Padmanaban, J. B. Holm-Nielsen, O. P. Mahela, and P. Kaliannan, "Comprehensive review on detection and classification of power quality disturbances in utility grid with renewable energy penetration," *IEEE Access*, vol. 8, pp. 146 807–146 830, 2020.

[9] S. A. Mohamed, "Enhancement of power quality for load compensation using three different facts devices based on optimized technique," *International Transactions on Electrical Energy Systems*, vol. 30, no. 3, p. e12196, 2017.

[10] M. A. Mansor, K. Hasan, M. M. Othman, S. Z. B. M. Noor, and I. Musirin, "Construction and performance investigation of three-phase solar pv and battery energy storage system integrated upqc," *IEEE Access*, vol. 8, pp. 103 511–103 538, 2020.

[11] A. Amirullah, A. Adiananda, O. Penangsang, and A. Soeprijanto, "Load active power transfer enhancement using upqc-pv-bes system with fuzzy logic controller," *International Journal of Intelligent Engineering and Systems*, vol. 13, no. 2, pp. 329–349, 2020.

[12] W. Ahamd and I. Ullah, "Unified power quality conditioner based power quality improvement in micro-grid," in *2025 IEEE Texas Power and Energy Conference (TPEC)*, 2025, pp. 1–6.

[13] A. Metia and S. Ghosh, "Power quality improvement by upqc in a distribution network using a novel srf based control approach," in *2023 International Conference on Energy, Materials and Communication Engineering (ICEMCE)*, 2023, pp. 1–6.

[14] N. Zanib, M. Batool, S. Riaz, and F. Nawaz, "Performance analysis of renewable energy based distributed generation system using ann tuned upqc," *IEEE Access*, vol. 10, pp. 110 034–110 049, 2022.

[15] K. Sarita, S. Kumar, A. S. S. Vardhan, R. M. Elavarasan, R. K. Saket, G. M. Shafiullah, and E. Hossain, "Power enhancement with grid stabilization of renewable energy-based generation system using upqc-flc-eva technique," *IEEE Access*, vol. 8, pp. 207 443–207 464, 2020.

[16] T.-U. Hassan, R. Abbassi, H. Jerbi, K. Mehmood, M. F. Tahir, K. M. Cheema, R. M. Elavarasan, F. Ali, and I. A. Khan, "A novel algorithm for mppt of an isolated pv system using push pull converter with fuzzy logic controller," *Energies*, vol. 13, no. 15, p. 4007, 2020.

[17] U. Yilmaz, A. Kircay, and S. Borekci, "Pv system fuzzy logic mppt method and pi control as a charge controller," *Renewable and Sustainable Energy Reviews*, vol. 81, pp. 994–1001, 2018.

[18] A. K. Srivastava, A. A. Kumar, and N. N. Schulz, "Impact of distributed generations with energy storage devices on the electric grid," *IEEE Systems Journal*, vol. 6, no. 1, pp. 110–117, 2012.

[19] V. Khadkikar, "Enhancing electric power quality using upqc: A comprehensive overview," *IEEE Transactions on Power Electronics*, vol. 27, no. 5, pp. 2284–2297, 2012.

[20] S. A. Pasha and N. P. Kumar, "Model predictive controller based unified power quality conditioner for voltage regulation studies in 33-bus closed loop distribution system," in *E3S Web of Conferences*, vol. 184. EDP Sciences, 2020, p. 01073.

APPENDIX A: CODES AND DATA

Solar PV FUZZY Code of Model

```
[System]
Name='pv11'
Type='mamdani'
Version=2.0
NumInputs=2
NumOutputs=1
NumRules=9
AndMethod='min'
OrMethod='max'
ImpMethod='min'
AggMethod='max'
DefuzzMethod='centroid'

[Input1]
Name='Voltage'
Range=[0 2000]
NumMFs=3
MF1='LV':'trapmf',[0 0 300 800]
MF2='MV':'trapmf',[700 1100 1400 1700]
MF3='HV':'trapmf',[1600 1800 2000 2000]

[Input2]
Name='Current'
Range=[0 42]
NumMFs=3
MF1='LI':'trapmf',[0 0 4.5 8.281]
MF2='MI':'trapmf',[7.679 13.08 21.83 26.52]
MF3='HI':'trapmf',[25.56 33.72 42 42]

[Output1]
Name='DutyCycle'
Range=[0.4 1]
NumMFs=3
```

```
MF1='LD':'trapmf',[0.4 0.4 0.5 0.6]
MF2='MD':'trapmf',[0.578 0.628 0.7865 0.834]
MF3='HD':'trapmf',[0.8 0.85 1 1]

[Rules]
1 1, 3 (1) : 1
1 2, 2 (1) : 1
1 3, 2 (1) : 1
2 1, 3 (1) : 1
2 2, 2 (1) : 1
2 3, 2 (1) : 1
3 1, 2 (1) : 1
3 2, 1 (1) : 1
3 3, 1 (1) : 1
```

Solar PV FUZZY Code of Real System

```
[System]
Name='pv11'
Type='mamdani'
Version=2.0
NumInputs=2
NumOutputs=1
NumRules=9
AndMethod='min'
OrMethod='max'
ImpMethod='min'
AggMethod='max'
DefuzzMethod='centroid'

[Input1]
Name='Voltage'
Range=[0 700]
NumMFs=3
MF1='LV':'trapmf',[0 0 100 200]
MF2='MV':'trapmf',[180 300 400 500]
MF3='HV':'trapmf',[480 600 700 700]
```

```
[Input2]
Name='Current'
Range=[0 90]
NumMFs=3
MF1='LI':'trapmf',[0 0 10 20]
MF2='MI':'trapmf',[18 35 50 65]
MF3='HI':'trapmf',[60 75 90 90]

[Output1]
Name='DutyCycle'
Range=[0.4 1]
NumMFs=3
MF1='LD':'trapmf',[0.4 0.4 0.5 0.6]
MF2='MD':'trapmf',[0.578 0.628 0.7865 0.834]
MF3='HD':'trapmf',[0.8 0.85 1 1]

[Rules]
1 1, 3 (1) : 1
1 2, 2 (1) : 1
1 3, 2 (1) : 1
2 1, 3 (1) : 1
2 2, 2 (1) : 1
2 3, 2 (1) : 1
3 1, 2 (1) : 1
3 2, 1 (1) : 1
3 3, 1 (1) : 1
```

Energy Storage System FLC Code of Model/Real System

```
[System]
Name='BCMS11'
Type='sugeno'
Version=2.0
NumInputs=1
NumOutputs=2
NumRules=2
AndMethod='prod'
OrMethod='probor'
```

```
ImpMethod='prod'
AggMethod='sum'
DefuzzMethod='wtaver'

[Input1]
Name='Error'
Range=[-60000 60000]
NumMFs=2
MF1='lowError':'trapmf',[-60000 -60000 -30000 0]
MF2='mf3':'trapmf',[0 30000 60000 60000]

[Output1]
Name='BC'
Range=[0 1]
NumMFs=2
MF1='mf1':'constant',[0]
MF2='mf3':'constant',[1]

[Output2]
Name='BD'
Range=[0 1]
NumMFs=2
MF1='mf1':'constant',[0]
MF2='mf3':'constant',[1]

[Rules]
1, 1 2 (1) : 1
2, 2 1 (1) : 1
```

Data of Cesar Apartment, Sanepa, Lalitpur

The following data has been obtained from Gham Power Pvt. Ltd. for Cesar Apartment, located in Lalitpur, where a solar PV system along with a battery energy storage system has been installed.

Real System Data of
Cesar Apartment, Sanepa, Lalitpur, Nepal

Time	Active_Power_ Load	Reactive_Power_ Load	Apparent_Power_ Load	Current_A_THD	Current_B_THD	Current_C_THD	Frequency	PF	Voltage_AN_ THD	Voltage_BN_ THD	Voltage_CN_ THD	Solar_Active_ Power_Gen
3/1/2025 0:00	6468.516	-1432.99	6631.908	51.49	43.43	16.4	49.996	0.975	2.96	3.16	3.19	33.134
3/1/2025 1:00	16067.125	-524.584	16075.687	46.37	61.93	50	49.983	1	2.33	1.9	2.05	32.068
3/1/2025 2:00	52942.809	48356.91	71641.406	7.48	6.43	6.07	49.989	-0.737	2.3	2.49	2.54	31.515
3/1/2025 3:00	7794.473	-1689.385	7975.195	30.91	46.58	18.18	50.046	0.977	2.88	2.9	3.01	33.82
3/1/2025 4:00	52565.383	45674.902	69637.039	8.34	7.7	7.19	50.051	-0.754	2.1	2.36	2.38	31.823
3/1/2025 5:00	46947.398	30383.025	55998.82	17.34	17.1	15.28	50.008	-0.84	1.98	2.05	2.04	30.412
3/1/2025 6:00	19237.23	6607.406	22202.215	20	20.23	19.41	50.077	-0.947	2.1	2.15	1.94	655.254
3/1/2025 7:00	5776.272	152.337	5787.206	61.71	110.46	96.23	50.035	1	1.62	1.6	1.27	6663.33
3/1/2025 8:00	-4342.18	-393.19	4356.041	71.91	21.31	181.02	49.965	-0.995	1.95	2.28	1.59	15285.664
3/1/2025 9:00	-4778.36	6221.051	7850.084	30.62	32.11	52.79	49.987	0.609	2.17	1.79	1.96	22455.064
3/1/2025 10:00	2259.163	8022.98	8309.738	40.39	41.91	47.62	50.045	-0.26	1.59	2.02	1.68	27506.537
3/1/2025 11:00	-18369.389	681.882	18257.785	16.96	17.64	29.73	49.939	-1	1.75	2.08	1.66	31499.895
3/1/2025 12:00	25192.184	41873.07	48938.062	11.77	11.38	12.27	49.852	-0.519	1.99	2.08	2.01	29686.732
3/1/2025 13:00	12884.014	-1283.297	12937.236	41.12	25.03	21.54	50.031	0.995	1.67	2.01	1.73	28.193
3/1/2025 14:00	-11868.685	968.26	11908.114	30.17	30.01	32.18	49.942	0.996	1.77	2.07	1.96	20600.51
3/1/2025 15:00	-4492.974	1064.821	4633.992	114.99	86.42	80.99	50.008	0.974	1.66	2.15	2.22	13818.885
3/1/2025 16:00	17105.711	7392.685	18636.254	37.4	29.31	27.77	49.97	-0.917	1.78	2.24	1.99	4301.135
3/1/2025 17:00	15584.427	-636.027	15597.4	41.08	38.17	43.27	50.108	1	1.99	1.92	2.23	33.797
3/1/2025 18:00	18836.764	-2947.991	19097.854	41.1	24.92	35.96	50.006	0.988	1.88	2.27	2.22	29.153
3/1/2025 19:00	13821.52	-2289.036	13996.845	38.87	54.56	34.49	50.003	0.986	2	3.09	2.75	30.253
3/1/2025 20:00	18778.232	4607.724	19202.775	36.91	19.51	10.54	49.99	-0.97	2.97	2.74	3.08	30.297
3/1/2025 21:00	19654.34	-849.322	19675.215	44.55	49.81	34.93	49.99	1	2.28	2.76	2.25	29.319
3/1/2025 22:00	10276.854	-1929.135	10457.868	30.93	39.03	21.33	49.938	0.982	2.96	3.45	3.18	30.999
3/1/2025 23:00	7146.651	-1808.874	7406.646	54.63	46.9	17.28	49.986	0.969	2.99	3.35	3.3	31.918
3/2/2025 0:00	18870.494	5540.6	19820.801	36.66	29.05	17.74	49.978	-0.96	2.61	3.01	2.87	30.646
3/2/2025 1:00	5530.018	-2658.637	6133.415	67.37	47.9	17.99	49.964	0.901	2.85	3.06	3.19	30.162
3/2/2025 2:00	6767.57	-1794.875	7001.222	60.05	39.24	13.68	50.033	0.966	2.99	3.07	3.2	28.94
3/2/2025 3:00	6528.371	-1751.334	6755.772	51.43	44.23	13.43	50.006	0.965	2.96	3.08	3.21	31.259
3/2/2025 4:00	7580.406	-1486.561	7753.274	50.97	46.55	23.15	49.965	0.982	2.68	2.73	2.86	30.184
3/2/2025 5:00	6969.732	-1761.916	7321.045	55.85	46.74	23.6	50.09	0.97	2.58	2.73	2.81	29.856
3/2/2025 6:00	3788.164	-537.922	3826.166	85.61	66.61	35.04	50.004	0.99	3	2.77	2.85	301.876
3/2/2025 7:00	853.29	-94.577	858.515	131.59	52.35	267.95	50.085	0.994	2.35	2.21	2.09	6160.656
3/2/2025 8:00	7452.209	5791.263	9535.957	50.46	49.98	34.62	49.959	-0.794	1.49	1.63	1.59	12396.866
3/2/2025 9:00	-4822.893	1410.833	5025.012	291.8	94.87	110.08	50.037	0.959	1.63	1.66	1.65	22005.66
3/2/2025 10:00	1280.872	7748.948	7894.857	49.69	118.94	52.35	49.986	-0.205	2.04	1.65	1.72	20525.201
3/2/2025 11:00	-11922.366	-185.076	11919.395	49.66	16.59	10.53	49.875	-1	2.79	2.34	2.68	21186.676
3/2/2025 12:00	-11341.785	280.094	11381.827	30.15	27.58	13.03	50	-1	2.44	2.47	2.63	21110.518
3/2/2025 13:00	2297.524	7501.592	7692.775	21.28	66.72	33.67	49.984	-0.246	2.9	2.37	2.81	15753.427
3/2/2025 14:00	4767.116	2509.386	4164.488	145.26	154.36	62.7	49.941	-0.796	1.99	1.83	2.13	10677.772
3/2/2025 15:00	-163.25	-82.562	182.94	90.92	107.78	48.09	49.897	-0.954	2.71	2.7	2.79	8478.549
3/2/2025 16:00	10180.401	-484.571	10177.724	87.83	37.09	13.95	49.814	1	21.13	19.59	3.36	2653.377
3/2/2025 17:00	23741.668	6225.901	24541.438	32.349	25.26	20.91	49.981	-0.965	2.51	2.22	2.31	76.727
3/2/2025 18:00	59450.789	42664.191	73124.828	11.84	10.09	8.52	50.041	-0.812	2.13	2.16	1.94	31.227
3/2/2025 19:00	17349.1	-2385.597	17516.717	39.2	30.53	33.16	50.003	0.99	2.25	2.81	2.76	33.848
3/2/2025 20:00	16845.018	-2529.227	17033.053	36.09	34.88	37.78	50.005	0.989	2.66	3.17	2.95	31.966
3/2/2025 21:00	21584.467	4431.026	22030.246	23.2	19.98	15.14	50.031	-0.979	3.3	3.49	3.59	30.608
3/2/2025 22:00	7356.53	-1688.833	7547.892	42.91	42.91	28.34	50.006	0.974	3	3.73	3.51	30.26
3/2/2025 23:00	12154.4	-1693.132	11884.529	61.55	58.13	48.21	50.01	0.989	3.15	3.36	3.31	31.237
3/3/2025 0:00	16328.591	6452.202	17560.746	23.43	16.7	9.61	50.006	-0.93	3.23	3.47	3.64	32.244
3/3/2025 1:00	21435.215	16865.852	26591.646	20.73	18.28	14.46	49.88	-0.773	2.45	2.76	2.86	31.289
3/3/2025 2:00	49728.172	46671.492	68104.484	6.03	6.41	6.44	2.51	-0.728	43261.809	30398.221	8.149	28.185
3/3/2025 3:00	55616.219	46939.684	72853.305	11.5	9.83	9.39	50.026	-0.764	2.14	2.36	2.59	28.477
3/3/2025 4:00	54655.449	43047.242	69579.938	9.84	8.16	7.45	50.045	-0.785	2.15	2.35	2.34	27.921
3/3/2025 5:00	5745.739	-1685.967	5943.578	49.91	39.14	16.049	50.093	0.958	3.04	3.15	3.1	31.759
3/3/2025 6:00	5009.512	-280.645	4884.44	45.76	58.39	33.17	50.036	0.998	2.57	2.51	2.41	560.296
3/3/2025 7:00	5820.364	-411.709	5858.548	84.09	37.51	48.72	50.037	0.997	1.85	1.65	1.73	3385.38
3/3/2025 8:00	10429.19	-375.663	10436.105	52.89	50.41	28.74	50.136	1	1.64	1.58	1.62	2940.157
3/3/2025 9:00	5110.373	6694.598	8437.48	59.02	120.16	28.68	50.036	-0.608	1.67	1.72	1.56	15355.575
3/3/2025 10:00	-6123.386	935.081	6156.672	44.01	176.74	66.88	50.023	0.988	1.86	1.86	1.62	18556.445
3/3/2025 11:00	11237.948	6973.921	13226.001	53.83	95.1	32.74	50.001	-0.849	1.55	1.62	1.49	12543.946
3/3/2025 12:00	12049.241	211.2	12051.035	72.22	90.58	43.35	50.022	-0.997	1.5	1.66	1.31	3829.932
3/3/2025 13:00	3322.442	-568.345	3388.324	102.17	167.07	48.77	50.237	0.985	1.97	2.19	1.77	9479.839
3/3/2025 14:00	5110.042	5853.433	7333.2	30.92	110.29	45.4	49.957	-0.674	1.97	2.02	1.79	17735.295
3/3/2025 15:00	318.123	-106.371	354.835	99.1	111.77	353.83	49.924	0.952	1.86	2.08	1.92	11418.431
3/3/2025 16:00	9126.272	-138.779	9108.26	60.22	59.33	44.57	49.984	1	1.93	1.96	1.85	2522.606
3/3/2025 17:00	12809.497	-1189.602	12864.618	47.4	43.29	33.98	50.001	0.995	2.14	2.12	2.15	71.794
3/3/2025 18:00	19319.57	-1291.013	19511.143	26.95	46.1	24.91	50.004	0.997	2.31	2.69	2	30.472
3/3/2025 19:00	13587.831	-1183.098	14015.723	50.78	46.02	17.8	50.073	0.985	2.47	2.79	2.21	30.278
3/3/2025 20:00	58324.016	44661.781	73152.766	9.75	10.3	9.66	50.033	-0.793	2.26	2.38	2.26	30.409
3/3/2025 21:00	58577.984	47454.344	75387.633	11.21	10.62	9.29	49.993	-0.777	2.42	2.41	2.51	30.8
3/3/2025 22:00	56468.621	45222.188	72798.664	12.26	9.45	9.25	50.05	-0.783	2.27	2.5	2.5	30.695
3/3/2025 23:00	52366.637	44210.828	68552.109	11	8.95	8.81	50.116	-0.764	2.07	2.3	2.36	28.405
3/4/2025 0:00	7839.116	-1705.919	8019.482	15.46	11.49	9.27	50.01	0.977	2.74	3.09	3.23	32.197
3/4/2025 1:00	6980.094	-1805.457	7200.527	53.44	44.99	22.21	49.977	0.968	2.71	2.88	2.95	32.632
3/4/2025 2:00	7358.513	-1712.974	7544.742	55.15	44.25	21.25	49.971	0.974	2.69	2.89	3	31.951
3/4/2025 3:00	8940.535	-1487.884	9065.445	55.8	48.99	30.83	50.022	0.986	2.75	2.82	2.96	33.852
3/4/2025 4:00	9270.674	-1463.854	9385.534	56.68	45.82	30.67	50.089	0.988	2.48	2.8	2.87	33.548
3/4/2025 5:00	5618.313	-2314.058	6076.208	55.09	38.49	16.99	50.038	0.924	2.74	2.93	2.93	30.644
3/4/2025 6:00	5035.086	-676.371	5088.177	43.85	54.59	28.31	50.034	0.992	2.47	2.47	2.2	337.629
3/4/2025 7:00	19163.264	5436.433	19718.814	24.95	40.7	32.32	49.999	-0.961	1.49	1.68	1.25	6134.527
3/4/2025 8:00	32038.129	41912.645	52875.801	8.85	5.23	7.98	50.05	-0.609	1.45	1.76	1.56	21100.863
3/4/2025 9:00	-15195.206	2082.244	15337.21	25.64	26.64	30.2	50.003	0.99	1.67	1.95	1.55	29358.645
3/4/2025 10:00	-11781.272	7457.28	14007.309	31.28	18.8	51.58	49.924	0.846	1.66	1.87	1.66	36709.098
3/4/2025 11:00	-23605.424	1584.115	23658.518	18.8	14.51	14.98	50.026	0.997	1.95	2.09	2	37924.945
3/4/2025 12:00	-14193.986	7495.75	16035.62	32.439	40.63	26.39	50.001	0.884	2.09	1.77	1.97	40136.078
3/4/2025 13:00	-18191.918	722.337	19299.033	17.05	25.04	15.27	50.004	-1	2.25	2.39	2.3	30090.719
3/4/2025 14:00	-18037.045	240.742	18038.65	17.01	28.13	21.15	49.968	-1	2.19	2.24	2.3	31162.322
3/4/2025 15:00	4428.159	-317.793	4439.548	206.69	54.53	107.31	49.942	0.997	1.94	2.2	2.12	5937.858
3/4/2025 16:00	7695.487	-1243.504	9178.709	181.08	32.84	44.23	49.987	0.99	2.45	2.52	2.61	5692.843

3/4/2025 17:00	53148.391	38007.414	65402.375	8.43	9.25	9.14	50.022	-0.819	1.88	2.03	1.99	387.604
3/4/2025 18:00	14099.851	-283.952	14390.793	48.78	50.01	29.48	49.962	1	2.21	2.64	2.27	30.313
3/4/2025 19:00	61140.832	38401.598	72140.016	13.11	10.2	10.1	50.048	-0.846	2.07	2.07	2.15	27.869
3/4/2025 20:00	13240.056	-1283.297	13284.988	51.15	52.4	35.3	50.096	0.995	2.49	2.47	2.51	31.074
3/4/2025 21:00	52903.785	44817.645	69374.766	12.46	9.58	9.59	50.022	-0.763	2.43	2.66	2.38	31.385
3/4/2025 22:00	16681.326	4678.602	17322.781	28.5	15.6	9.4	50.023	-0.962	3.01	3.32	3.21	29.933
3/4/2025 23:00	28436.031	16331.896	32849.629	63.61	46.61	37.44	50.013	-0.867	2.42	2.76	2.92	29.786
3/5/2025 0:00	47588.828	47923.926	67538.133	8.61	6.05	6.79	50.006	-0.704	2.68	2.66	2.8	32.021
3/5/2025 1:00	11745.889	-1638.679	11868.487	67.12	62.49	49.28	49.956	0.99	2.41	2.55	2.67	31.394
3/5/2025 2:00	53217.277	29445.301	47560.82	8	5.42	5.72	50.037	-0.785	2.48	2.66	2.63	30.08
3/5/2025 3:00	6226.451	-2195.23	6602.101	57.35	36.56	14.05	50.042	0.942	2.95	3.05	3.23	30.79
3/5/2025 4:00	8498.953	-2111.566	8797.565	69.33	55.83	36.74	50.036	0.97	2.69	2.9	2.91	29.624
3/5/2025 5:00	7370.859	-2206.253	7838.653	65.47	51.21	30.62	50.025	0.959	2.56	2.62	2.81	30.703
3/5/2025 6:00	56559.895	46441.664	73209.57	4.28	5.17	5.45	50.02	-0.773	2.01	1.85	1.73	1927.31
3/5/2025 7:00	-4582.261	-758.161	4657.283	24.46	69.28	118.16	50.036	-0.986	2.13	1.97	1.56	10979.999
3/5/2025 8:00	33063.047	41223.598	52727.059	5.48	6.32	7.98	50.031	-0.623	1.56	1.75	1.8	21455.188
3/5/2025 9:00	32699.289	42583.723	53727.754	10.68	8.89	10.93	50.126	-0.609	1.45	1.55	1.38	29083.297
3/5/2025 10:00	-20720.154	617.839	20868.082	13.3	21.54	17.17	50.068	-1	1.74	1.96	1.55	34708.992
3/5/2025 11:00	-28229.242	783.404	28495.307	11.14	12.43	15.33	50.004	-1	2.3	2.28	2.16	37469.871
3/5/2025 12:00	-33270.832	571.983	33295.254	4.37	8.76	6.24	49.97	-1	2.71	2.73	2.69	40377.719
3/5/2025 13:00	-28042.953	653.663	28015.781	4.54	7.86	10.67	49.986	-1	2.78	2.72	2.6	36460.109
3/5/2025 14:00	-24302.738	298.502	24436.838	5.83	9.34	15.84	50.073	-1	2.74	2.85	2.71	30270.26
3/5/2025 15:00	-12116.262	-542.441	12121.79	21.13	13.57	23.49	49.878	-1	2.63	2.77	2.71	19846.797
3/5/2025 16:00	-1578.273	-213.846	1584.721	69.31	69.69	125.58	49.907	-0.992	2.73	2.89	2.6	8365.952
3/5/2025 17:00	11715.465	182.21	11788.191	41.47	41.53	36.62	50.008	1	1.9	2.32	2.49	241.816
3/5/2025 18:00	17297.402	-615.855	17332.156	54.23	36.52	33.29	50.035	0.998	2.16	2.45	2.42	30.463
3/5/2025 19:00	20830.934	2734.806	21009.688	41.73	40.68	24.08	50.047	-0.991	2.87	2.16	2.52	30.637
3/5/2025 20:00	16878.637	-1894.963	17026.086	57.64	55.82	25.35	50.018	0.993	2.25	2.76	2.34	31.267
3/5/2025 21:00	21560.768	5570.142	22270.795	37.26	33.25	18.44	50.01	-0.968	3.18	2.69	3.14	29.915
3/5/2025 22:00	19156.543	5378.232	19903.354	25.42	29.14	12.62	49.953	-0.962	2.77	3.04	3.1	31.775
3/5/2025 23:00	6277.378	-1866.414	6527.733	51.65	49.81	17.87	49.941	0.958	2.83	3.12	3.13	30.427
3/6/2025 0:00	5893.777	-1805.677	6157.643	53.55	46.02	17.53	50.013	0.956	2.65	3.19	3.18	32.387
3/6/2025 1:00	48259.242	47581.219	67771.141	8.09	6.13	6.4	49.907	-0.712	2.52	2.79	2.8	33.058
3/6/2025 2:00	5889.589	-1523.599	6078.155	50.84	39.55	18.14	49.967	0.966	2.82	2.87	3.05	35.04
3/6/2025 3:00	6420.015	-1525.472	6602.302	56.18	38.85	17.15	49.974	0.974	2.76	2.82	2.98	33.56
3/6/2025 4:00	5750.258	-1714.186	5991.347	50.18	44	18.53	50.016	0.958	2.78	3.03	2.94	32.123
3/6/2025 5:00	8867.122	-1714.517	9025.621	46.7	15.3	18.84	49.834	0.981	2.8	2.81	2.79	30.201
3/6/2025 6:00	11940.114	5935.775	13334.158	15.38	18.77	12.25	49.994	-0.895	2.17	2.41	2.18	1845.639
3/6/2025 7:00	12185.486	13891.404	18478.561	11	13.96	17.14	50.073	-0.659	1.87	1.96	1.68	9839.54
3/6/2025 8:00	-9481.544	-51.918	9220.113	14.85	25.91	81.06	49.989	-1	2.14	2.09	1.76	20172.938
3/6/2025 9:00	-11827.568	7785.324	13610.772	14.93	27.74	26.7	50.041	0.808	1.92	1.99	2.18	28850.193
3/6/2025 10:00	-16550.043	-122.575	16550.496	12.5	19.95	31.02	50.01	-1	2.27	2.58	2.34	24814.465
3/6/2025 11:00	0	0	0	0	0	0	0	0	0	0	0	0
3/6/2025 12:00	-15848.649	1886.145	15960.49	22.58	28.31	30.96	49.945	0.993	2.34	2.29	1.76	32164.748
3/6/2025 13:00	-24322.029	1343.703	24360.658	11.32	22.23	22.64	49.983	0.998	4.22	2.19	1.95	36953.598
3/6/2025 14:00	-16452.711	1136.691	17857.529	26.32	37.82	35.16	50.048	0.997	1.82	2.02	2	30887.762
3/6/2025 15:00	55842.738	47990.836	73631.047	8.54	9.37	9.04	49.956	-0.758	2.01	1.89	1.98	9290.829
3/6/2025 16:00	2412.273	375.663	2477.515	169.27	178.48	113.18	50.01	-0.988	2.33	1.99	2.34	7889.741
3/6/2025 17:00	22029.355	5114.121	22622.598	22.63	27.04	19.85	50.067	-0.974	2.25	2.26	2.08	161.012
3/6/2025 18:00	0	0	0	0	0	0	0	0	0	0	0	0
3/6/2025 19:00	25893.027	4788.942	26706.189	42.07	39.57	25.93	50.099	-0.983	2.55	2.01	1.98	47.562
3/6/2025 20:00	68295.969	48829.793	84359.484	11.81	10.81	9.21	49.998	-0.815	2.35	2.29	2.29	48.511
3/6/2025 21:00	54903.578	45002.941	71103.641	13.25	11.23	9.68	49.987	-0.774	2.48	2.5	2.55	48.51
3/6/2025 22:00	46073.605	47731.574	66340.641	10.11	6.97	7.82	49.951	-0.694	2.81	3.02	3	47.852
3/6/2025 23:00	15991.507	-847.117	16896.801	42.93	59.12	47.69	49.935	0.998	2.65	2.71	2.59	48.299
3/7/2025 0:00	5844.174	-1664.914	6076.702	55.63	43.41	14.11	49.984	0.961	2.92	3.4	3.31	50.098
3/7/2025 1:00	12629.602	-868.061	12659.399	65.04	62.2	49.37	49.991	0.997	2.18	2.51	2.44	51.64
3/7/2025 2:00	5950.325	-1812.842	6215.395	52.23	40.97	15.2	49.98	0.956	2.91	3.19	3.29	52.426
3/7/2025 3:00	5939.523	-1576.95	6145.299	54.21	41.67	15.47	49.967	0.965	2.86	3.25	3.2	51.182
3/7/2025 4:00	5780.02	-1682.44	6082.309	51.73	43.22	15.99	50.015	0.96	2.9	3.3	3.21	50.307
3/7/2025 5:00	5822.458	-1549.833	6015.399	48.86	38.57	15.92	50.008	0.966	2.97	3.29	3.28	49.636
3/7/2025 6:00	16706.68	6078.523	17778.121	28.84	27.89	22.55	49.871	-0.939	1.85	2.01	1.78	1690.334
3/7/2025 7:00	-1215.616	561.842	1339.175	27.18	153.83	174.16	50.011	0.906	2.05	1.97	1.95	9979.296
3/7/2025 8:00	31810.504	39580.176	50840.016	7.31	7.15	8.56	50.028	-0.627	1.76	1.79	1.76	19855.514
3/7/2025 9:00	-21812.533	355.05	21815.422	12.82	10.3	13.7	50.04	-1	2.33	2.47	2.34	29818.193
3/7/2025 10:00	-8216.654	7232.19	10959.771	19.4	40.31	51.06	49.991	0.748	2.05	1.96	1.87	34581.742
3/7/2025 11:00	-14002.077	9480.662	17281.846	17.16	40.1	26.72	49.997	0.833	2.07	1.98	1.99	37377.754
3/7/2025 12:00	-26498.189	863.541	26496.613	10.71	19.89	12.7	50.007	-1	2.26	2.3	2.34	37118.246
3/7/2025 13:00	22988.688	41064.863	47079.688	10.86	11.38	11.93	49.978	-0.489	2.02	2.13	1.91	34299.445
3/7/2025 14:00	-8074.237	7103.111	11292.649	23.79	35.06	49.69	49.971	0.777	2.11	2.26	2.17	27642.184
3/7/2025 15:00	-10007.12	412.48	10034.562	32.099	42.37	37.26	49.958	-1	2.23	2.42	2.38	18313.793
3/7/2025 16:00	15642.078	6109.056	16901.912	24.55	49.38	31.16	49.958	-0.932	2.2	2.34	2.19	7738.393
3/7/2025 17:00	14299.587	-747.69	14319.121	58.94	39.89	38.05	50.063	0.998	2.19	2.45	2.41	274.859
3/7/2025 18:00	59135.969	36803.812	69568.172	11.64	12.94	9.77	49.938	-0.848	2.29	2.41	2.14	29.548
3/7/2025 19:00	56587.453	39633.309	68881.539	11.24	9.98	9.36	50.003	-0.818	2.82	2.71	2.85	31.635
3/7/2025 20:00	11639.186	-2376.007	11894.997	54.27	40.59	32.55	49.992	0.979	3.01	3.64	3.1	31.155
3/7/2025 21:00	8811.015	-1784.072	8920.688	46.84	37.13	34.57	49.989	0.979	3.25	3.64	3.76	32.238
3/7/2025 22:00	7376.481	-2039.475	7653.23	59.69	44.11	27.74	49.999	0.963	2.77	3.28	3.2	31.276
3/7/2025 23:00	6080.948	-1760.814	6337.722	62.41	43.32	19.77	50.047	0.96	3.02	3.5	3.29	32.528
3/8/2025 0:00	5794.57	-1406.755	5956.994	67.43	39.12	18.35	49.993	0.97	2.96	3.5	3.36	30.833
3/8/2025 1:00	7060.342	-1081.797	7142.738	49.5	39.33	16.44	50.01	0.988	3.21	3.6	3.36	31.779
3/8/2025 2:00	52742.852	47336.73	70903.031	8.53	6.76	6.73	50.046	-0.744	2.8	2.79	3.01	32.31
3/8/2025 3:00	5659.869	-1501.663	5856.223	64.32	40.63	17.61	50.065	0.966	2.89	3.34	3.33	33.668
3/8/2025 4:00	6021.314	-1142.313	6136.942	51.86	39.23	19.41	50.018	0.982	3.27	3.32	3.23	29.777
3/8/2025 5:00	38586.121	28026.748	45459.941	9.82	6.82	6.73	49.962	-0.787	2.6	2.95	2.86	27.928
3/8/2025 6:00	18074.082	11228.028	21120.168	25.16	16.209	16.26	50.024	-0.846	2.25	2.4	2.33	2111.126
3/8/2025 7:00	6305.376	6315.627	8920.579	35.46	36.57	27.27	50.02	-0.705	1.93	2.27	2.03	10426.938
3/8/2025 8:00	2119.502	8367.779	8661.636	61.55	131.78	59.69	49.942	-0.258	1.72	1.71	1.54	21125.881
3/8/2025 9:00	-20953.289	-128.197	20953.676	8.71	15.4	12.28	49.941	-1	2.25	2.51	2.23	28422.102
3/8/2025 10:00	-19964.639	1103.402	20019.318	14.77	24.64	26.53	50.028	0.998	1.99	2.29	1.78	34874.32
3/8/2025 11:00	-8178.405	7200.995	10906.914	24.9	38.1	61.98	49.969	0.749	1.79	1.84	1.78	36848.922
3/8/2025 12:00	9821.383	31481.576	32978.012	14.31	20.6	15.66	50.001	-0.297	1.95	1.91	1.86	37008.152
3/8/2025 13:00	-20908.979	1397.936	21075.102	22.55	36.16	31.66	50.078	0.997	2.45	2.11	2.42	33974.98
3/8/2025 14:00	-20913.387	195.437	20914.299	14.23	15.72	12.41	50.03	-1	3.06	2.76	2.71	26666.82
3/8/2025 15:00	-10039.418	68.783	9999.199	22.85	48.75	19.29	49.961	-1	2.56	2.64	2.68	16245.17

3/8/2025 16:00	12001.291	6512.057	14319.771	27.73	20.5	23.15	50.025	-0.89	2.72	2.9	2.62	6525.568
3/8/2025 17:00	6362.475	-1328.051	6489.248	51.15	65.129	37.78	50.016	0.98	2.8	3.24	3.28	258.815
3/8/2025 18:00	52833.238	40134.41	66754.367	10.06	12.08	7.01	50.025	-0.799	2.91	2.85	9.67	28.042
3/8/2025 19:00	7856.863	-2059.978	8114.103	62.26	54.94	23.67	50.051	0.967	3.29	3.82	4.12	30.39
3/8/2025 20:00	9620.434	-531.088	9635.081	30.26	49.64	22.79	50.029	0.998	3.44	3.85	4.08	30.272
3/8/2025 21:00	7582.831	-1327.83	7683.034	63.94	31.83	21.07	49.97	0.985	3.46	3.75	3.91	30.25
3/8/2025 22:00	6933.026	-2147.06	7257.872	59.48	46.84	20.78	49.962	0.955	2.72	3.53	3.38	30.838
3/8/2025 23:00	5910.532	-1767.427	6167.76	57.66	47.45	17.5	49.994	0.957	2.95	3.58	3.55	30.015
3/9/2025 0:00	15879.072	6210.578	17053.895	25.42	20.75	10.47	49.967	-0.931	3.14	3.38	3.43	30.468
3/9/2025 1:00	6145.984	-1832.573	6405.246	60.34	46.86	23.96	49.978	0.958	2.9	3.36	3.4	32.037
3/9/2025 2:00	5846.379	-1761.916	6106.102	61.04	50.32	24.69	49.992	0.957	2.96	3.28	3.29	34.416
3/9/2025 3:00	5552.395	-1804.134	5838.149	59.84	49.85	23.52	49.992	0.951	2.99	3.23	3.23	32.583
3/9/2025 4:00	5197.455	-1811.409	5504.066	66.07	51.74	24.37	49.98	0.944	2.77	3.47	3.18	30.462
3/9/2025 5:00	5611.698	-1438.17	5791.988	55.58	46.65	16.29	49.956	0.968	2.91	3.25	3.15	30.805
3/9/2025 6:00	2275.147	-325.509	2295.15	119.27	89.91	49.72	50.048	0.99	2.42	2.81	2.6	2179.173
3/9/2025 7:00	42681.938	41366.785	59430.926	5.23	5.91	6.06	50.073	-0.717	2.04	2.11	2.05	9085.932
3/9/2025 8:00	-3197.772	6517.348	7265.86	19.96	52.53	34.7	50.018	0.442	2.43	2.01	2.32	18004.85
3/9/2025 9:00	-9915.96	6510.735	12798.494	19.28	34.3	23.22	50.036	0.86	2.04	2.16	2.55	28188.566
3/9/2025 10:00	-21913.504	102.183	21913.744	23	15.82	29.28	50.005	-1	2.64	2.69	2.55	31233.256
3/9/2025 11:00	-18707.244	6771.428	19903.865	17.52	13.4	15.06	50.01	0.939	2.26	2.53	2.64	34563.746
3/9/2025 12:00	46896.254	40236.152	61798.891	9.25	7.68	8.33	50.051	-0.759	2.42	2.44	2.57	9022.439
3/9/2025 13:00	-23981.859	337.854	24037.145	12.01	17.94	8.89	50.011	-1	2.67	3.07	2.93	32856.578
3/9/2025 14:00	-19927.932	899.366	19932.643	10.48	14.14	11.01	49.987	0.998	2.63	2.95	2.63	25544.906
3/9/2025 15:00	-12003.496	-416.118	11951.99	20.14	22.15	19.14	49.837	-1	2.98	3.16	3.15	17384.924
3/9/2025 16:00	-1159.289	-109.899	1186.655	104.01	112.71	181.87	49.949	-0.995	2.42	2.97	2.9	6638.754
3/9/2025 17:00	59400.301	48330.234	76578.109	8.84	9.45	6.06	50.065	-0.775	2.21	2.25	2.6	309.252
3/9/2025 18:00	8884.868	-2736.57	9297.861	63.34	59.11	32.169	49.766	0.955	3.22	3.3	3.39	28.173
3/9/2025 19:00	11964.144	-1550.825	12070.358	32.279	52	19.51	49.973	0.991	3.12	3.54	3.7	32.569
3/9/2025 20:00	8854.665	-2428.807	9181.732	64.21	37.5	25.17	50.076	0.964	3.76	3.89	4.29	30.097
3/9/2025 21:00	8989.588	-2445.893	9316.387	56.16	38.88	26.93	50.004	0.964	3.83	3.67	3.98	32.377
3/9/2025 22:00	7269.227	-1804.575	7502.254	61.61	42.71	16.37	49.955	0.97	2.9	3.67	3.54	31.327
3/9/2025 23:00	16057.535	6376.474	17265.074	29.69	19.1	9.04	50.016	-0.929	3.36	3.65	3.94	32.119
3/10/2025 0:00	6479.76	-1673.07	6700.273	63.76	45.44	17.28	49.914	0.968	2.86	3.45	3.46	29.109
3/10/2025 1:00	6158.55	-1576.619	6362.166	68.99	44.41	17.66	49.969	0.968	2.88	3.59	3.45	30.54
3/10/2025 2:00	5773.847	-1739.87	6019.004	66.72	43.58	16.53	49.978	0.957	2.83	3.44	3.31	30.915
3/10/2025 3:00	51913.484	47334.086	70287.758	9.18	7.02	6.68	49.97	-0.739	2.79	2.86	3.03	35.848
3/10/2025 4:00	5840.977	-1881.846	6131.5	64.82	46.98	19.37	49.945	0.951	3.4	3.34	3.61	29.132
3/10/2025 5:00	6912.964	-1966.393	7178.183	62.43	32.2	15.17	50.018	0.961	2.76	3.25	3.23	31.9
3/10/2025 6:00	3705.491	-677.473	3765.671	91.88	53.04	39.46	49.991	0.983	2.47	2.73	2.51	2042.092
3/10/2025 7:00	5985.268	5215.422	8182.039	33.71	35.1	21.12	50.047	-0.828	2.24	2.01	1.97	9240.141
3/10/2025 8:00	-11867.803	1918.002	12021.791	19.69	29.92	30.5	50.01	0.987	2.33	2.34	2.07	18915.236
3/10/2025 9:00	-11420.82	5372.72	12385.467	18.52	23.33	20.14	49.993	0.901	2.34	2.08	2.12	25171.584
3/10/2025 10:00	-24591.871	1240.638	24623.146	7.9	16.24	13.35	49.963	0.998	2.74	2.31	2.27	33241.129
3/10/2025 11:00	-23555.158	248.458	23603.205	8.41	16.65	13.13	49.993	-1	2.63	2.29	2.35	35774.617
3/10/2025 12:00	-6474.359	7602.122	9749.751	28.55	41.3	55.33	49.949	0.626	2.04	2.11	2	34607.504
3/10/2025 13:00	-2841.839	-362.987	3851.713	43.56	70.93	301.17	50.009	-0.995	1.95	2.03	1.94	14202.541
3/10/2025 14:00	36439.945	37690.395	52507.879	9.29	11.17	9.24	49.984	-0.696	1.82	1.84	1.81	20302.732
3/10/2025 15:00	-2410.73	-1089.844	2645.634	107.64	46.2	252.9	49.884	-0.911	2.73	2.67	2.53	15367.489
3/10/2025 16:00	4876.465	-358.578	4889.63	116.56	190.32	40.91	49.957	0.997	2.38	2.21	2.32	5680.43
3/10/2025 17:00	54149.055	40008.531	68087.352	10.41	13.1	9.97	50.033	-0.802	1.76	1.79	1.71	280.433
3/10/2025 18:00	13878.288	-1703.494	13982.446	58.34	55.41	34.07	50.002	0.992	2.85	2.3	2.46	30.015
3/10/2025 19:00	23179.164	3976.767	23517.83	35.14	39.52	17.64	50.097	-0.985	2.73	2.24	2.49	30.794
3/10/2025 20:00	13559.062	-1296.304	13647.771	55.51	53.01	34.73	50.03	0.995	2.61	3.14	2.86	30.876
3/10/2025 21:00	10533.027	-1032.193	10583.482	51.24	53.33	32.189	50.08	0.995	2.58	3.08	2.95	32.81
3/10/2025 22:00	10598.394	-1492.624	10702.985	54.24	51.35	30.2	50.006	0.99	3	3.68	3.3	30.515
3/10/2025 23:00	9423.783	-1468.263	9486.943	57.58	55.16	34.15	50.02	0.988	3.3	3.24	3.26	29.54
3/11/2025 0:00	12466.792	-577.605	12528.726	70.44	65.94	48.23	49.968	0.998	2.81	2.76	2.73	34.089
3/11/2025 1:00	6654.695	-1432.549	7042.135	74.37	51.72	31.1	49.945	0.979	2.95	3.15	3.07	30.268
3/11/2025 2:00	7698.022	-2405.218	8065.129	23.87	46.82	23.29	49.952	0.954	3.11	3.29	3.35	30.052
3/11/2025 3:00	8542.053	-2116.636	8800.388	65.35	56.75	37.17	50	0.97	2.51	2.76	2.86	30.903
3/11/2025 4:00	5212.115	-2125.785	5628.953	62.04	42.13	22.32	50.009	0.926	2.73	3.23	3.21	32.338
3/11/2025 5:00	5370.074	-2122.258	5757.11	48.39	44.43	24.51	49.962	0.929	2.89	3.16	3.05	31.173
3/11/2025 6:00	7066.405	83.774	7079.686	61.43	68.09	49.98	49.994	1	2.15	2.08	1.87	1355.481
3/11/2025 7:00	1487.002	3397.178	3688.485	48.48	256.73	58.35	50.087	-0.47	1.71	2.03	1.93	9214.056
3/11/2025 8:00	-7164.068	979.393	7088.534	26.62	27.02	122.39	50.02	0.99	2.33	2.18	7.17	15825.458
3/11/2025 9:00	-18030.32	2343.159	18216.439	14.67	22.19	23.95	49.942	0.991	2.18	2.28	2.42	25173.129
3/11/2025 10:00	-8136.297	7088.23	10820.049	29.9	39.44	49.96	50.012	0.684	1.91	2.09	1.98	31241.717
3/11/2025 11:00	-17186.4	70.767	17179.822	14.45	18.32	48.84	49.89	-1	1.87	1.92	1.84	30801.275
3/11/2025 12:00	-18247.916	589.84	18308.016	15.54	23.18	20.86	49.955	-1	1.84	2.17	1.73	28227.279
3/11/2025 13:00	-15723.648	-765.657	15731.932	14.8	52.09	19.7	49.851	-0.998	2.24	2.21	2.43	28662.41
3/11/2025 14:00	-12439.676	365.743	12445.35	20.83	21.07	55.61	50.016	-1	2.01	2.14	2.02	22300.41
3/11/2025 15:00	4936.54	5581.055	7451.013	61.26	103.62	40.45	49.886	-0.662	1.97	1.9	1.9	14090.853
3/11/2025 16:00	9366.795	-634.263	9234.391	103.62	25.05	64.48	49.853	0.997	1.97	2.19	2.2	3996.542
3/11/2025 17:00	52733.258	42292.387	67597.648	11.04	10.7	10	50.096	-0.78	1.94	2.05	1.95	263.562
3/11/2025 18:00	9820.61	-2780.331	10210.099	59.23	55.74	38.88	49.916	0.962	2.87	3.01	2.58	29.999
3/11/2025 19:00	29205.881	17281.748	34502.688	24.79	30.96	18.53	50.029	-0.865	2.71	2.82	2.57	29.552
3/11/2025 20:00	16363.974	-2592.719	16568.098	35.33	60.29	39.36	50.049	0.987	2.78	3.12	2.87	31.257
3/11/2025 21:00	8528.385	-2632.843	8925.537	55.91	61.85	33.6	49.893	0.955	3.47	3.37	3.9	32.442
3/11/2025 22:00	17895.4	5230.965	18648.699	33.92	28.42	12.65	50.008	-0.959	3.26	3.26	3.65	32.289
3/11/2025 23:00	5885.841	-1781.757	6154.47	60.5	45.41	19.32	50.016	0.955	3.01	3.74	3.86	31.115
3/12/2025 0:00	5854.756	-1782.639	6104.84	59.81	47.02	19.76	49.899	0.956	3.1	3.65	3.68	30.309
3/12/2025 1:00	6092.081	-1628.317	6312.116	61.16	43.42	19.85	49.924	0.964	3.11	3.58	3.52	30.798
3/12/2025 2:00	6223.365	-1542.668	6411.716	62.1	43.32	18.56	49.963	0.97	3.08	3.59	3.67	31.471
3/12/2025 3:00	5739.896	-1683.653	5981.73	60.36	46.98	17.62	49.915	0.959	3.07	3.49	3.57	31.166
3/12/2025 4:00	49967.59	44000.066	66483.195	9.11	7.09	6.69	50.034	-0.749	2.89	2.95	3.06	27.674
3/12/2025 5:00	7480.097	-1684.204	7653.487	56.9	42.64	10.37	50.008	0.975	2.87	3.31	3.34	29.717
3/12/2025 6:00	21772.078	6343.846	22678.004	40.2	26.95	31.44	50.038	-0.96	1.63	1.69	1.56	2460.478
3/12/2025 7:00	1996.375	685.961	2168.468	252.28	308.08	193.07	50.116	-0.948	1.39	1.43	1.41	9624.275
3/12/2025 8:00	-6529.694	-654.876	6564.974	33.41	27.19	95.74	50.039	-0.995	2.34	2.36	1.69	17571.668
3/12/2025 9:00	-6604.43	6052.068	8953.465	19.25	15.75	31.47	50.054	0.736	2.37	2.41	2.2	26145.678
3/12/2025 10:00	22004.994	39640.254	45382.809	8.96	14.18	12.03	49.97	-0.486	1.98	1.81	1.79	32221.793
3/12/2025 11:00	-8177.743	5910.643	10086.849	18.2	43.2	70.97	49.903	0.81	2.1	1.96	1.92	32279.646
3/12/2025 12:00	-20496.387	774.916	20537.027	11.97	20.9	19.21	49.963	-1	2.39	2.32	2.31	32339.789
3/12/2025 13:00	-19223.01	962.197	19233.756	13.21	17.75	27	50	0.998	2.58	2.37	2.42	29337.576
3/12/2025 14:00	-14869.917	95.238	14870.223	23.48	20.53	21.47	49.878	-1	2.27	2.02	2.12	24337.859

3/12/2025 15:00	2710.555	6618.099	7151.668	52.88	82.77	47.58	49.899	-0.39	2.39	2.1	1.96	16230.375
3/12/2025 16:00	3306.679	547.953	3351.773	234.71	70.15	129.28	49.923	-0.986	1.83	2.03	1.9	8018.663
3/12/2025 17:00	14849.305	4814.956	15611.148	18.77	29.67	15.71	50.001	-0.951	3.25	2.37	2.79	347.085
3/12/2025 18:00	10461.047	-2237.558	10699.313	55.77	59.73	26.21	49.852	0.977	3.33	3.11	3.24	31.002
3/12/2025 19:00	23375.264	3976.216	23711.035	23.15	33.96	18.62	50.04	-0.985	3.07	2.66	3.03	32.754
3/12/2025 20:00	65073.621	55146.086	85297.531	9.97	16.61	10.98	49.946	-0.762	8.73	7.06	9.15	31.578
3/12/2025 21:00	8583.609	-2506.409	8940.051	53.59	57.66	32.7	50.025	0.959	3.64	3.27	3.59	32.122
3/12/2025 22:00	22757.203	6752.249	23737.803	38.75	38.31	26.56	49.991	-0.958	2.99	3.07	3.15	35.137
3/12/2025 23:00	5410.86	-2391.88	5914.304	53.64	50.35	22.11	50.025	0.914	3.39	3.52	3.46	31.337
3/13/2025 0:00	5652.594	-1713.745	5906.669	54.31	49.31	22.4	50.003	0.957	2.93	3.62	3.22	31.636
3/13/2025 1:00	5752.463	-1482.703	5961.825	53.53	49.13	16.78	49.949	0.967	2.96	3.39	3.41	31.43
3/13/2025 2:00	5383.853	-1603.185	5618.642	53.27	50.22	16.75	49.953	0.956	3	3.52	3.49	32.813
3/13/2025 3:00	59411.434	58300.648	91291.508	12.06	11.48	10.99	50.036	-0.788	2.25	2.1	2.37	34.306
3/13/2025 4:00	5380.656	-1712.202	5645.147	54.34	50.19	19.64	50.019	0.953	2.89	3.37	3.15	31.393
3/13/2025 5:00	10115.146	-1398.929	9293.671	61.5	62.84	48.54	49.945	0.988	2.18	2.47	2.39	32.369
3/13/2025 6:00	14647.361	6557.803	16048.364	15.01	24.63	15.78	49.834	-0.912	2.24	2.48	2.23	1960.718
3/13/2025 7:00	-2844.816	-580.691	2867.413	30.63	71.53	142.83	50.01	-0.979	2.26	1.8	1.62	9472.965
3/13/2025 8:00	-5415.93	828.158	5469.245	112.97	95.76	165.11	50.027	0.988	1.99	1.56	1.54	18143.641
3/13/2025 9:00	41249.168	52549.945	66661.375	9.57	9.33	10.18	50.049	-0.617	1.83	1.77	1.77	26322.244
3/13/2025 10:00	-24706.4	901.13	24712.586	12.03	12.82	17.66	50.052	-1	2.59	2.4	2.29	33128.953
3/13/2025 11:00	-15929.999	7006.77	17390.656	14.62	27.3	37.9	50.022	0.915	2.35	2.27	2.12	35359.977
3/13/2025 12:00	-26070.938	874.675	26102.242	12.44	18.28	16.54	50.018	-1	2.39	2.26	2.32	35579.465
3/13/2025 13:00	19290.141	41935.789	46165.578	6.21	7.45	8.09	49.984	-0.418	2.42	2.42	2.38	32062.254
3/13/2025 14:00	-16689.484	708.117	16695.357	17.74	18.19	24.9	49.936	-1	2.3	2.79	2.28	24540.168
3/13/2025 15:00	-7485.94	538.583	7486.488	41.62	45.19	72.11	49.962	0.997	2.13	2.31	1.96	15412.183
3/13/2025 16:00	3505.093	-109.458	3510.458	350.41	69.96	110.63	49.934	0.998	1.93	2.12	1.97	6262.132
3/13/2025 17:00	9073.582	-587.305	9092.569	46.16	52.37	40.79	49.957	0.997	2.41	2.51	2.35	367.319
3/13/2025 18:00	12351.822	-2271.84	12559.011	57.53	59.87	35.12	49.935	0.983	2.57	2.95	2.71	27.967
3/13/2025 19:00	23854.654	4806.8	24324.404	39.24	38.96	22.06	50.093	-0.98	3.22	2.76	2.95	30.774
3/13/2025 20:00	63324.824	55029.242	83866.523	10.99	10.78	8.93	50.008	-0.753	2.94	2.88	3.06	29.48
3/13/2025 21:00	13121.447	1710.99	13232.53	44.84	43.39	24.74	49.947	-0.991	3.08	3.17	3.34	32.768
3/13/2025 22:00	65680.766	60166.289	97055.43	7.8	6.08	6.79	50.101	-0.784	2.78	3.07	2.94	31.627
3/13/2025 23:00	7842.864	-2126.667	8107.574	61.37	48.78	16.33	50.019	0.965	3.17	3.9	3.47	33.541
3/14/2025 0:00	6066.839	-1717.493	6304.837	54.7	46.79	17.04	49.891	0.962	2.95	3.65	3.46	34.771
3/14/2025 1:00	5703.19	-1647.387	5933.279	63.3	46.23	17.77	49.954	0.959	2.85	3.55	3.3	35.692
3/14/2025 2:00	6066.949	-1414.03	6229.554	61.84	46.47	18.81	50.006	0.974	2.88	3.47	3.2	37.131
3/14/2025 3:00	5383.964	-1667.339	5636.23	63.19	48.78	18.04	49.947	0.955	2.89	3.57	3.31	32.078
3/14/2025 4:00	5644.548	-1419.872	5820.391	61.44	46.02	15.82	49.945	0.968	2.8	3.47	3.2	32.673
3/14/2025 5:00	5955.616	-1645.072	6178.643	53.9	39.52	15.57	50.025	0.963	2.78	3.26	3.19	33.261
3/14/2025 6:00	1481.711	-1127.101	1859.48	100.7	101.77	44.2	49.959	0.795	2.68	2.34	2	2289.043
3/14/2025 7:00	13265.85	9287.869	16197.754	19.49	29.14	15.4	49.888	-0.819	4.62	4.84	3.59	9431.256
3/14/2025 8:00	3152.026	-635.475	2809.492	37.74	105.63	43.59	49.947	0.974	4.46	4.06	3.79	6121.112
3/14/2025 9:00	-19344.043	881.95	19364.139	9.09	13.05	23.6	50.018	0.998	2.4	2.38	2.22	27377.371
3/14/2025 10:00	-19167.123	4374.257	19070.195	5.85	15.53	26.03	49.987	0.973	2.98	2.52	2.42	32145.945
3/14/2025 11:00	-18278.008	2464.853	18490.869	16.049	42.64	24.5	49.983	0.991	2.16	2.05	2.06	33246.906
3/14/2025 12:00	-23905.471	454.919	23882.355	5.11	12.74	10.27	49.98	-1	2.76	2.56	2.64	34884.934
3/14/2025 13:00	-12130.37	6888.934	13915.058	6.52	25.24	29.69	49.983	0.868	2.85	2.46	2.27	31407.969
3/14/2025 14:00	-18114.867	386.356	18106.645	7.59	13.78	8.93	49.991	-1	2.38	2.86	2.53	24239.158
3/14/2025 15:00	-10989.71	124.008	10990.41	57.27	61.6	78.26	49.965	-1	2.71	2.66	2.49	17183.766
3/14/2025 16:00	12285.465	5953.412	12790.995	20.12	27.55	22.45	49.904	-0.885	2.8	2.99	2.8	7164.624
3/14/2025 17:00	5715.535	-787.042	5893.654	51.02	60.93	39.14	50.016	0.99	3.06	3.03	3.11	346.112
3/14/2025 18:00	8516.26	-1421.085	8601.222	72.16	54.2	30.51	49.941	0.986	3.1	3.26	3.08	28.879
3/14/2025 19:00	22127.57	8921.906	23866.715	28.5	28.04	10.25	50.019	-0.927	3.04	2.89	3.18	29.069
3/14/2025 20:00	29834.742	5098.468	30206.727	36.21	41.64	23.04	49.972	-0.985	2.71	2.31	2.66	28.188
3/14/2025 21:00	13662.457	-735.675	13666.729	56.62	52.52	32.119	50.042	0.998	3.24	3.29	3.29	32.915
3/14/2025 22:00	16801.258	5372.941	17622.877	34.24	22.02	14.73	49.961	-0.952	3.06	3.49	3.42	30.293
3/14/2025 23:00	7061.003	-2011.807	7339.359	67.5	53.73	24.7	50.005	0.961	2.81	3.4	3.29	28.974
3/15/2025 0:00	5573.118	-1659.071	5810.395	57.78	50.77	22.56	50.061	0.958	2.9	3.5	3.17	29.652
3/15/2025 1:00	5279.686	-1598.004	5507.044	55.85	45.65	25.57	50.02	0.957	2.75	3.63	3.25	31.125
3/15/2025 2:00	5744.636	-1661.055	5984.304	56.39	50.29	25.61	49.958	0.96	2.67	3.18	3.18	33.535
3/15/2025 3:00	5119.081	-1539.913	5349.483	56.53	47.08	26.54	49.983	0.957	2.74	3.29	3.12	33.128
3/15/2025 4:00	5444.921	-1554.683	5662.527	57.96	41.28	17.67	49.94	0.959	2.75	3.27	3.15	30.414
3/15/2025 5:00	4868.859	-1652.678	5152.458	54.93	49.09	19.8	49.934	0.947	2.8	3.28	2.99	29.23
3/15/2025 6:00	11172.472	5332.156	12393.534	18.27	25.91	13.9	50.007	-0.902	2.32	2.66	2.5	2335.869
3/15/2025 7:00	-443.675	-309.856	541.164	256.06	116.91	74.03	50.069	-0.819	1.94	2.01	2.17	9692.311
3/15/2025 8:00	-12351.603	1225.978	12412.296	19.41	21.47	30.25	50.017	0.995	1.88	2.46	2.14	18571.082
3/15/2025 9:00	-6857.187	7246.74	9955.825	21.62	32.74	47.52	50.012	0.685	1.88	1.98	1.86	27010.428
3/15/2025 10:00	-23203.746	597.115	23206.361	12.57	17.17	15.16	50.031	-1	2.38	2.38	2.29	33187.164
3/15/2025 11:00	32678.234	48469.344	58456.34	7.12	5.69	8.26	50.023	-0.559	2.6	2.31	2.35	35561.043
3/15/2025 12:00	-28226.043	310.407	28226.65	5.47	7.31	17.56	49.997	-1	2.64	2.71	2.52	35368.254
3/15/2025 13:00	-10874.521	9917.393	14717.671	13.62	15.2	23.05	49.986	0.738	2.56	2.58	2.71	31584.41
3/15/2025 14:00	-21222.252	139.992	21222.713	9.44	10.33	11.43	49.938	-1	2.68	2.75	2.65	26010.168
3/15/2025 15:00	-9595.852	1013.895	9649.267	35.52	39.25	41.31	49.9	0.994	2.24	2.25	1.95	17048.773
3/15/2025 16:00	1013.454	-171.407	1027.847	533	169.8	148.86	49.881	0.986	2.38	2.34	2.53	7019.384
3/15/2025 17:00	17430.229	5748.715	18353.764	20.85	15.27	14.45	50.008	-0.949	3.24	3.17	2.58	512.446
3/15/2025 18:00	12647.019	-1952.063	12796.782	58.96	59.71	41.22	49.909	0.988	2.15	2.69	2.56	28.694
3/15/2025 19:00	6698.677	-2820.896	7254.187	72.38	61.56	21.14	50.037	0.921	3.36	3.41	3.75	31.11
3/15/2025 20:00	6083.704	-2740.538	6677.004	60.71	44.96	24.14	-2748.915	0.911	3.43	3.76	3.89	30.783
3/15/2025 21:00	7571.148	-1122.472	7670.258	60.64	27.26	25.85	50.041	0.989	3.18	3.8	3.89	29.797
3/15/2025 22:00	15128.737	4373.706	15763.308	36.88	27.05	10.39	49.936	-0.96	3.44	3.3	3.48	28.551
3/15/2025 23:00	9706.743	-1512.686	9919.434	59.86	35.38	37.18	49.986	0.987	2.44	3.18	2.86	29.65
3/16/2025 0:00	14171.72	4789.052	14974.698	32.85	18.97	9.34	50.016	-0.947	2.9	3.44	3.3	30.621
3/16/2025 1:00	4470.488	-2164.586	5009.348	79.28	46.12	18.03	50.023	0.9	3.21	3.65	2.87	30.86
3/16/2025 2:00	4365.218	-2276.911	4944.284	62.84	46.79	22.55	50.026	0.883	3	3.37	3.13	31.783
3/16/2025 3:00	4385.39	-2223.78	4907.363	62.42	47.46	21.77	50.004	0.889	3.02	3.42	3.04	30.745
3/16/2025 4:00	4377.784	-2211.654	4914.575	63.22	46.98	22.01	49.956	0.891	3.09	3.29	3.08	28.9
3/16/2025 5:00	4547.759	-2113.439	5014.852	58.73	49.75	23.82	49.995	0.906	2.78	3.26	2.89	31.471
3/16/2025 6:00	3733.49	-814.93	3923.66	151.64	115.34	60.03	50.04	0.978	1.61	2.01	2.23	2495.009
3/16/2025 7:00	-6545.237	-353.507	6554.777	24.37	32.86	71.13	50.101	-0.998	2.41	2.43	2.03	10184.897
3/16/2025 8:00	-2197.655	5706.055	6132.193	39.62	43.51	55.2	50.06	0.366	2.06	1.96	2.03	20107.992
3/16/2025 9:00	-17733.252	1138.786	17769.779	28.31	22.23	29.82	50.01	0.997	2.16	2.02	2.13	28154.631
3/16/2025 10:00	-23949.453	818.347	23916.828	19.14	16.71	22.62	49.985	-1	1.97	2.07	2.06	34281.703
3/16/2025 11:00	-25099.043	-331.902	25080.83	15.8	16.45	25.31	50.018	-1	2.32	2.36	2.53	35430.188
3/16/2025 12:00	-15653.542	6933.356	17120.303	28.83	20.54	29.56	49.966	0.914	2.13	2.27	2.18	35663.59
3/16/2025 13:00	-10168.607	1072.427	10097.63	21.82	68.05	27.33	49.927	0.994	1.93	2.45	2.38	20586.824

3/16/2025 14:00	-1340.286	181.989	1352.585	81.81	155.17	196.61	49.934	0.99	2.12	2.27	2.17	11094.897
3/16/2025 15:00	-1152.675	4145.75	4299.34	53.67	210.32	60.76	49.941	0.264	3.28	2.72	3.4	12208.347
3/16/2025 16:00	-136.134	-1095.024	1106.596	75.89	160.56	172.12	50.053	-0.119	3.32	3.02	3.15	4833.372
3/16/2025 17:00	7500.489	-1690.046	7688.536	118.01	26.5	48.04	50.061	0.976	3.35	3	3.32	707.63
3/16/2025 18:00	22025.717	5730.747	23239.316	34.94	39.09	20.88	49.991	-0.969	2.56	2.39	2.43	28.221
3/16/2025 19:00	13699.164	-2898.608	14004.947	70.79	39.15	35.95	50.09	0.978	2.89	2.83	2.78	31.208
3/16/2025 20:00	7076.104	-1803.252	7347.023	82.79	49.45	35.82	50.028	0.969	3.67	4.09	3.65	30.767
3/16/2025 21:00	28320.734	20123.369	32408.312	68.06	47.97	8.93	50.031	-0.783	3.77	3.84	3.63	30.316
3/16/2025 22:00	11701.906	2860.137	12052.687	35.23	35.35	17.25	49.88	-0.971	3.64	3.59	3.83	30.143
3/16/2025 23:00	13707.872	-767.972	13729.368	65.46	66.01	48.55	49.98	0.998	2.18	2.84	2.78	28.463
3/17/2025 0:00	5822.458	-1692.361	6076.762	72.04	44.35	20.28	50.051	0.959	2.49	3.54	3.44	29.604
3/17/2025 1:00	5952.089	-1735.571	6206.739	71.97	46.76	23.09	50.008	0.96	2.57	3.23	3.22	29.043
3/17/2025 2:00	12625.304	-650.577	12537.585	68.91	70.97	49.47	49.966	0.998	2.13	2.74	2.58	30.92
3/17/2025 3:00	5241.105	-1868.839	5577.101	72.53	47.07	22.02	49.928	0.94	2.45	3.29	3.08	32.013
3/17/2025 4:00	6617.879	-1667.339	6808.653	70.98	45.82	23.15	50.048	0.969	2.48	3.27	3.13	30.091
3/17/2025 5:00	6056.697	-1692.802	6284.176	73.51	31.04	19.52	50.033	0.963	2.51	2.95	2.92	29.771
3/17/2025 6:00	1680.566	-495.924	1753.586	210.51	103.1	69.42	50.042	0.959	2.48	2.65	2.35	2475.416
3/17/2025 7:00	-3429.145	568.015	3690.384	70.23	78.3	142.31	50.087	0.987	1.79	1.34	1.61	10679.427
3/17/2025 8:00	0	0	0	0	0	0	0	0	0	0	0	0
3/17/2025 9:00	-5702.639	6703.306	10573.847	12.45	24.62	37	49.997	0.773	2.91	2.44	2.34	29481.484
3/17/2025 10:00	-19941.158	1905.876	19967.508	27.88	29.25	57.94	49.97	0.995	2	1.86	1.71	35753.586
3/17/2025 11:00	-30533.27	1025.028	30550.473	5.12	8.06	12.94	49.971	-1	2.84	2.74	2.67	37973.086
3/17/2025 12:00	-29025.434	1927.481	29141.055	6.37	7.28	7.67	50.044	0.997	2.99	2.74	2.56	35966.246
3/17/2025 13:00	-17652.123	1546.747	17749.627	7.77	16.11	14.76	50.041	0.996	2.75	2.31	2.58	25987.867
3/17/2025 14:00	-20516.891	652.892	20527.275	6.17	18.76	9.35	49.915	-1	2.2	2.54	2.43	25812.205
3/17/2025 15:00	47071.629	46570.742	66216.102	5.03	5.8	5.96	49.836	-0.71	2.36	2.39	2.13	16868.939
3/17/2025 16:00	3.306	-218.034	226.326	71.48	91.13	448.04	50.052	0.03	2.65	2.66	2.49	6538.045
3/17/2025 17:00	10558.381	-371.364	10572.731	53.12	52.56	42.38	50.055	1	2.23	2.21	1.98	462.512
3/17/2025 18:00	10704.986	-1533.299	10814.145	54.65	53.3	37.28	50.038	0.989	2.45	2.54	2.37	29.182
3/17/2025 19:00	9443.294	-2304.688	9721.64	24.21	51.61	26.17	50.017	0.971	2.7	3.03	3.26	29.548
3/17/2025 20:00	7290.612	-2254.865	7627.133	57.98	49.56	35.02	49.995	0.955	3.4	3.43	3.51	32.204
3/17/2025 21:00	7030.91	-2009.382	7315.08	65.089	47.36	28.98	50.062	0.961	3.25	3.81	3.82	30.789
3/17/2025 22:00	6208.815	-1740.421	6447.498	63.92	47.54	23.94	50.04	0.962	3.09	3.72	3.75	31.041
3/17/2025 23:00	7086.025	-1739.76	7291.87	67.79	42.74	10.85	50.015	0.971	2.54	3.63	3.51	33.02
3/18/2025 0:00	5454.842	-1302.147	5613.363	59.95	40.82	18.04	49.998	0.971	2.68	3.53	3.22	34.781
3/18/2025 1:00	5558.899	-1243.174	5687.584	63.97	36.73	18.38	50.001	0.974	2.81	3.43	3.25	32.392
3/18/2025 2:00	5169.015	-1339.845	5339.841	62.36	45.82	18.98	50.006	0.968	2.64	3.41	3.15	30.08
3/18/2025 3:00	5007.528	-1495.159	5229.557	61.55	43	17.19	50	0.958	2.59	3.18	3.08	30.699
3/18/2025 4:00	5137.489	-1412.046	5329.139	56.08	45.53	16.85	50.032	0.964	2.68	3.2	3.02	29.981
3/18/2025 5:00	14665.771	-432.432	14688.23	63.65	41.55	51.89	50.054	1	1.9	2.38	2.13	32.73
3/18/2025 6:00	1606.161	-91.16	1608.746	207.37	108.34	51.14	50.006	0.998	2.43	2.52	2.47	2866.671
3/18/2025 7:00	7558.03	5939.964	9612.855	29.29	77.87	30.96	50.116	-0.786	1.64	1.69	1.71	10603.024
3/18/2025 8:00	16319.222	11655.169	20089.373	37.82	53.52	29.38	50.054	-0.814	1.32	1.71	1.38	19447.729
3/18/2025 9:00	-17342.156	858.14	17343.775	17.67	17.15	33.31	49.982	0.998	1.9	2.11	1.36	27650.713
3/18/2025 10:00	-24512.396	1268.747	24536.732	12.18	12.22	16.34	50.054	0.998	2.2	2.32	2.22	32552.008
3/18/2025 11:00	-21917.912	1658.079	21934.596	13.42	19.25	25.25	50.006	0.997	2.23	2.22	1.69	33310.75
3/18/2025 12:00	-14350.844	7377.694	16136.204	16.309	23.08	35.21	49.996	0.888	2.01	2.17	1.86	34644.332
3/18/2025 13:00	-16219.572	747.8	16236.801	19.29	18.12	36.73	50.028	0.998	2.17	2.28	1.77	29654.273
3/18/2025 14:00	-16516.201	-266.866	16511.965	8.189	12.07	34.15	49.874	-1	2.77	2.85	2.69	24659.895
3/18/2025 15:00	-7973.597	113.757	7950.381	34.39	33.07	56.35	49.901	-1	2.24	2.56	2.31	14462.598
3/18/2025 16:00	-254.08	-534.615	591.921	122.63	110.62	127.06	50.003	-0.429	2.16	2.58	2.37	5457.976
3/18/2025 17:00	8399.306	-832.567	-855.164	56.53	21.59	44.78	50.054	0.994	3.02	2.87	2.96	448.772
3/18/2025 18:00	10562.569	-2123.029	10684.568	57.94	58.71	42.9	49.929	0.98	2.42	2.81	2.5	28.846
3/18/2025 19:00	12253.057	-1812.401	12346.245	56.07	40.5	32.82	50.041	0.989	2.76	2.8	2.69	31.197
3/18/2025 20:00	19521.732	6302.62	20472.109	31.26	22.77	17.17	50.052	-0.951	3.16	3.03	3.14	28.017
3/18/2025 21:00	11603.802	-1713.415	11739.435	60.45	53.14	26.87	49.996	0.989	2.45	3.17	2.85	27.855
3/18/2025 22:00	7169.69	-1589.847	7462.288	54.18	43.41	22.66	49.997	0.976	2.82	3.46	3.34	30.34
3/18/2025 23:00	6316.51	-1513.678	6493.757	47.95	43.77	20.94	49.988	0.972	2.69	3.36	3.16	29.012
3/19/2025 0:00	5891.793	-1802.37	6339.792	56.6	45.33	19.28	50.002	0.958	2.69	3.56	3.37	29.832
3/19/2025 1:00	57277.938	47271.477	52622.828	7.47	5.86	6.4	50.004	-0.769	2.89	2.88	3.13	28.556
3/19/2025 2:00	7554.723	-1404.109	7686.344	27.58	41.21	18.74	49.982	0.982	3.04	3.41	3.23	30.222
3/19/2025 3:00	16728.064	5561.655	17654.439	19.72	15.16	8.34	49.993	-0.949	2.88	3.29	3.21	28.545
3/19/2025 4:00	7152.383	-1676.488	7351.818	30.91	43.38	18.79	49.999	0.973	2.81	3.17	3.07	29.396
3/19/2025 5:00	14059.947	-590.391	14076.521	46.83	61.95	50.82	49.977	1	2.24	2.47	2.19	28.86
3/19/2025 6:00	4943.154	-453.486	4956.228	35.51	47.41	58.21	49.966	0.995	2.55	2.71	2.53	2495.31
3/19/2025 7:00	-1776.356	90.939	1758.382	179.64	114.16	74.95	50.05	0.998	2.19	2.37	2.09	9829.379
3/19/2025 8:00	3625.685	10719.316	11315.534	20	45.01	21.42	50.065	-0.324	2.49	2.23	2.36	18715.898
3/19/2025 9:00	-14230.143	524.694	14268.433	24.79	29.05	29.72	50.012	-1	2.02	2.06	1.89	26083.477
3/19/2025 10:00	-21045.002	1143.305	21198.98	19.5	20.66	14.27	50.025	0.998	2.16	2.08	2.16	31735.914
3/19/2025 11:00	-26523.654	994.054	26534.156	11.83	14.8	11.37	49.947	-1	1.71	2.07	2.05	36583.055
3/19/2025 12:00	-15625.874	7244.426	17148.002	20.28	18.6	21.42	49.963	0.906	2.04	2.19	2.07	35547.887
3/19/2025 13:00	-20680.361	453.376	20740.211	23.37	15.52	14.68	49.963	-1	2.25	2.36	2.21	31435.648
3/19/2025 14:00	-10978.798	1220.576	11026.061	91.17	27.32	26.03	49.955	0.993	2.17	2.26	2.07	23793.74
3/19/2025 15:00	-2806.455	808.647	2920.634	61.11	65.63	112.02	49.998	0.96	2.23	2.1	2.2	13901.818
3/19/2025 16:00	2542.565	-870.817	2687.556	47.2	51.67	148.06	50.045	0.946	2.85	2.59	2.8	5163.226
3/19/2025 17:00	10173.898	-807.765	10196.545	56.89	42.24	44.38	50.014	0.996	2.36	2.37	2.03	751.132
3/19/2025 18:00	17972.23	-2037.16	18030.691	58.16	36.32	41.54	50.006	0.993	2.43	2.66	2.55	32.696
3/19/2025 19:00	28118.24	4220.596	28433.236	39.24	37.77	24.32	50.045	-0.988	2.86	2.28	2.71	29.877
3/19/2025 20:00	23849.252	5299.528	24430.961	39.08	29.42	19.55	50.018	-0.976	3.11	2.98	2.92	30.508
3/19/2025 21:00	14931.755	-1093.591	14962.395	58.35	29.37	32.93	49.991	0.997	3.18	3.28	3.25	30.198
3/19/2025 22:00	6920.46	-1693.794	7135.004	52.67	44.43	17.15	50.003	0.971	3.4	3.66	3.71	31.391
3/19/2025 23:00	5985.82	-1672.519	6217.739	55.26	45.11	15.49	49.959	0.961	3	3.38	3.35	31.731
3/20/2025 0:00	5233.389	-1790.355	5543.961	56.64	47.48	18.64	49.966	0.946	3	3.28	3.35	33.389
3/20/2025 1:00	64871.789	57655.805	86556.469	7.16	6.13	6.17	49.993	-0.745	2.52	2.66	2.78	29.577
3/20/2025 2:00	5655.46	-1704.706	5901.039	54.52	46.89	16.94	50.002	0.958	3.03	3.15	3.16	33.368
3/20/2025 3:00	59460.047	54152.141	80452.43	7.14	6.22	5.84	50.014	-0.739	2.31	2.53	2.69	29.344
3/20/2025 4:00	5609.384	-1700.408	5861.448	54.76	41.45	20.76	41.54	0.957	20.08	3.13	3.4	32.477
3/20/2025 5:00	5776.933	-1552.92	5982.016	53.78	39.67	18.51	50.027	0.965	2.72	3.02	3.14	31.689
3/20/2025 6:00	19478.633	10997.427	22368.74	8.78	15.78	8.64	50.037	-0.87	2.68	2.57	2.35	248.484
3/20/2025 7:00	7640.702	-1309.312	7723.391	79.1	33.15	40.4	50.108	0.985	2.6	2.13	2.64	940.756
3/20/2025 8:00	7547.338	-1144.518	7672.969	41.62	123.31	25.94	50.067	0.988	2.38	2.53	2.29	3400.932
3/20/2025 9:00	33739.086	30210.406	45287.91	11.41	15.37	13.56	49.98	-0.744	1.8	1.77	1.62	1147.135
3/20/2025 10:00	7452.209	-21.715	7453.45	87.21	62.01	38.32	50.084	1	1.83	1.73	1.78	2501.128
3/20/2025 11:00	63353.039	45547.477	78149.453	7.42	7.99	7.74	49.92	-0.812	1.62	1.57	1.69	3720.018
3/20/2025 12:00	7591.209	-543.544	7613.832	68.93	73.71	31.12	50.01	0.997	2.17	2.08	2.22	2007.986

3/20/2025 13:00	5970.608	-532.962	5977.111	106.51	103.23	50.7	50.006	0.996	2.15	1.87	1.96	4083.249
3/20/2025 14:00	9701.453	-534.064	9727.883	83.07	38.87	52.06	49.905	0.998	3.25	3.18	3.94	3759.015
3/20/2025 15:00	4342.842	-730.273	4400.988	190.76	118.97	81.23	49.827	0.986	2.02	1.63	1.93	5629.955
3/20/2025 16:00	18585.439	5436.213	19364.168	29.31	40.18	19.78	49.926	-0.959	2.01	1.79	1.94	1594.619
3/20/2025 17:00	12857.117	-1593.484	13149.025	50.98	47.84	39.59	50.073	0.992	2.48	2.05	2.25	89.781
3/20/2025 18:00	16726.301	-1611.121	16803.715	44.82	41.73	32.58	50.047	0.995	2.65	1.89	2.13	32.307
3/20/2025 19:00	9357.204	-2998.255	9825.757	66.11	49.73	23.89	49.993	0.952	2.77	2.82	3.29	34.456
3/20/2025 20:00	13473.633	-2492.63	13696.734	54.73	27.52	19.8	49.961	0.983	3.52	2.89	3.31	30.892
3/20/2025 21:00	55265.129	44096.52	70666.172	12.67	12.41	10.63	50.05	-0.781	2.56	2.43	2.66	31.903
3/20/2025 22:00	22159.979	5846.379	22895.73	27.82	31.52	21.19	50	-0.966	2.81	3.17	3.06	31.526
3/20/2025 23:00	10442.639	-1606.822	10576.65	60.83	57.7	35.56	49.961	0.988	2.71	2.86	2.79	33.701
3/21/2025 0:00	9208.614	-1651.906	9355.606	61.97	61.27	37.51	49.947	0.984	2.62	2.67	2.61	33.136
3/21/2025 1:00	8755.349	-1506.623	8884.794	62.4	60.33	33.24	49.966	0.986	2.49	2.57	2.61	33.74
3/21/2025 2:00	9440.538	-1320.224	9532.406	60.54	55.17	32.689	49.902	0.991	2.72	2.65	2.66	32.781
3/21/2025 3:00	5887.384	-1763.68	6145.882	54.35	46.56	20.73	50	0.957	2.89	2.97	3.03	33.591
3/21/2025 4:00	6017.896	-1691.369	6256.158	47.86	45.38	19.5	50.018	0.962	2.86	2.87	3	33.72
3/21/2025 5:00	47545.945	45311.914	65709.281	7.26	6.58	6.64	50.027	-0.724	2.49	2.55	2.69	30.827
3/21/2025 6:00	14025.775	5627.351	15112.56	13.9	29.29	14.15	49.995	-0.928	2.45	2.41	2.42	815.417
3/21/2025 7:00	1247.252	264	1021.164	69.67	67.24	405.01	50.052	-0.965	1.74	1.95	1.99	7457.332
3/21/2025 8:00	-9531.258	6529.805	11562.135	17.41	21.82	46.86	50.068	0.825	2.45	2.09	2.13	28523.492
3/21/2025 9:00	4532.768	5725.566	7290.719	24.68	75.35	21.71	49.985	-0.619	2.49	2.23	2.21	11564.962
3/21/2025 10:00	-24198.682	1206.026	24329.561	16.46	18.73	23.05	50.039	0.998	2.06	2.07	1.98	35024.277
3/21/2025 11:00	37348.793	41483.406	55398.766	7.52	8.21	9.18	49.859	-0.662	1.77	1.96	1.93	20304.111
3/21/2025 12:00	4259.728	158.29	4288.224	238.81	155.32	46.61	49.926	1	1.82	2.16	1.85	12234.261
3/21/2025 13:00	9446.711	-539.134	9469.017	45.12	34.47	69.92	49.949	0.998	2.13	2.06	1.93	4664.614
3/21/2025 14:00	8437.225	-749.233	8470.426	53.79	59.5	38.79	49.962	0.996	1.98	2.06	1.87	877.548
3/21/2025 15:00	11859.094	-821.985	11887.547	63	27.47	41.77	49.949	0.997	1.8	1.74	1.79	849.941
3/21/2025 16:00	5780.24	-1371.481	5939.754	66.22	73.24	43.34	50.009	0.973	2.66	2.56	2.49	948.388
3/21/2025 17:00	12500.192	-1016.1	13104.683	52.92	40.64	31.72	49.973	0.996	2.37	2.47	2.04	73.369
3/21/2025 18:00	13099.292	-2246.487	13122.597	65.42	58.77	40.25	49.905	0.985	2.04	2.19	2.22	29.423
3/21/2025 19:00	11380.366	-2339.962	11619.907	58.21	51.51	39.88	49.994	0.979	2.47	2.73	2.29	27.539
3/21/2025 20:00	20568.258	5730.858	21351.719	33.49	29.76	18.42	49.997	-0.963	2.44	2.23	2.46	28.134
3/21/2025 21:00	12678.324	-623.681	13021.975	61.52	38.93	34.41	50.05	0.998	2.8	2.89	2.79	31.847
3/21/2025 22:00	14057.191	-1419.542	14132.633	36.66	61.25	20.44	49.987	0.994	2.92	2.96	3.04	28.49
3/21/2025 23:00	6454.407	-1656.316	6676.886	60.73	38.65	16.28	49.963	0.968	2.85	3.12	3.2	31.358
3/22/2025 0:00	7506.552	-1651.135	7667.913	31.84	44.26	16.17	49.953	0.977	3.05	3.22	3.22	31.12
3/22/2025 1:00	7224.915	-1517.536	7357.326	31.41	44.32	16.67	49.917	0.977	3.04	3.33	3.18	31.684
3/22/2025 2:00	7265.921	-1636.584	7443.007	33.23	45.34	15.75	49.983	0.975	3.14	3.32	3.33	31.831
3/22/2025 3:00	5172.763	-1662.378	5437.729	62.7	47.41	17.53	49.951	0.951	2.96	3.23	3.27	29.026
3/22/2025 4:00	5291.15	-1637.907	5557.294	54.4	46.68	19.21	49.975	0.955	3.04	3.15	3.22	28.294
3/22/2025 5:00	5079.618	-1459.114	5250.077	52.22	46.94	16.43	50.06	0.96	2.55	3.16	3.11	28.973
3/22/2025 6:00	13852.384	5849.685	15036.867	17.06	19.8	13.05	49.997	-0.921	2.86	2.57	2.69	1686.58
3/22/2025 7:00	104.387	-749.453	756.688	123.56	150.6	196.4	50.027	0.145	2.04	2.32	2.02	5280.596
3/22/2025 8:00	127.095	128.638	180.834	39.21	42.34	184.75	50.012	-0.662	2.23	2.29	1.98	9544.878
3/22/2025 9:00	-2847.792	1417.116	3181.889	48.28	231.14	234.19	50	0.895	2.02	1.75	1.75	17181.854
3/22/2025 10:00	-18310.416	1670.756	18386.482	27.08	22.88	20.36	49.937	0.995	2.02	1.88	1.7	36267.715
3/22/2025 11:00	-21926.732	816.583	22372.283	19.12	14.65	19.66	50.012	-1	2.28	2.39	2.15	38016.168
3/22/2025 12:00	5892.014	989.534	5746.372	33.94	173.4	130.399	49.98	-0.985	2.31	2.07	2.1	7432.465
3/22/2025 13:00	0	0	0	0	0	0	0	0	0	0	0	36068.641
3/22/2025 14:00	-18816.48	708.999	18829.834	15.65	15.38	15.83	49.907	-1	2.37	2.51	2.52	28868.457
3/22/2025 15:00	5379.995	-1053.798	5497.05	48.52	121.86	91.29	49.951	0.981	2.03	2.06	2.04	4979.413
3/22/2025 16:00	12275.322	-1545.975	12239.641	35.31	50.49	40.93	50.012	0.992	2.34	2.35	2.11	1448.642
3/22/2025 17:00	13242.48	-210.098	13245.689	26.33	49.04	39.72	49.986	1	2.05	2.22	2.35	116.029
3/22/2025 18:00	0	0	0	0	0	0	0	0	0	0	0	0
3/22/2025 19:00	66262.672	50499.781	83286.094	10.2	9.4	9.57	50.026	-0.795	2.15	2.4	2.3	27.602
3/22/2025 20:00	12521.025	-1494.388	12611.421	58.64	42.99	34.46	49.979	0.992	2.59	3.03	2.87	30.002
3/22/2025 21:00	9626.938	-2357.709	9943.245	55.37	48.31	19.11	49.962	0.971	3.38	3.64	3.47	29.908
3/22/2025 22:00	6849.582	-2031.428	7139.504	54.13	35.49	24.52	49.912	0.958	3.45	3.69	3.55	29.261
3/22/2025 23:00	6888.493	-1823.975	7117.254	54.68	39.56	21.76	49.892	0.966	3.29	3.68	3.52	29.085
3/23/2025 0:00	17877.432	6095.719	18906.361	20.04	18.29	12.71	49.901	-0.946	3.34	3.52	3.42	28.976
3/23/2025 1:00	7702.652	-1670.535	7877.736	30.66	46.82	21.17	50.016	0.977	3.55	3.52	3.52	29.885
3/23/2025 2:00	7892.357	-1366.521	8010.004	29.1	45.61	17.87	49.967	0.985	3.38	3.43	3.43	31.602
3/23/2025 3:00	7506.662	-1636.364	7696.302	32.39	47.12	19.87	49.992	0.975	3.2	3.28	3.42	29.799
3/23/2025 4:00	7187.657	-1694.786	7384.762	31.59	44.67	17.56	50.003	0.973	3.29	3.37	3.58	29.135
3/23/2025 5:00	8126.156	-1725.43	8307.317	29.76	26.33	21.43	50.052	0.978	2.69	3.54	3.43	31.869
3/23/2025 6:00	7198.018	-506.617	7215.824	29.18	33.63	35.15	50.005	0.997	2.93	2.8	3.02	523.258
3/23/2025 7:00	6831.614	-820.441	6880.703	37.89	89.23	54.34	50.068	0.992	2.36	2.16	2.27	1727.379
3/23/2025 8:00	12387.316	6015.802	13770.82	27.04	29.98	22.01	49.961	-0.899	1.98	2.19	2.15	5882.796
3/23/2025 9:00	-4325.535	134.26	4375.876	46.68	66.1	89.04	49.983	-1	2	2.21	2.1	13446.168
3/23/2025 10:00	-5412.513	1601.201	5757.695	51.74	53.69	83.84	50	0.959	1.92	2.42	2.2	18371.324
3/23/2025 11:00	0	0	0	0	0	0	0	0	0	0	0	0
3/23/2025 12:00	0	0	0	0	0	0	0	0	0	0	0	7188.857
3/23/2025 13:00	0	0	0	0	0	0	0	0	0	0	0	0
3/23/2025 14:00	7749.279	5177.503	9417.504	31.2	41.97	16.83	49.943	-0.835	2.73	2.65	2.54	9480.467
3/23/2025 15:00	7348.813	-1186.185	7443.93	52.88	57.07	17.29	50.037	0.986	2.82	2.67	2.9	674.044
3/23/2025 16:00	3640.235	-1172.847	3824.815	111.72	80.58	52.68	49.997	0.95	2.49	2.74	2.78	2644.564
3/23/2025 17:00	16154.427	5542.144	16933.902	30.79	33.82	12.68	49.989	-0.945	2.58	2.52	2.74	172.548
3/23/2025 18:00	8067.623	-2933.33	8584.345	64.44	58.13	44.86	50.018	0.939	3.58	2.79	3.3	35.349
3/23/2025 19:00	7709.266	-2148.493	8003.049	66.63	56.07	26.32	50.008	0.963	3.24	3.08	3.31	39.747
3/23/2025 20:00	8543.155	-1830.258	8737.011	60.01	39.28	26.63	50.027	0.977	3.77	2.9	3.34	29.498
3/23/2025 21:00	22534.318	5349.903	23160.676	36.44	33.64	18.38	49.973	-0.972	2.87	3.2	2.92	45.222
3/23/2025 22:00	6441.4	-1568.352	6629.583	52.16	50.74	20.13	49.955	0.971	3.85	4.07	3.9	42.609
3/23/2025 23:00	22357.84	438.605	11147.044	40.78	28.98	9.44	50.013	1	3.35	4.02	3.64	45.655
3/24/2025 0:00	22584.916	19820.127	30060.992	13.73	9.98	8.31	49.966	-0.654	3.16	3.29	3.32	42.005
3/24/2025 1:00	5390.026	-1413.148	5572.197	62.24	52.52	22.89	49.967	0.965	4.03	4.05	3.85	45.591
3/24/2025 2:00	5535.089	-1379.969	5704.518	54.41	51.89	22.65	49.965	0.97	3.58	3.7	3.58	45.536
3/24/2025 3:00	5208.808	-1427.478	5400.868	63.92	53.82	21.97	49.962	0.964	3.95	3.83	3.61	37.588
3/24/2025 4:00	5281.781	-1596.461	5517.78	60.04	53.63	25.45	50.026	0.957	3.56	3.88	3.64	31.388
3/24/2025 5:00	5105.964	-1380.3	5295.042	43.05	54.62	24.32	50.044	0.965	3.29	3.62	3.18	31.061
3/24/2025 6:00	48996.906	43684.039	65642.914	5.14	5.65	6.39	50.037	-0.746	2.13	2.19	2.01	2132.235
3/24/2025 7:00	-2611.238	196.319	2618.608	44.59	111.87	128.74	50.059	0.997	2.46	2.06	2.3	7735.353
3/24/2025 8:00	-4012.151	6805.82	7900.414	14.64	41.2	38.35	49.941	0.507	2.57	2.86	1.89	18914.555
3/24/2025 9:00	-11669.829	845.905	11700.448	37.22	46.28	58.06	50.035	0.997	1.86	1.74	2.23	29102.881
3/24/2025 10:00	-9570.94	945.112	9617.49	20.54	84.6	171.12	50.048	0.995	2.14	2.01	2.02	22058.609
3/24/2025 11:00	47251.191	44604.238	64373.895	12.12	10.88	11.45	50.023	-0.728	10.92	2.32	1.9	20590.322

3/24/2025 12:00	-23684.789	1044.208	23688.855	7.13	14.74	8.76	49.99	-1	2.85	2.88	2.93	36960.02
3/24/2025 13:00	-4549.964	697.315	4603.088	36.79	69	76.87	49.978	0.988	2.79	2.61	2.86	9555.555
3/24/2025 14:00	28649.109	43349.492	52014.211	6.6	6.82	7.62	49.897	-0.551	2.43	2.51	2.39	18661.705
3/24/2025 15:00	7344.073	5855.087	9407.246	30.62	42.22	30.84	49.929	-0.782	3.11	2.95	2.79	10019.882
3/24/2025 16:00	4641.785	112.655	4637.642	136.53	120.63	85.89	49.857	1	2.5	2.54	2.37	4726.398
3/24/2025 17:00	14502.189	5403.695	15475.086	35.64	38.66	31.83	50.021	-0.937	3.23	2.77	2.66	322.948
3/24/2025 18:00	13424.471	-1975.762	13553.054	48.48	36.52	37.37	49.982	0.989	2.82	2.5	2.6	26.729
3/24/2025 19:00	10207.85	-1646.836	10326.562	54.41	55.72	37.97	49.947	0.987	2.97	2.69	3	30.374
3/24/2025 20:00	12544.395	-1342.27	12626.194	46.66	51.13	26.88	50.006	0.994	3.1	3.34	3.09	31.704
3/24/2025 21:00	12262.316	-1768.199	12401.909	58.91	34.97	28.73	49.968	0.989	3.58	3.84	3.61	30.617
3/24/2025 22:00	18169.102	5758.746	19059.889	25.46	14.42	12.06	50.012	-0.953	3.89	4.11	3.83	30.86
3/24/2025 23:00	6081.499	-1508.607	6265.823	53.63	39.86	20.03	49.913	0.984	3.55	3.92	3.61	30.93
3/25/2025 0:00	7954.968	-1541.346	8087.118	23.78	40.64	20.6	49.997	0.981	3.44	3.77	3.55	31.134
3/25/2025 1:00	5374.594	-1539.582	5580.798	53.89	42.49	17.08	50.035	0.961	3.32	3.74	3.66	30.73
3/25/2025 2:00	5721.708	-1489.207	5907.64	44.45	40.22	17.89	50.022	0.967	3.47	3.67	3.51	32.61
3/25/2025 3:00	5482.399	-1466.279	5676.583	51.4	40.37	18.28	49.98	0.966	3.33	3.61	3.58	35.235
3/25/2025 4:00	5426.843	-1491.963	5634.041	53.13	42.52	19.25	49.974	0.962	2.93	3.7	3.45	32.146
3/25/2025 5:00	4600.559	-1060.081	4701.781	33.6	36.69	15.7	50.073	0.975	3.38	3.6	3.38	31.93
3/25/2025 6:00	46568.645	44839.359	64678.637	5.45	6.71	6.41	50.033	88.516	2.3	2.28	2.29	4405.544
3/25/2025 7:00	5918.8	6869.313	9067.505	25.76	33.04	26.6	50.112	-0.651	2.67	2.3	2.42	12641.801
3/25/2025 8:00	614.752	6576.322	6609.595	36.41	44.29	21.94	50.021	-0.073	2.42	2.11	2.28	21268.072
3/25/2025 9:00	-21538.391	650.577	21943.652	12.48	14.64	10.48	50.031	-1	3.09	2.53	2.79	30214.408
3/25/2025 10:00	-10810.036	9280.704	14126.842	15.04	27.45	23.16	50.039	0.753	3.09	2.72	2.75	35964.926
3/25/2025 11:00	-19530.332	1919.986	19624.48	14.41	75.68	18.92	49.989	0.995	2.55	1.85	2.31	38275.012
3/25/2025 12:00	-20556.021	2237.448	20677.432	16.01	31.52	21.73	49.957	0.998	2.51	2.18	2.42	37201.176
3/25/2025 13:00	-26240.029	1437.619	26927.844	14.91	27.69	14.07	50.02	0.998	2.51	2.36	2.6	38111.762
3/25/2025 14:00	-14876.311	691.252	14829.818	29.24	37.13	21.02	49.926	0.998	2.54	2.54	2.53	30173.594
3/25/2025 15:00	46.627	-527.23	529.287	205.24	149.26	361.62	49.854	-0.861	2.33	2.41	1.92	10559.224
3/25/2025 16:00	16134.917	6529.143	17404.568	27.38	35.21	21.92	49.763	-0.926	2.6	2.7	2.71	1918.664
3/25/2025 17:00	23976.898	5450.873	24589.443	27.77	20.34	18.24	50.037	-0.975	3.33	2.96	2.81	314.84
3/25/2025 18:00	12104.356	-2120.384	12290.16	48.04	58.6	35.62	49.986	0.985	2.63	2.99	2.74	27.346
3/25/2025 19:00	13348.191	-2006.957	13500.787	55.29	52.61	38.71	50.031	0.988	3.08	2.77	2.72	29.793
3/25/2025 20:00	23554.498	4834.577	24056.002	30.24	31.25	18.37	50.022	-0.979	3.46	3.35	3.52	31.549
3/25/2025 21:00	12365.602	-2074.198	12538.356	54.53	46.37	40.42	49.991	0.986	3.39	3.75	3.37	31.341
3/25/2025 22:00	9985.625	-1475.538	10094.055	54.56	48.96	31.42	49.975	0.989	3.52	3.91	3.81	33.684
3/25/2025 23:00	6031.455	-1220.687	6153.74	46.64	37.85	17.99	49.978	0.98	3.8	4.21	3.96	33.49
3/26/2025 0:00	5772.414	-1404.22	5837.668	51.47	40.84	19.36	49.903	0.97	3.56	4.07	3.82	32.976
3/26/2025 1:00	9410.225	-898.815	9207.505	57.59	48.03	40.71	49.968	0.995	3.29	3.64	3.45	31.585
3/26/2025 2:00	5717.85	-1239.867	5855.15	49.9	37.53	17.56	50.015	0.977	3.43	3.98	3.85	32.256
3/26/2025 3:00	5809.01	-1105.055	5918.057	50.73	38.27	15.58	50.042	0.982	5923.606	3.77	3.6	33.031
3/26/2025 4:00	13175.682	-456.682	13187.781	61.57	59.23	50.2	50.066	1	2.98	2.96	2.91	33.113
3/26/2025 5:00	14987.312	6427.952	16308.217	12.85	15.26	10.99	49.972	-0.919	3.51	3.28	3.42	30.45
3/26/2025 6:00	10449.474	265.213	10452.839	62.75	45.73	50.82	50.01	1	2.34	1.95	2	2014.489
3/26/2025 7:00	9557.271	5015.795	10783.253	31.25	43.89	23.36	50.025	-0.885	2.56	2.14	1.99	6063.757
3/26/2025 8:00	-5327.085	-120.15	5328.44	50.53	48.76	55.16	50.035	-1	2.27	2.72	2.32	12417.395
3/26/2025 9:00	31050.357	46636.66	67744.172	11.55	9.59	10.32	49.968	-0.725	1.8	1.95	1.96	22492.48
3/26/2025 10:00	-11925.563	1730.611	12050.479	20.61	67.35	41.93	50.041	0.992	2.14	2.37	2.18	27014.312
3/26/2025 11:00	-24304.943	1203.932	24385.387	19	13.28	13.95	49.983	0.998	2.59	2.54	2.53	37131.828
3/26/2025 12:00	-8825.455	1130.739	8897.597	25.67	59.29	44.9	49.991	0.991	2.51	2.22	2.37	17756.162
3/26/2025 13:00	-3481.504	551.48	3283.546	121.56	163	260.17	49.986	0.985	2.04	2.46	2.36	12378.863
3/26/2025 14:00	-9747.309	1310.745	9971.291	23.58	33.82	89.05	50.013	0.991	2.47	2.09	2.57	20683.182
3/26/2025 15:00	-7403.487	812.725	7447.962	38.58	50.37	90.46	49.935	0.994	2.32	2.42	1.93	15925.918
3/26/2025 16:00	9591.112	4208.581	10473.854	49.44	54.15	38.9	49.968	-0.915	2.38	2.45	2.6	4198.991
3/26/2025 17:00	13031.722	-894.406	12917.221	49.04	36.15	29.67	49.961	0.997	2.55	2.54	2.56	277.669
3/26/2025 18:00	7148.305	-2063.064	7206.528	57.41	47.74	35.4	51612.617	0.958	34429.754	3.23	3.37	26.931
3/26/2025 19:00	12301.778	-1705.919	12414.364	55.87	47.98	25.49	50.031	0.99	3.07	3.45	2.89	30.939
3/26/2025 20:00	10147.443	-1050.712	10206.959	27.29	48.68	34.55	50.041	0.987	3.88	3.92	3.99	32.047
3/26/2025 21:00	8605.325	-1581.028	8755.755	47.15	34.99	24.09	50.034	0.983	3.72	4.07	3.82	29.854
3/26/2025 22:00	6589.219	-1727.524	6810.952	50.03	44.59	20.43	49.987	0.967	3.54	3.89	3.71	31.898
3/26/2025 23:00	6625.153	-1620.932	6935.186	64.559	39.72	17.14	50.023	0.971	3.17	3.4	3.49	30.618
3/27/2025 0:00	5788.067	-1468.373	5969.175	59.71	41.92	17.99	50.04	0.969	3.08	3.46	3.53	30.76
3/27/2025 1:00	5488.352	-1583.674	5722.12	59.35	41.04	19.15	49.974	0.961	2.98	3.32	3.22	30.036
3/27/2025 2:00	5436.433	-1720.028	5704.987	56.25	43.24	19	50.026	0.953	3.23	3.44	3.27	30.304
3/27/2025 3:00	5696.466	-1606.492	5920.039	59.14	37.14	16.99	50.003	0.964	3.15	3.35	3.37	32.155
3/27/2025 4:00	5838.993	-1407.416	6002.79	61.11	41.34	18.07	50.022	0.972	2.6	3.44	3.19	30.009
3/27/2025 5:00	4862.135	-1074.191	4968.404	27.5	42.51	14.41	50.044	0.974	3.32	3.4	3.46	31.422
3/27/2025 6:00	1652.788	-243.387	1660.362	162.47	106.25	69.99	50.025	0.989	2.61	2.77	2.75	3361.975
3/27/2025 7:00	-1705.037	-117.835	1973.504	40.22	108.77	85.39	50.09	-0.998	2.38	2.26	2.25	8564.725
3/27/2025 8:00	13887.216	6902.823	15508.184	43.01	39.18	25.74	50.027	-0.895	2.13	2.03	1.96	9427.936
3/27/2025 9:00	-2735.578	274.142	2749.28	62.79	310.71	102.75	49.959	0.995	1.72	2.08	1.89	12784.143
3/27/2025 10:00	3626.236	1116.74	3794.298	108.54	140.99	42.12	49.965	-0.955	2.08	2.16	2.26	6822.394
3/27/2025 11:00	-18232.482	967.598	18531.793	20.89	23.7	17.39	49.998	0.998	2.2	2.26	2.39	31125.631
3/27/2025 12:00	21199.543	41867.117	47081.758	10.36	13.13	12.88	50.03	-0.437	2.39	2.18	2.35	35207.066
3/27/2025 13:00	6628.461	5878.566	8852.375	46.39	93.05	37.86	49.908	-0.749	2.31	2.11	2.36	11543.803
3/27/2025 14:00	52817.035	37089.531	64603.078	8.02	9.01	8.87	49.834	-0.818	2.11	2.16	2.21	3332.596
3/27/2025 15:00	7877.917	-464.068	7893.555	54.22	47.25	42.84	49.803	0.998	2.53	2.26	2.37	1063.095
3/27/2025 16:00	8660.22	-313.604	8694.624	44.12	41.17	41.15	49.827	1	2.67	2.48	2.65	1595.6
3/27/2025 17:00	9104.557	-1083.23	9125.974	48.96	50.83	39.9	50.036	0.993	2.63	2.65	2.69	356.936
3/27/2025 18:00	11567.315	-2766.442	11890.021	53.04	55.01	36.52	50.04	0.972	2.37	2.62	2.38	28.488
3/27/2025 19:00	13877.406	-1665.575	13110.611	49.63	49.1	34.25	49.904	0.991	2.76	2.45	2.48	27.976
3/27/2025 20:00	18660.064	3296.979	18947.898	28.45	32.82	13.47	49.971	-0.984	2.83	2.92	2.93	28.021
3/27/2025 21:00	7395.44	-2226.536	7715.214	56.28	47.81	25.29	50.035	0.957	3.34	3.74	3.61	30.946
3/27/2025 22:00	9236.723	-1295.533	12702.346	62.46	55.97	46.98	49.957	0.994	2.98	3.32	3.19	29.56
3/27/2025 23:00	8909.561	-1693.243	9070.435	54.23	46.16	30.83	50.013	0.982	3.31	3.57	3.46	30.734
3/28/2025 0:00	7768.128	-1342.16	7883.223	55.54	41.89	31.34	49.961	0.986	3.03	3.27	3.25	32.216
3/28/2025 1:00	5689.962	-1553.471	5886.731	47.38	41.5	18.46	49.984	0.964	3.19	3.47	3.38	31.735
3/28/2025 2:00	0	0	0	0	0	0	0	0	0	0	0	0
3/28/2025 3:00	6114.789	-1324.633	6239.923	42.71	37.41	16.61	50.019	0.975	3.31	3.31	3.36	32.446
3/28/2025 4:00	9187.45	-1379.197	9092.374	51.46	42.52	34.58	50.008	0.988	2.48	2.82	2.78	29.1
3/28/2025 5:00	7412.527	-1257.062	7549.444	55.47	46.74	33.08	49.997	0.986	2.18	2.83	2.48	28.512
3/28/2025 6:00	17583.34	1720.028	7483.253	30.81	38.01	23.27	50.054	-0.973	2.54	2.7	2.54	244.625
3/28/2025 7:00	17424.938	5343.289	19097.824	15.63	12.36	13.19	50.126	-0.96	2.37	2.45	2.33	1411.286
3/28/2025 8:00	11692.868	-204.145	11694.65	99.88	43.42	41.71	50.077	1	1.49	2	1.59	3877.17
3/28/2025 9:00	8958.172	-834.661	8998.803	115.5	31.55	57.73	50.013	0.995	1.9	2.07	1.69	3868.568
3/28/2025 10:00	21218.283	13299.359	24234.695	21.98	20.63	23.03	49.861	-0.835	1.83	1.87	1.68	5550.258

3/28/2025 11:00	-8015.375	-158.731	7839.29	16.61	48.34	50.38	49.872	-1	3.31	3.35	2.9	14328.577
3/28/2025 12:00	-823.087	-261.686	853.366	83.98	116.42	91.73	49.878	-0.951	2.69	2.94	2.76	12130.317
3/28/2025 13:00	6651.719	5968.182	8936.698	57.09	58.79	43.87	49.993	-0.745	3.22	2.68	2.91	13298.625
3/28/2025 14:00	16129.734	8598.271	18286.828	25.48	39.09	27.69	50.037	-0.882	2.93	2.91	2.72	8096.135
3/28/2025 15:00	61061.027	43831.305	75045.523	8.55	8.33	9.3	49.953	-0.811	2.55	2.49	2.46	6967.673
3/28/2025 16:00	8110.943	-385.474	8105.832	53.69	43.08	56.91	49.953	0.998	2.85	3.05	2.69	2853.648
3/28/2025 17:00	10503.597	-567.133	10516.365	44.57	31.65	40.57	50.025	0.998	3.05	3.38	2.95	576.589
3/28/2025 18:00	13130.487	-2508.835	13384.044	45.11	44.77	25.37	49.957	0.982	3.36	3.79	3.19	29.821
3/28/2025 19:00	12584.519	-1531.645	12677.383	45.45	36.27	35.64	49.954	0.992	3.57	3.8	3.35	29.666
3/28/2025 20:00	13796.167	-1600.319	13888.674	47.63	53.04	20.73	49.959	0.993	3.63	3.66	3.29	29.322
3/28/2025 21:00	11824.482	-2222.898	12061.295	26.85	45.88	18.27	49.927	0.982	4.2	4.28	4.16	30.545
3/28/2025 22:00	10820.508	-2177.924	11063.127	20.32	49.67	20.4	49.759	0.98	3.99	4.27	4.13	29.63
3/28/2025 23:00	8941.857	-1716.501	9105.119	30.17	41.26	19.78	50	0.982	3.75	4.27	4.01	31.872
3/29/2025 0:00	8105.543	-2193.687	8401.191	36.75	44.6	37.94	50.025	0.965	3.77	4.17	3.81	33.424
3/29/2025 1:00	10140.278	-1864.981	10298.69	38.74	53.94	38.5	50.024	0.983	3.32	3.78	3.56	31.133
3/29/2025 2:00	5653.917	-1814.826	5938.045	53.35	40.9	30.85	49.965	0.952	3.62	3.99	3.78	32.753
3/29/2025 3:00	5592.298	-1595.91	5815.559	49.89	43.5	29.93	50.057	0.961	3.7	4.09	3.72	32.391
3/29/2025 4:00	11329.77	-894.736	11348.233	67.23	58.81	51.19	50.034	0.996	3.25	3.24	3.43	29.878
3/29/2025 5:00	6604.21	-1321.327	6737.549	51.86	45.71	33.07	50.053	0.98	2.88	3.3	3.01	29.628
3/29/2025 6:00	3619.622	-792.663	3696.14	117.79	56.81	51.28	50.02	0.977	2.94	3.06	2.76	1518.872
3/29/2025 7:00	9796.36	4628.888	10819.166	28.34	33.58	22.43	50.031	-0.903	2.63	2.89	2.5	5924.411
3/29/2025 8:00	-1126.22	5314.188	5634.244	52.47	142.76	70.25	49.968	0.332	2.34	2.17	2.51	16912.223
3/29/2025 9:00	-4342.29	8090.882	9182.476	65.17	97.19	91.43	50.021	0.472	2.12	1.72	2.03	27502.402
3/29/2025 10:00	35216.281	53290.91	63508.086	9.51	11.53	11.54	49.925	-0.543	2.54	2.51	2.33	36210.109
3/29/2025 11:00	327.603	6410.095	5854.669	30.29	63.08	47.31	50.02	-0.055	3.43	2.93	3.06	17438.473
3/29/2025 12:00	-6013.267	-191.8	6016.325	24.02	71.09	66.58	50.04	-1	3.42	3.38	3.49	12313.894
3/29/2025 13:00	28005.365	44800.449	52833.516	7.38	9.08	8.8	50.025	-0.53	3.12	3	2.86	36958.594
3/29/2025 14:00	0	0	0	0	0	0	0	0	0	0	0	0
3/29/2025 15:00	0	0	0	0	0	0	0	0	0	0	0	0
3/29/2025 16:00	0	0	0	0	0	0	0	0	0	0	0	0
3/29/2025 17:00	9670.367	-1256.07	9775.432	64.949	21.43	42.74	50.007	0.991	3.83	3.64	2.98	218.264
3/29/2025 18:00	12234.538	-1770.845	12359.086	59.59	56.41	40.86	49.993	0.989	3.24	3.15	2.99	29.8
3/29/2025 19:00	7006.219	-2422.083	7411.881	64.51	47.91	37.44	49.984	0.945	3.54	3.87	3.23	30.025
3/29/2025 20:00	19034.736	-1086.096	19006.707	49.28	56.93	37.02	49.991	0.998	3.48	2.92	2.92	32.082
3/29/2025 21:00	14014.421	-1161.383	14084.761	50.69	51.99	39.93	50.037	0.996	3.34	3.55	3.33	30.419
3/29/2025 22:00	6962.568	-1551.156	7549.676	43.18	37.95	25.21	49.888	0.978	3.77	4.27	3.77	31.472
3/29/2025 23:00	8417.384	-1946.331	8635.824	23.91	46.6	23.76	50.022	0.974	3.81	4.03	3.75	29.075
3/30/2025 0:00	5572.788	-1810.748	5859.588	51.92	42.33	21.56	49.951	0.951	3.43	3.86	3.67	30.624
3/30/2025 1:00	5549.088	-1675.055	5810.643	51.54	41.11	27.92	49.999	0.957	3.52	3.77	3.68	31.71
3/30/2025 2:00	6483.397	-1783.19	6749.557	54.76	41.69	35.6	50.012	0.964	3.15	3.62	3.35	32.715
3/30/2025 3:00	6033.769	-1561.518	6232.552	53.01	44.96	26.18	50.004	0.967	3.27	3.63	3.52	32.226
3/30/2025 4:00	5332.596	-1538.369	5550.06	52.95	39.1	17.47	50	0.96	3.25	3.85	3.58	30.623
3/30/2025 5:00	11511.649	-742.839	11597.412	54.34	48.93	47.19	50.03	0.997	2.67	2.92	2.81	32.135
3/30/2025 6:00	1249.346	-411.157	1312.807	167.7	85.53	66.64	49.997	0.949	2.82	3.1	2.93	2734.534
3/30/2025 7:00	9986.948	4468.724	10952.615	66.57	71.93	62.06	50.069	-0.913	2.2	2.19	1.72	6617.916
3/30/2025 8:00	-5061.1	6497.617	8286.021	13.04	28.86	36.37	50.034	0.62	2.49	2.55	2.66	22340.072
3/30/2025 9:00	-17950.623	326.831	18280.6	14.5	24.93	63.6	49.978	-1	2.44	2.17	2.09	32027.594
3/30/2025 10:00	5309.228	6767.019	8604.334	27.98	40.27	19.91	50.008	-0.617	3.24	2.72	2.91	14195.121
3/30/2025 11:00	-34663.805	581.242	34608.48	5.8	8.59	6.41	49.976	-1	3.3	3.32	3.25	41003.086
3/30/2025 12:00	-33741.293	454.037	33744.348	5.65	8.08	5.59	49.975	-1	3.27	3.28	3.36	39559.41
3/30/2025 13:00	-31535.922	52883.48	31515.789	5.83	14.38	6.67	47139.305	35014.023	5744.177	3.23	3.38	37975.133
3/30/2025 14:00	-21036.623	-145.172	20981.457	12.94	12.01	10.59	49.919	-1	3.19	3.28	3.3	30671.83
3/30/2025 15:00	1272.715	-470.13	1336.3	243.07	121.95	184.73	49.908	0.952	3.26	3.2	3.2	5306.701
3/30/2025 16:00	1533.74	-829.15	1743.516	88.02	95.43	205.9	49.989	0.879	2.69	3.02	2.85	8374.066
3/30/2025 17:00	8837.801	-2068.796	10391.395	24.99	55.5	40.22	49.991	0.976	3.2	3.44	3.43	342.924
3/30/2025 18:00	8081.182	-2948.542	8597.217	58.51	44.34	33.69	49.995	0.939	3.45	3.79	3.05	28.514
3/30/2025 19:00	15486.323	-2110.904	15723.136	46.99	33.01	26.41	50.08	0.99	3.38	3.25	3.13	28.265
3/30/2025 20:00	16901.016	4099.123	17391.006	25.03	26.27	13.49	50.029	-0.971	3.94	4.14	3.98	28.055
3/30/2025 21:00	7487.372	-2759.938	7982.953	56.81	47.67	27.95	50.072	0.938	3.6	3.93	3.68	30.464
3/30/2025 22:00	12521.577	-3156.105	13430.1	65.89	63.74	31.28	49.994	0.971	3.15	3.71	3.66	30.914
3/30/2025 23:00	6610.933	-2107.597	6938.761	59.01	41.95	24.35	49.996	0.952	3.53	4.28	3.93	31.431
3/31/2025 0:00	6082.601	-1779.002	6317.427	66.73	43.03	21.16	49.968	0.96	3.36	4.02	3.68	32.692
3/31/2025 1:00	7469.736	-1913.262	7702.523	35.98	40.31	23.55	50	0.968	3.3	3.89	3.62	33.705
3/31/2025 2:00	7408.117	-1720.469	7611.18	35.96	39.07	21.51	49.978	0.974	3.3	3.76	3.57	31.176
3/31/2025 3:00	6920.35	-1837.313	7149.868	35.97	41.39	19.06	49.977	0.966	3.29	3.75	3.63	30.469
3/31/2025 4:00	7689.424	-1826.731	7897.53	35.27	40.98	19.45	49.959	0.971	3.03	3.91	3.43	29.697
3/31/2025 5:00	6221.161	-1303.469	6361.317	13.92	39.22	16.98	49.998	0.978	3.01	3.81	3.56	30.973
3/31/2025 6:00	7415.723	266.977	7420.528	71.76	107.26	89.74	50.062	1	2.04	2.14	2.1	5108.27
3/31/2025 7:00	-9167.499	-209.326	9169.889	14.69	37.04	38.57	50.07	-1	2.5	2.69	2.35	14149.103
3/31/2025 8:00	3780.558	10645.903	11298.433	53.51	81.18	60.07	49.998	-0.334	2.16	2.25	2.06	24821.994
3/31/2025 9:00	-11034.354	6707.385	12831.447	29.62	64.75	60.77	49.971	0.852	2.31	2.13	2.15	33956.371
3/31/2025 10:00	-34367.18	732.147	34289.344	5.62	7.88	10.22	49.942	-1	3.28	3.27	3.14	41058.055
3/31/2025 11:00	-33204.805	5720.606	33693.98	5.6	8.75	9.3	50.016	0.985	3.27	3.39	3.35	46293.238
3/31/2025 12:00	-24411.094	8095.511	25397.787	5.87	16.45	13.75	50.025	0.947	3.58	3.24	3.26	45482.297
3/31/2025 13:00	-31140.084	517.088	31172.812	5.3	11.14	10.81	50.028	-1	3.45	3.54	3.25	41384.434
3/31/2025 14:00	-22355.967	106.482	22356.234	10.12	12.78	11.92	49.93	-1	3.22	3.33	3.21	32415.82
3/31/2025 15:00	-5924.531	4883.299	7677.675	13.8	35.84	55.09	49.816	0.77	3.1	2.83	3.1	21551.582
3/31/2025 16:00	3159.302	-1078.049	3338.17	253.58	99.74	44.11	49.959	0.946	3.02	3.42	3.18	4080.174
3/31/2025 17:00	2303.255	-989.534	2506.824	258.34	103.29	78.36	49.947	0.918	3.2	3.47	3.19	3417.536
3/31/2025 18:00	8381.558	-2309.979	8692.883	47.51	46.9	32.7	50.055	0.964	3.38	4.39	3.44	27.831
3/31/2025 19:00	8597.829	-1359.576	8650.793	45.3	53.8	28.96	49.995	0.987	3.87	3.98	3.99	28.115
3/31/2025 20:00	8599.152	-2785.181	9048.81	53.29	49.5	33.12	50	0.951	3.85	4.23	3.41	30.978
3/31/2025 21:00	56665.277	39545.672	69021.945	10.04	7.82	7.66	50.003	-0.819	3.26	3.43	3.33	30.561
3/31/2025 22:00	10997.537	-2002.438	11237.688	61.47	52.52	28.39	50.016	0.984	3.22	3.42	3.41	31.81
3/31/2025 23:00	6607.297	-1811.078	6828.903	62.49	42.63	21.67	50.03	0.964	3.37	3.73	3.74	29.852

APPENDIX B: PUBLICATION

Conference paper

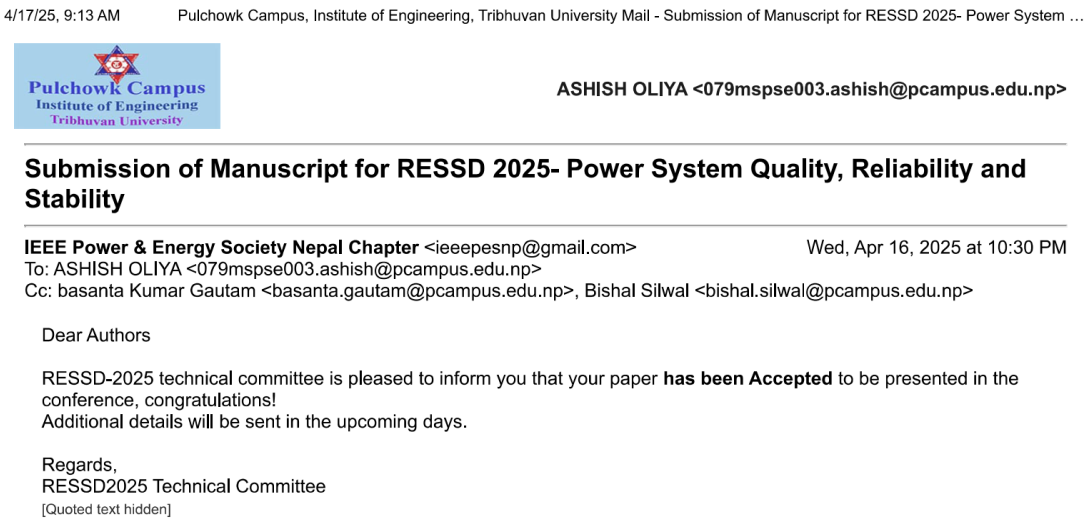

4/17/25, 9:13 AM Pulchowk Campus, Institute of Engineering, Tribhuvan University Mail - Submission of Manuscript for RESSD 2025- Power System …

Pulchowk Campus
Institute of Engineering
Tribhuvan University

ASHISH OLIYA <079mspse003.ashish@pcampus.edu.np>

Submission of Manuscript for RESSD 2025- Power System Quality, Reliability and Stability

IEEE Power & Energy Society Nepal Chapter <ieeepesnp@gmail.com> Wed, Apr 16, 2025 at 10:30 PM
To: ASHISH OLIYA <079mspse003.ashish@pcampus.edu.np>
Cc: basanta Kumar Gautam <basanta.gautam@pcampus.edu.np>, Bishal Silwal <bishal.silwal@pcampus.edu.np>

Dear Authors

RESSD-2025 technical committee is pleased to inform you that your paper **has been Accepted** to be presented in the conference, congratulations!
Additional details will be sent in the upcoming days.

Regards,
RESSD2025 Technical Committee
[Quoted text hidden]

Acceptance email for the paper titled ”Performance Evaluation Of PV-ESS-Integrated Grid Using ANN Tuned UPQC For Power Quality Enhancement” at the RESSD-2025 Conference of IEEE PES Nepal Chapter.

Performance Evaluation Of PV-ESS-Integrated Grid Using ANN Tuned UPQC For Power Quality Enhancement

*

Ashish Oliya
Department of Electrical Engineering
IOE, Pulchowk Campus
Tribhuwan University
Lalitpur, Nepal
ashisholiya123@gmail.com

Bishal Silwal
Department of Electrical Engineering
IOE, Pulchowk Campus
Tribhuwan University
Lalitpur, Nepal
bishal.silwal@pcampus.edu.np

Basanta Kumar Gautam
Department of Electrical Engineering
IOE, Pulchowk Campus
Tribhuwan University
Lalitpur, Nepal
basanta.gautam@pcampus.edu.np

***Abstract*—This paper proposes the use of an Artificial Neural Network (ANN) based control method for Unified Power Quality Control (UPQC) to improve power quality in a grid-connected Photovoltaics (PV)-Energy Storage System (ESS). UPQC utilizes the Neutral Point Clamped (NPC) converter topology to obtain the series and shunt active filter behavior. The study examines Total Harmonic Distortion (THD) improvement, Power Factor (PF) compensation, voltage regulation under nonlinear loads, grid disturbances, and faults (L-G and L-L-L-G) in ANN-tuned UPQC against PI-controlled UPQC. The series voltage conditioner mitigates voltage magnitude sagging, swelling, and imbalance, whereas the shunt current conditioner mitigates harmonic distortion, load imbalance, and reactive power. FUZZY logic MPPT is implemented for optimal PV extraction with fast and stable convergence. In addition, ESS with FUZZY Logic Control (FLC) supports grid stability by handling power variations and improving dynamic response. MATLAB/Simulink simulations verify THD reduction, PF improvement, and grid stability of the system and establish the dominance of ANN-based control over traditional ones.**

***Index Terms*—Unified Power Quality Control, Artificial Neural Network, FUZZY Logic Controller, Renewable Energy, Power Quality, Neutral Point Clamped Converter, Total Harmonic Distortion**

I. Introduction

The increasing socioeconomic environmental issues of large-scale power plants have led researchers and policy makers to explore alternative energy solutions, such as hybrid renewable energy systems, which integrate multi-renewable sources to improve energy efficiency and reliability, resulting in greater diversity and resilience in the current power infrastructure [1]. The research emphasizes that while Variable Renewable Energy Resources (VRER) provide material environmental, sustainability, and economic benefits, barriers may exist regarding the stability, reliability, and variability in their integration into the grid. The results of our study indicate that successful integration of VRER can lead to a much more sustainable, resilient, and cost-effective energy future [2].

The integration of renewable energy sources necessitates power electronic devices like converters and inverters, causing power quality degradation on both source and load sides. Harmonics from non-linear loads at the point of common coupling add more challenges, causing voltage sags, swells, flicker, and harmonic distortions [3]. THD is an essential concern of PV systems with respect to the grid system, which affects the load voltage and currents in the resultanting ways. These include FACTS devices such as UPFC, UPFC-FLC, GUPFC, UPQC, and SVC, which are used to mitigate THD and enhance power quality for bettering grid performance [4].

In [5], this study deals with the use of UPQC to alleviate harmonic disturbances and power network disturbances through PV-BESS. A PV-BESS integrated UPQC ensures voltage support and stable power even in times of voltage interruptions. This too is far superior to SVC, Statcom, and DVR with respect to voltage enhancement, harmonic alleviation, current enhancement, and improvement of system power quality [6].

In comparison with the classical PI controller, the UPQC-ANN-RE system is able to achieve slightly better THD in load-side voltage and currents, while being capable of eliminating harmonics due to the operation of nonlinear loads. Both systems meet IEEE 519 harmonic distortion standards [7]. UPQC has shown quicker response, better restoration of voltage and greater THD reduction which improves the stability and reliability of operations therefore proving UPQC as a more effective solution in improving power quality for renewable-integrated microgrids [8]. The SRF and dq0 concept based control strategies are used for series and shunt connected active

power filter of UPQC. UPQC reduces voltage fluctuations and harmonic distortions with series and shunt active power filters implemented with SRF and dq0 strategies [9]. The FLC-based MPPT is superior to ANN-based MPPT in PV, Wind, and ESS for an efficient and economical use of power. They give electric vehicles the flexibility to consume power and assist the grid during peak load and off-peak periods if proper controllability and grid integration are provided [10]. Uncertainty in RESs can be avoided when using FLC-based MPPT algorithms. The FLC-based MPPT is known to have been carried out for avoiding the uncertainties from climate conditions related to solar, Several parameters, such as irradiation and temperature, must be analyzed when modeling PV systems, as RESs are sensitive to both weather and location [11].

The main contributions made by the present work is that this model gives efficient voltage regulation, harmonic elimination, and perform active/reactive power compensation to improve PF compared to traditional controllers. There is a formulation of the introduction, methodology, results, and conclusions.

II. Methodology

The ANN Tuned UPQC, PV-ESS system methodology integrates the UPQC with the ANN for the action of enhancing and managing power quality using a PV-ESS-enabled setup. The ANN optimizes the control strategy of the UPQC to the current load, solar irradiation, and grid status. The PV-ESS system assures that renewable energies are produced while also ensuring the storage of excess power for stable and sufficient supply for all the units. Fig. 1 illustrates a overall DG System. A three-phase, three-wire grid with PV-ESS, through a phase inverter is proposed. The working conditions have voltage dips, swells, and harmonic disturbances from the equivalent non linear loads and faults. The AC L-L voltage is 400 V which is stepdown from 11/0.4 kV transformer, and the frequency is kept constant at 50 Hz. In the study, model PV system consists of First Solar FS-272 modules connected with 26 series-connected modules per string and 33 parallel strings for efficient power. For ESS, in conjunction with a solar

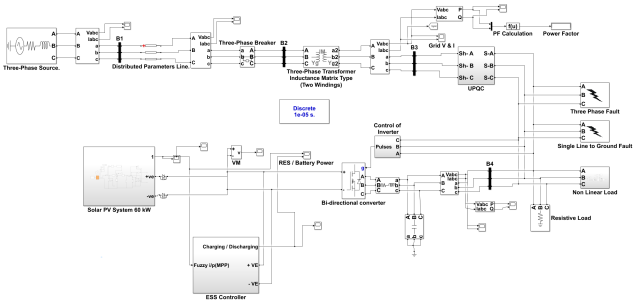

Fig. 2. Modelling of System on Matlab

PV system of approximately 60 kW is used an open circuit voltage (Voc) equal to 94.57 V, a short circuit current (Isc) 1.18 A, a maximum power point voltage (Vmp) 70.56 V and a maximum power point current (Imp) 1.01 A under STC conditions. For ESS, a nine 48V 30Ah battery with rated capacity 13kWH with a battery bank linked via a bidirectional converter is used in conjunction with The FLC method has developed the proposed MPPT and ESS controllers and ANN is used as a controller in NPC converter inside UPQC in the present study. Both resistive and non linear load are present in the system and a fault block indicates possible disruptions in the system. Overall system modeling is shown in Fig. 2.

A. ANN Tuned UPQC, PV-ESS TOPOLOGY

Below Structure Fig. 3 symbolizes the architecture of a UPQC-ANN, PV-ESS system planned to boost the power quality in an integrated green energy setup. This system utilizes the dual compentation approach as it consists of a shunt NPC converter utilizing its power architecture to compensate for current, connected through a shunt coupling transformer to regulate reactive power and neutralize harmonics and the series-connected NPC converter through a series coupling transformer provides for voltage compensation through appropriate voltage injection. The two converters are linked by a DC Link which maintains power balance. The ANN-based control keeps optimizing

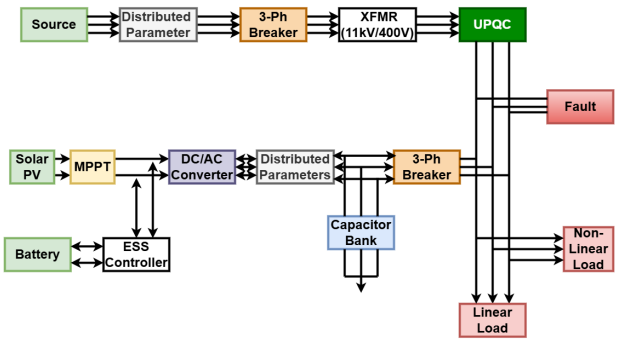

Fig. 1. Overall Proposed System

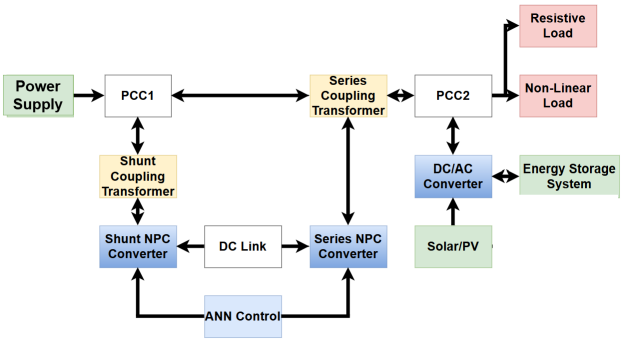

Fig. 3. UPQC-ANN, PV-ESS Topology

UPQC performance by instantaneously modifying its operation in instances of disturbances.

1) NPC Shunt Inverter Control: The load currents i_{La}, i_{Lb}, i_{Lc} are transformed into the $dq0$ frame using Park's transformation:

$$\begin{bmatrix} i_d \\ i_q \\ i_0 \end{bmatrix} = \frac{2}{3} \begin{bmatrix} \cos\theta & \cos(\theta - 120°) & \cos(\theta + 120°) \\ \sin\theta & \sin(\theta - 120°) & \sin(\theta + 120°) \\ \frac{1}{2} & \frac{1}{2} & \frac{1}{2} \end{bmatrix} \begin{bmatrix} i_{La} \\ i_{Lb} \\ i_{Lc} \end{bmatrix} \tag{1}$$

The low-pass filter (LPF) removes oscillating components in i_d and i_q. The compensating current reference is generated:

$$i_{dsh} = i_d - i_{dref}, \quad i_{qsh} = i_q - i_{qref} \tag{2}$$

The reference current is then computed and converted back to the *abc* frame using inverse Park transformation and the Voltage Source Inverter (VSI) injects the compensatory current using switching pulses produced by the hysteresis current controller. The shunt inverter regulates DC-link voltage and compensates for reactive power and current harmonics using an ANN-based control strategy.

2) NPC Series Inverter Control: The reference voltage is extracted using the SRF theory: Convert supply voltage V_s to $dq0$ frame:

$$\begin{bmatrix} V_d \\ V_q \\ V_0 \end{bmatrix} = \frac{2}{3} \begin{bmatrix} \cos\theta & \cos(\theta - 120°) & \cos(\theta + 120°) \\ \sin\theta & \sin(\theta - 120°) & \sin(\theta + 120°) \\ \frac{1}{2} & \frac{1}{2} & \frac{1}{2} \end{bmatrix} \begin{bmatrix} V_{sa} \\ V_{sb} \\ V_{sc} \end{bmatrix} \tag{3}$$

The oscillating components in V_d and V_q are removed using an LPF. The reference voltage is calculated:

$$V_{ds} = V_d - V_{dref}, \quad V_{qs} = V_q - V_{qref} \tag{4}$$

The compensatory voltage is computed and returned to the abc frame after filtering. The gate pulses for the series inverter are produced using a Sinusoidal Pulse Width Modulation (SPWM) approach. The series inverter compensates for voltage sags/swells by injecting appropriate voltage using an ANN-based controller.

B. Artificial Neural Network

The ANN model is generated using the Neural Fitting Tool (nftool) of the MATLAB using Levenberg-Marquardt backpropagation(LMBP) for training and hence gives great convergence and accuracy because it uses the approximation of the Hessian matrix instead of simple gradient descent. In this study, an ANN based UPQC is constructed to enhance the power quality of the distribution system with the following parameters of ANN: number of hidden layers: 10, number of epochs: 5000, number of inputs: 1 and outputs: 1 of error controllers (PI or P).

C. PV Modelling

The PV system uses a FLC to accomplish MPPT, which optimizes power extraction by dynamically regulating the duty cycle of the boost converter. Table I shows the FUZZY rules for the PV MPPT system.

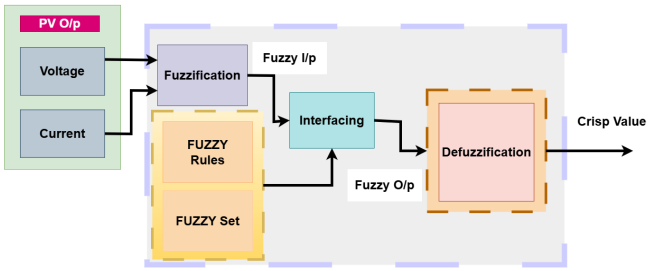

Fig. 4. Block diagram of FLC-based MPPT controller used to regulate the duty cycle of the boost converter for PV system

TABLE I
FUZZY CONTROL RULES FOR MPPT V & I AS INPUT

V \ I	Low Current	Medium Current	High Current
Low Voltage	High Duty	Medium Duty	Medium Duty
Medium Voltage	High Duty	Medium Duty	Medium Duty
High Voltage	Medium Duty	Low Duty	Low Duty

The FLC-based MPPT provides better flexibility and decision-making, allowing for more effective tracking in dynamic situations than conventional MPPT methods like Perturb and Observe (P & O) and Incremental Conductance, which have trouble with abrupt changes in irradiance and partial shading [9].

D. ESS Modelling

The power management strategy determines how much power is transferred to and from the battery, PV system, and grid, aiming to get an optimal power flow. The FLC approach is developed to manages power imbalance by setting battery discharging (BD = High, BC = Low) during a power deficit (Error 0), and enabling battery charging (BC = High, BD = Low) when there is excess power (Error $>$ 0). Table II shows the FUZZY rules for the ESS controller.

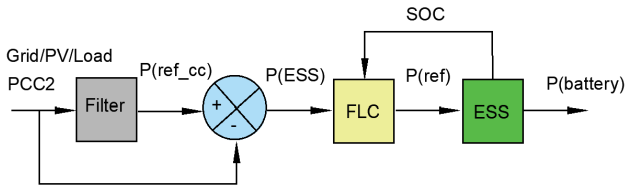

Fig. 5. FLC-based control of ESS connected with grid.

TABLE II
FUZZY CONTROL RULES FOR ERROR, BC, AND BD

Rule No.	Error (Input1)	BC (Output1)	BD (Output2)
1	Low Error ($\leq$ 0)	High (1)	Low (0)
2	High Error ($>$ 0)	Low (0)	High (1)

III. Results and Discussion

In this section, we describe the simulation results and analysis the performance of system which is tested under different conditions. Some overview of data and concept of project are shown in Table III. From the graph, Fig. 6. , the Maximum Power Point (MPP) occurs at 1 kW/m^2 of irradiation, with a voltage of approx. 1800-1850 V and current somewhere 30-35 A. Thus,maximum power output of 60KW can achieved at ideal case. As irradiance declines, parameters such as current and power drop proportionately, affecting energy generation overall. Same data can be seen through simulation plot in Fig. 6.

AFter using FUZZY as MPPT, the simulation results indicate that, the PV system has reached a stable maximum output of approx. 57.5 kW with a corresponding voltage of approx. 1800v and a current of approx. 32 A with efficiency of nearly 96%. The system is fast and smooth in tracking with minimum oscillations as shown in Fig. 7. The power flow characteristics of the ESS indicating that it can be utilized for charging (negative values) in Fig. 8 during normal load cases and discharging (positive values) as in Fig. 9 is supplying power to the grid or load during peak hours. The ESS functions as an energy balancing solution between energy supplied by the grid and energy supplied by the solar array.

Under the normal Operating condition, the grid voltage remains approx. 230V (L-Ph). However, the introduction of non-linear loads, PV-ESS integration and faults causes significant waveform distortions in V-I waveform in Fig. 10. In Fig. 11 During an L-G fault at (0.2s-0.4s), the R phase (1st) drops to Zero, while the current surges from approx. 250 to 2000A, marking 8 times/ 800% increase. Similarly, during L-L-L-G fault at (0.6s-0.8s) in Fig. 12 , the three phase voltage collapses to nearly zero and the current spikes to approx.. 2500A i.e. 9 times/1900% increases, indicating extreme instability.

TABLE III
System Components and Specifications

Category	Component	Specifications/Details
Source & Grid	Three-phase YG Source	11kV (L-L), 50 Hz
	Transmission Line	Distributed parameter, 100 km
	Step-down Transformer	11kV → 0.4kV (L-L)
	Swing Bus	100 kW power
RE & Storage	PV System	60 kW, 1kW/m^2, 25°C, Fuzzy MPPT
	Battery Storage	30Ah, 13kWH
	ESS	Fuzzy-based controller, Manages power flow
Power Electronics	Buck-Boost Converter	MOSFETs, IGBTs, Fuzzy Logic Control
	NPC Converter	PI/ANN Controller
Loads	Linear Grid Load	30 kW Resistive
	Nonlinear Load	100 kW (Diode Bridge + RLC)
Quality & Control	UPQC	Voltage Regulation & Harmonic Mitigation
	Shunt Inverter (NPC)	Current Compensation
	Series Inverter (NPC)	Voltage Sag/Swells Compensation
Control Strategies	MPPT	Fuzzy Logic
	PI/ANN Controller	NPC Converter

UPQC controlled by ANN and PI both restores V-I waveforms under different operating conditions, hence reduce harmonic distortions and improved power stability. In connectivity with PV-ESS, faults, and some non-linear loads, the voltage stays stable while drastically reducing

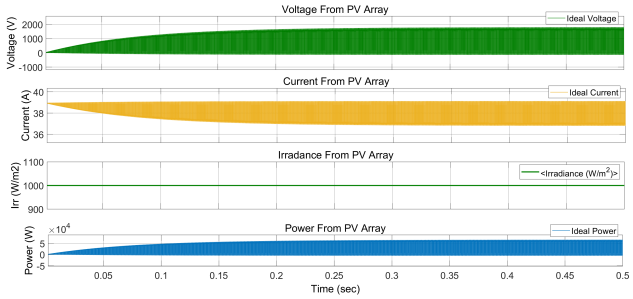

Fig. 6. Ideal Voltage, Current, Irradance, Power Plot of array at 25 deg.c

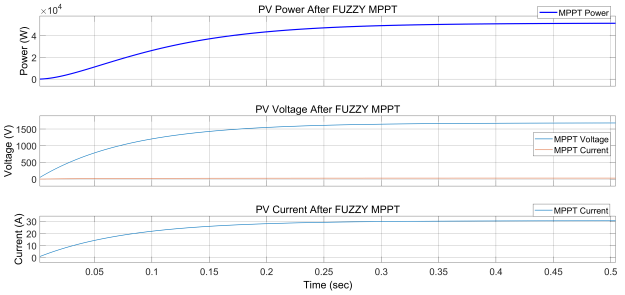

Fig. 7. Power,Voltage, Current Plot After FUZZY MPPT

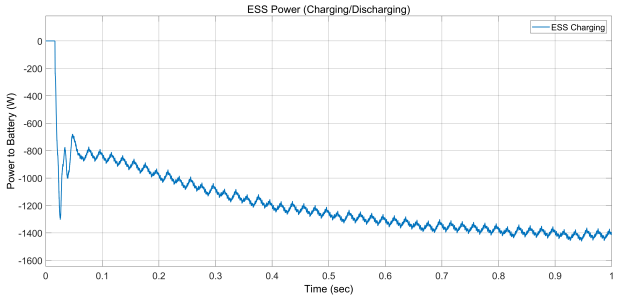

Fig. 8. Charging Power Plot of ESS

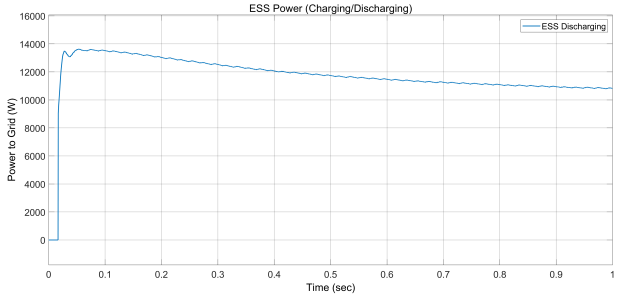

Fig. 9. Discharging Power Plot of ESS

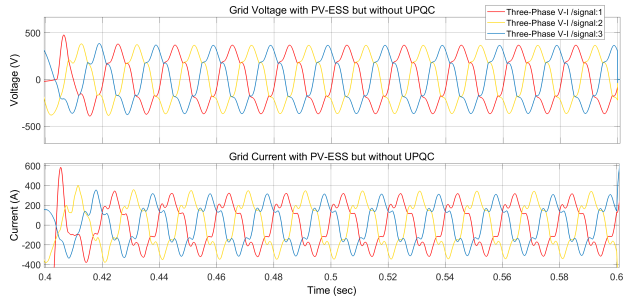

Fig. 10. Grid V-I Waveform with PV-ESS, Fault and Non-Linear load but without UPQC

Fig. 11. Grid V-I Waveform with L-G fault but without UPQC

current distortion; hence, this validates that the UPQC has the capacity to filter power quality issues.

With ANN Tuned UPQC in Fig. 14 all distortion are significantly mitigated. During L-G fault (0.2s-0.4s), the voltage remain close to its rated value and current distortion also reduced to approx. 500A i.e. 2 times to original value. In Fig. 15 For L-L-L-G fault at (0.6s-0.8s), voltage stabilizes with less than 10% fluctuation instead of dropping to zero, similarly current value decreased to 500A showing drastic improvement over the 2200A spike in the uncontrolled case.

The THD is measured up to 20th harmonics(i.e 1000Hz) over five cycles from 0.5 s.After integration of the PV-ESS system, the voltage and the current THD rise to 13.17% and 21.30%, respectively, due to the fluctuating generating capacity of renewable resources, and power factor (PF) of 0.86 was observed. Implementing UPQC along with a PI

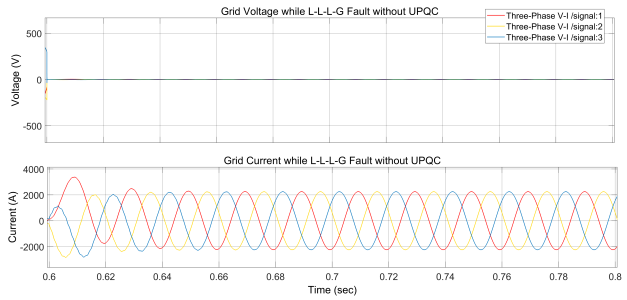

Fig. 12. Grid V-I Waveform with L-L-L-G fault but without UPQC

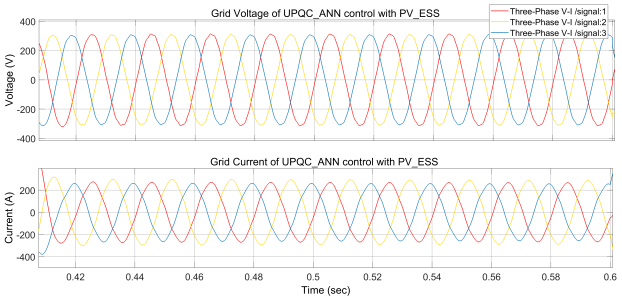

Fig. 13. Grid V-I Waveform with PV-ESS, Fault and Non-Linear load and ANN Tuned UPQC

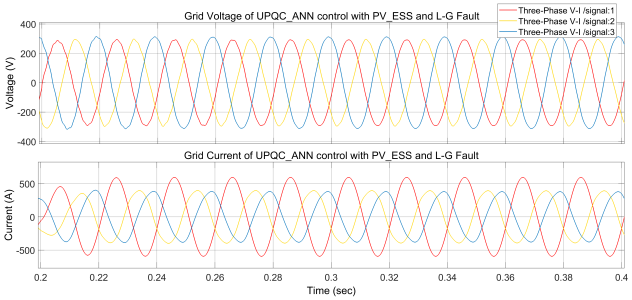

Fig. 14. Grid V-I Waveform with L-G fault but without UPQC

controller will act effectively to reduce harmonics, as the voltage and current THD was brought down to 3.13% and 3.11% respectively, which is under the IEEE 519 standard and PF improves to 0.95. Finally, using an ANN-based controller instead of a PI controller further enhances the performance of UPQC and THD of voltage and THD of current were reduced to 1.66% and 2.48%, with stabilization over time and PF is optimized at 0.99. Therefore, PI-controlled UPQC demonstrates similar improvement in each test case so that both controllers are capable of improving power quality. However, adaptive control-oriented dynamic features are assumed to be fulfilled more appropriately by ANN-tuned UPQC.

A THD Table IV in different cases seen at 0.5s through five cycles and upto 20th harmonics (1000Hz) are as follows.

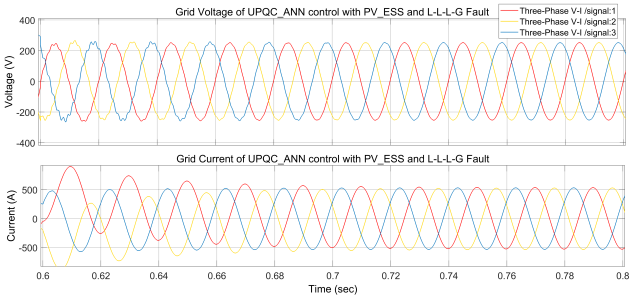

Fig. 15. Grid V-I Waveform with L-L-L-G fault and ANN Tuned UPQC

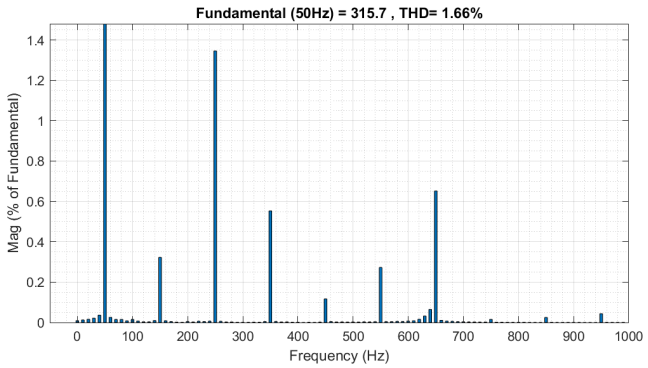

Fig. 16. FFT of measured Voltage signal with ANN Tune UPQC

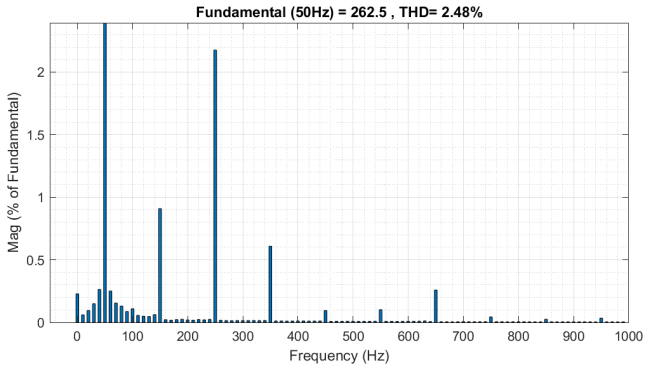

Fig. 17. FFT of measured Current signal with ANN Tuned UPQC

TABLE IV
GRID THD ANALYSIS UNDER DIFFERENT CONDITIONS

Condition	Phase I (%)	Phase II (%)	Phase III (%)
With Non-Linear Load but without UPQC			
Voltage THD	11.54	11.53	11.54
Current THD	17.55	17.54	17.58
With PV-ESS, Non-Linear Load but without UPQC			
Voltage THD	13.17	13.68	13.57
Current THD	21.30	20.46	22.93
With PV-ESS, Non-Linear Load & PI Controlled UPQC			
Voltage THD	3.13	3.25	3.26
Current THD	3.11	3.21	3.39
With PV-ESS, Non-Linear Load & ANN Tuned UPQC			
Voltage THD	1.66	1.81	1.79
Current THD	2.48	2.66	2.87

IV. CONCLUSION

The proposed PV-ESS with FLC integrated UPQC system based on ANN-tuned, brings about great improvements in power quality and system stability under various working situations and fault conditions. The fuzzy MPPT controller extracts power efficiently from the PV system, converging to the maximum power point quickly with great stability and efficiency. The PI-controlled UPQC notably reduces the total harmonic distortion (THD) levels, while the ANN-based UPQC would achieve even better harmonic attenuation, giving both excellent performance to keep harmonics well below the IEEE-519 standard. The ANN-based approach effects power factor correction much more effectively than the PI controller against the original, achieving very nearly unity power factor operation. Furthermore, the ESS satisfactorily maintains a balanced power transfer with a load and grid support, with controlled discharge. In conclusion, the proposed system improves power quality, reduces harmonic distortion, and strengthens the resilience of the grid to disturbances, providing reliable and efficient solutions for modern power systems.

REFERENCES

[1] Dolf Gielen, Francisco Boshell, Deger Saygin, Morgan D. Bazilian, Nicholas Wagner, and Ricardo Gorini, "The role of renewable energy in the global energy transformation," Energy Strategy Reviews, 24:38–50, 2019.

[2] S. Garg and S. Tyagi, "A Comprehensive Review on Opportunities and Challenges of Grid Integration of Renewable Energy Resources," 2024 Second International Conference on Smart Technologies for Power and Renewable Energy (SPECon), Ernakulam, India, 2024, pp. 1-6, doi: 10.1109/SPECon61254.2024.10537518.

[3] Edward J. Coster, Johanna M. A. Myrzik, Bas Kruimer, and Wil L. Kling, "Integration issues of distributed generation in distribution grids," Proceedings of the IEEE, 99(1):28–39, 2011.

[4] S. A. Mohamed, "Enhancement of power qualityfor load compensation using three different factsdevices based on optimized technique," InternationalTransactions on Electrical Energy Systems, 30(3):e12196, 2017.

[5] M. A. Mansor, K. Hasan, M. M. Othman, S. Z. B. M. Noor and I. Musirin, "Construction and Performance Investigation of Three-Phase Solar PV and Battery Energy Storage System Integrated UPQC," in IEEE Access, vol. 8, pp. 103511-103538, 2020, doi: 10.1109/ACCESS.2020.2997056.

[6] S. Devassy and B. Singh, "Performance Analysis of Solar PV Array and Battery Integrated Unified Power Quality Conditioner for Microgrid Systems," in IEEE Transactions on Industrial Electronics, vol. 68, no. 5, pp. 4027-4035, May 2021, doi: 10.1109/TIE.2020.2984439

[7] N. Zanib, M. Batool, S. Riaz and F. Nawaz, "Performance Analysis of Renewable Energy Based Distributed Generation System Using ANN Tuned UPQC," in IEEE Access, vol. 10, pp. 110034-110049, 2022, doi: 10.1109/ACCESS.2022.3213948.

[8] W. Ahamd and I. Ullah, "Unified Power Quality Conditioner Based Power Quality Improvement in Micro-Grid," 2025 IEEE Texas Power and Energy Conference (TPEC), College Station, TX, USA, 2025, pp. 1-6, doi: 10.1109/TPEC63981.2025.10906828.

[9] A. Metia and S. Ghosh, "Power Quality Improvement by UPQC in a Distribution Network using a Novel SRF based Control Approach," 2023 International Conference on Energy, Materials and Communication Engineering (ICEMCE), Madurai, India, 2023, pp. 1-6, doi: 10.1109/ICEMCE57940.2023.10434113.

[10] K. Sarita et al., "Power Enhancement With Grid Stabilization of Renewable Energy-Based Generation System Using UPQC-FLC-EVA Technique," in IEEE Access, vol. 8, pp. 207443-207464, 2020, doi: 10.1109/ACCESS.2020.3038313.

[11] T.-U. Hassan, R. Abbassi, H. Jerbi, K. Mehmood, M. F. Tahir, K. M. Cheema, R. M. Elavarasan, F. Ali, and I. A. Khan, "A novel algorithm for mppt of an isolated pv system using push pull converter with fuzzy logic controller," Energies, 13(15):4007, 2020.

APPENDIX C: PLAGIARISM TEST REPORT

Ashish Oliya

Performance Evaluation of PV-ESS-Integrated Grid Using ANN Tuned UPQC For Power Quality Enhancement

Tribhuvan University

Document Details

Submission ID
trn:oid:::3117:451107753

Submission Date
Apr 21, 2025, 11:04 PM GMT+5:45

Download Date
Apr 21, 2025, 11:05 PM GMT+5:45

File Name
Finalthesisreportashisholiya.pdf

File Size
14.6 MB

67 Pages

13,450 Words

70,633 Characters

11% Overall Similarity

The combined total of all matches, including overlapping sources, for each database.

Filtered from the Report

- Bibliography

Match Groups

145 Not Cited or Quoted 10%
Matches with neither in-text citation nor quotation marks

7 Missing Quotations 1%
Matches that are still very similar to source material

5 Missing Citation 0%
Matches that have quotation marks, but no in-text citation

0 Cited and Quoted 0%
Matches with in-text citation present, but no quotation marks

Top Sources

7% Internet sources

9% Publications

0% Submitted works (Student Papers)

Integrity Flags

0 Integrity Flags for Review

No suspicious text manipulations found.

Our system's algorithms look deeply at a document for any inconsistencies that would set it apart from a normal submission. If we notice something strange, we flag it for you to review.

A Flag is not necessarily an indicator of a problem. However, we'd recommend you focus your attention there for further review.

Match Groups

- **145** Not Cited or Quoted 10%
  Matches with neither in-text citation nor quotation marks
- **7** Missing Quotations 1%
  Matches that are still very similar to source material
- **5** Missing Citation 0%
  Matches that have quotation marks, but no in-text citation
- **0** Cited and Quoted 0%
  Matches with in-text citation present, but no quotation marks

Top Sources

- 7% Internet sources
- 9% Publications
- 0% Submitted works (Student Papers)

Top Sources

The sources with the highest number of matches within the submission. Overlapping sources will not be displayed.

1	Internet	researchrepository.murdoch.edu.au <1%
2	Internet	www.researchgate.net <1%
3	Internet	www.mdpi.com <1%
4	Internet	ebin.pub <1%
5	Internet	www.frontiersin.org <1%
6	Publication	"Innovations in Electrical and Electronics Engineering", Springer Science and Busi... <1%
7	Publication	Nayar, Priya. "Planning and Management of a Solar Power-Based Distribution Sys... <1%
8	Publication	I. Mahendravarman, S. A. Elankurisil, M. Venkateshkumar, A. Ragavendiran, N. Ch... <1%
9	Publication	Omnia S. S. Hussian, Hany M. Elsayed, M. A. Moustafa Hassan. "Fuzzy Logic Contr... <1%
10	Publication	Amir, Aamir. "Single-phase Cascaded T And -Type Gridconnected PV Inverters wi... <1%

11 Publication

Noor Zanib, Munira Batool, Saleem Riaz, Fawad Nawaz. "Performance Analysis of ... <1%

12 Publication

Mohammed Abdul Khader Aziz Biabani, Mohd Akram, Ikram Ahmed Shareef. "Po... <1%

13 Internet

uu.diva-portal.org <1%

14 Publication

L. Ashok Kumar, S. Albert Alexander. "Computational Paradigm Techniques for En... <1%

15 Publication

Rodolfo Dufo-López, Jaroslaw Krzywanski, Jai Singh. "Emerging Developments in t... <1%

16 Internet

core.ac.uk <1%

17 Publication

Nsilulu T. Mbungu, Ramesh C. Bansal, Raj M. Naidoo. "Smart energy coordination ... <1%

18 Publication

Radian Belu. "Energy Storage, Grid Integration, Energy Economics, and the Enviro... <1%

19 Internet

fdocumenti.com <1%

20 Internet

docplayer.net <1%

21 Publication

Ting Lu, Zhengming Zhao, Yingchao Zhang, Liqiang Yuan, Chongjian Li, Zhihua ... <1%

22 Internet

zero.sci-hub.se <1%

23 Publication

D. Casadei, G. Grandi, C. Rossi. "Single-Phase Single-Stage Photovoltaic Generatio... <1%

24 Internet

www.goanaturalgas.com <1%

25 Publication
Sarthak Dash, Manas Kumar Jena, Pankaj Dilip Achlerkar, Priyabrata Shaw. "Explo... <1%

26 Internet
iq.opengenus.org <1%

27 Publication
Kumari Sarita, Sachin Kumar, Aanchal Singh S. Vardhan, Rajvikram Madurai Elava... <1%

28 Publication
Unal Yilmaz, Omer Turksoy, Ahmet Teke. "Improved MPPT method to increase ac... <1%

29 Internet
web.fe.up.pt <1%

30 Internet
www.jetir.org <1%

31 Publication
Avik Metia, Smarajit Ghosh. "Power Quality Improvement by UPQC in a Distributi... <1%

32 Internet
repositorio.ufsm.br <1%

33 Internet
www.yandy-ager.com <1%

34 Publication
P. Rajesh Kumar, Chapala Shravani, M. Rajitha, Ch. Lokeshwar Reddy. "A Review o... <1%

35 Internet
elibrary.tucl.edu.np <1%

36 Internet
ijisrt.com <1%

37 Internet
123dok.org <1%

38 Publication
Kumari Sarita, Sachin Kumar, Aanchal Singh S. Vardhan, Rajvikram Madurai Elava... <1%

39 Publication
Suresh Mikkili, Anup Kumar Panda. "Power Quality Issues - Current Harmonics", ... <1%

40 Internet
bibliotecadigital.udea.edu.co <1%

41 Internet
diversedaily.com <1%

42 Internet
kahedu.edu.in <1%

43 Internet
open.uct.ac.za <1%

44 Internet
pubs.aip.org <1%

45 Internet
www.enfsolar.com <1%

46 Publication
"Advanced Computational Methods in Energy, Power, Electric Vehicles, and Their ... <1%

47 Publication
Ammar Al-Gizi, Sarab Al-Chlaihawi, Aurelian Craciunescu. "Efficiency of Photovolt... <1%

48 Publication
Bogdan M. Wilamowski, J. David Irwin. "The Industrial Electronics Handbook - Fiv... <1%

49 Publication
France Lasnier, Tony Gan Ang. "Photovoltaic Engineering Handbook", CRC Press, ... <1%

50 Publication
Gan, Philipe Gunawan. "Process Integration and Optimisation of Particle-Based C... <1%

51 Publication
H. Rudnick, J. Dixon, L. Moran. "Delivering clean and pure power", IEEE Power and... <1%

52 Publication
Koganti Srilakshmi, Sravanthy Gaddameedhi, Alapati Ramadevi, Praveen Kumar ... <1%

53 Publication
Sambit Kumar Mishra, Zdzislaw Polkowski, Samarjeet Borah, Ritesh Dash. "AI in ... <1%

54 Publication
Suleiman M. Sharkh, Mohammad A. Abusara, Georgios I. Orfanoudakis, Babar Hu... <1%

55 Publication
Terciyanli, Alper. "Design and Implementation of a Current Source Converter Bas... <1%

56 Internet
download.bibis.ir <1%

57 Internet
era.library.ualberta.ca <1%

58 Internet
iieta.org <1%

59 Internet
ijeer.forexjournal.co.in <1%

60 Internet
ijirt.org <1%

61 Internet
ijpeds.iaescore.com <1%

62 Internet
inass.org <1%

63 Internet
louis.uah.edu <1%

64 Internet
ltce.in <1%

65 Internet
spectrum.library.concordia.ca <1%

66 Internet
tuprints.ulb.tu-darmstadt.de <1%

67 Internet
vdoc.pub <1%

68 Internet
www.diva-portal.org <1%

69 Internet
www.e3s-conferences.org <1%

70 Internet
www.hindawi.com <1%

71 Internet
www.ijmetmr.com <1%

72 Internet
www.slideshare.net <1%

73 Publication
Altinoz, Bilal Metin. "Grid integration of combined solar-wind-battery energy syst... <1%

74 Publication
Dutta, Rathindra Nath. "On Resource Efficient and Obstacle Aware Link Selection ... <1%

75 Publication
Himadri Lala, Subrata Karmakar. "Continuous wavelet transform and artificial ne... <1%

76 Publication
Ikić, Marko R.. "Komponente snaga i Harmonijska izobličenja napona i struja foto... <1%

77 Publication
Jaephil Cho, Sookyung Jeong, Youngsik Kim. "Commercial and research battery te... <1%

78 Publication
Luca Esposito, Giulia Romagnoli. "Overview of policy and market dynamics for th... <1%

79 Publication
Luna, Adriana C., Nelson L. Diaz, Fabio Andrade, Moises Graells, Josep M. Guerrer... <1%

80 Publication
Roland Kobla Tagayi, Jonghoon Kim. "Binary-phase service battery energy storag... <1%

81 Publication

S. Hasheminejad, S. Esmaeili, S. Jazebi. "Power Quality Disturbance Classification ... <1%

82 Publication

Vamsi Priya Goli, Sanjib Ganguly. "Optimal allocation of series and multiple PV-int... <1%

83 Publication

Yinglong Zhao, Yong Li, Yijia Cao, Li Jiang, Jianghu Wan, Christian Rehtanz. "An R... <1%

84 Publication

Yuriy Rozanov, Sergey E. Ryvkin, Evgeny Chaplygin, Pavel Voronin. "Power Electro... <1%

85 Internet

cdn.enfsolar.com <1%

86 Internet

digibuo.uniovi.es <1%

87 Internet

dokumen.pub <1%

88 Internet

ijrrr.com <1%

89 Internet

research.ou.nl <1%

90 Internet

scholarworks.rit.edu <1%

91 Internet

vbn.aau.dk <1%

92 Internet

www.coursehero.com <1%

93 Internet

www.kresttechnology.com <1%

94 Internet

www.techscience.com <1%

95 Publication

Hasan Ebrahimi, Saeed Rezaeian-Marjani, Mohammad Farhadi-Kangarlu, Sadjad ... <1%

96 Publication

Shazia Baloch, Sunil Srivatsav Samsani, Mannan Saeed Muhammad. "Fault Protec... <1%

97 Publication

Teixeira, Ana Cristina Ornelas. "Preparation of Carbon-Based Electrodes to be Use... <1%

98 Publication

Thamer A. H. Alghamdi, Fatih Anayi, Michael Packianather. "Modelling and Contr... <1%

99 Publication

Green Energy and Technology, 2014. <1%

100 Publication

Youssef A. Mohamed, Ahmed M. Zobaa, Ahmed M. Ibrahim, Tarek A. Boghdady. "... <1%